

**A Quantitative Assessment of Atmospherically generated Foam Cements: Insights,
Impacts, and Implications of Wellbore Integrity and Stability.**

by

Richard Edward Spaulding

BS, Environmental Science, Robert Morris University, 2012

Submitted to the Graduate Faculty of the
Dietrich School of Arts and Sciences in partial fulfillment
of the requirements for the degree of
Master of Science

University of Pittsburgh

2015

UNIVERSITY OF PITTSBURGH
KENNETH P. DIETRICH SCHOOL OF ARTS AND SCIENCES

This thesis was presented

by

Richard Spaulding

It was defended on

July 15, 2015

and approved by

Josef Werne, Ph.D., Associate Professor, Department of Geology and Planetary Science

Brian Stewart, Ph.D., Associate Professor, Department of Geology and Planetary Science

Thesis Advisor: William Harbert, Ph.D., Professor, Department of Geology and Planetary
Science

Copyright © by Richard Spaulding

2015

A QUANTITATIVE ASSESSMENT OF ATMOSPHERICALLY GENERATED FOAM CEMENTS: INSIGHTS, IMPACTS, AND IMPLICATIONS OF WELLBORE INTEGRITY AND STABILITY.

Richard Edward Spaulding, M.S.

University of Pittsburgh, 2015

The primary function of well cement is to provide casing support and zonal isolation for the life of a well (Thiercelin et al., 1998; Singamshetty, 2004; Iverson et al., 2008). Failure to achieve one or both of these conditions can lead to a migration of fluids up the wellbore and result in both economic and ecological disasters, as exemplified by the Deepwater Horizon oil spill on April 20, 2010. To avoid these kinds of failures, the cement must have sufficient strength to secure the casing in the hole and withstand the stresses of drilling, perforating, enhanced oil recovery, and hydraulic fracturing and also be able to keep the annulus sealed against the formation.

This thesis analyzes and presents in detail some of the mechanical and physical properties of atmospherically generated foamed cements typically used in deep offshore wells in the Gulf of Mexico. Both static and dynamic measurements were taken across a range of foam qualities and include permeability, porosity, compressive strength, Young's modulus (E), and Poisson's ratio (ν). Investigating the properties of a range of foam qualities and cement recipes provides better understanding of the effect that different amounts of entrained air can have on cement performance and reliability. To better represent the behavior of cements in the wellbore, we subjected cements to pressure cycling and the measurements were analyzed over the range of these pressures. Our results show how these foamed cements behave and will prove to be a good baseline for future testing on cements generated under in-situ conditions.

TABLE OF CONTENTS

PREFACE.....	XIV
1. INTRODUCTION	1
1.1 FOAM CEMENT	4
1.2 HYPOTHESES, SCIENTIFIC OBJECTIVES AND INTELLECTUAL MERIT... 	5
1.3 BACKGROUND.....	6
1.3.1 Foamed Cement.....	6
1.3.2 Factors effecting sheath integrity and zonal isolation.....	7
1.3.3 Mechanical Properties of Foam Cement.....	8
1.4 METHODS.....	9
1.4.1 Cement slurry/Sample Preparation.....	9
1.4.2 Helium Porosimetry	10
1.4.3 Nitrogen Permeability.....	11
1.4.4 Ultrasonic-waveforms and Velocity measurements.....	11
1.5 BROADER IMPACTS.....	12
2. FOAMED CEMENTS: CORRELATION OF FOAM QUALITY WITH STRENGTH, PERMEABILITY, AND POROSITY	13
2.1 INTRODUCTION	13
2.2 FOAMED CEMENT	19
2.3 MATERIALS AND METHODS.....	21
2.3.1 Sample Preparation	21
2.3.2 Porosity and Permeability Measurements	22

2.3.3 Effect of Variable Conditions on Cement Permeability	23
2.3.4 Strength Measurements – Comparisons of sample geometries	24
2.3.5 Strength Measurements – Foamed Cements	25
2.4 RESULTS	25
2.4.1 Effects of hydration age and temperature on Porosity and Permeability ...	25
2.4.2 Strength Measurements – Comparisons of sample geometries	27
2.4.3 Correlations between Foam Quality and Permeability, Porosity, Mechanical Properties	30
2.4.4 Permeability and Porosity	32
2.4.5 Mechanical Properties	36
2.4.6 Strength Permeability and Porosity Relationship.....	41
2.4.7 Modulus of elasticity (Young’s Modulus vs. Porosity, and Permeability)...	44
2.4.8 Poisson’s Ratio vs. Porosity, Permeability	47
2.4.9 Young’s Modulus vs. Compressive strength relation	48
2.5 DISCUSSION.....	49
3. AN ASSESSMENT OF THE DYNAMIC MODULUS OF ATMOSPHERICALLY GENERATED FOAM CEMENTS	52
3.1 INTRODUCTION AND LITERATURE REVIEW	52
3.2 MATERIALS AND METHODS.....	56
3.2.1 Cement Slurry and Sample Preparation	56
3.2.3 Foamed Cements	56
3.2.4 Ultrasonic-Waveforms, Velocity and Permeability Measurements	57
3.3 RESULTS.....	59

3.3.1 Neat Cement	60
3.3.2 Foam Quality 10%	60
3.3.3 Foam Quality 20%	61
3.3.4 Foam Quality 30%	62
3.4 DISCUSSION.....	62
3.4.1 Permeability.....	62
3.4.2 Poisson’s Ratio.....	65
3.4.3 Young’s Modulus	67
3.5 CONCLUSIONS.....	70
3.6 LESSONS LEARNED AND FUTURE WORK	71
4. COMPARITIVE ANALYSIS OF STATIC AND DYNAMIC YOUNG’S MODULUS	76
4.1 STATIC VS. DYNAMIC MECHANICAL PROPERTIES.....	76
4.2 CORRELATION BETWEEN STATIC AND DYNAMIC MEASUREMENTS ...	77
APPENDIX A :.....	79
BIBLIOGRAPHY	100

LIST OF TABLES

Table 1: Mechanical Properties of multiple variations of Cement Slurries (Iverson et al., 2008) .	9
Table 2: Young’s moduli of various materials (Nelson and Guillot, 2006 – adapted from Table 8.1)	17
Table 3: Poisson’s ratio of various materials (www.EngineeringToolBox.com; Nelson and Guillot 2006; Mueller et al., 2004).....	19
Table 4: Measured properties of the cement samples.	33
Table 5: Dynamic Moduli calculated from equations 10-12	58
Table 6: Young's Modulus, Poisson's ratio, and Permeability recorded by AutoLab 1500	59

LIST OF FIGURES

Figure 1: Modulus of Elasticity	16
Figure 2: Deformation measured by Poisson's Ratio.....	18
Figure 3: Temco, Inc. Helium porosimeter HP 401 (TEMCO, Inc.).....	23
Figure 4: Temco UltraPerm 500 Permeameter	23
Figure 5: Permeability measurements of Class H neat cement over a period of 28 days.....	26
Figure 6: Porosity measurements of Class H neat cement over a period of 28 days.....	26
Figure 7: The impact of hydration temperature on permeability.....	27
Figure 8: The compressive strength of the different slurry densities.....	28
Figure 9: Compressive Strength Comparisons of the 0.5-inch cylinder vs. the standard ASTM 2 inch cube	28
Figure 10: Compressive Strength Comparisons of the 1-inch cylinder vs. the standard ASTM 2 inch cube.	29
Figure 11: Compressive Strength Comparisons of the 1-inch cube vs. the standard ASTM 2 inch cube.....	29
Figure 12: Comparison of CT-derived porosity to foam quality	31
Figure 13: Comparison of foam quality and the bulk average density	31
Figure 14: 2D slices of reconstructed 3.7 μm resolution CT scans	32
Figure 15: 2-D slices of reconstructed 3.9 μm resolution CT scans.....	32
Figure 16: Permeability measurements of foamed cement recipe 1(a.) and 2 (b.) (FCR1 and FCR2)	34
Figure 17: Porosity measurements of foamed cement recipe 1(a.) and 2(b.) (FCR1 and FCR2)..	35

Figure 18: Plots of permeability versus porosity measurements of foamed cement recipe 1(a.) and 2(b.) (FCR1 and FCR2).	36
Figure 19: Compressive Strength as a function of foam quality	38
Figure 20: Young’s Modulus as a function of foam quality.....	39
Figure 21: Poisson’s Ratio as a function of foam quality.....	40
Figure 22: Compressive strength as a function of permeability.	42
Figure 23: Compressive strength as a function of porosity.	43
Figure 24: Young’s modulus as a function of porosity.....	45
Figure 25: Young’s modulus as a function of permeability.	46
Figure 26: Poisson’s ratio as a function of porosity.	47
Figure 27: Young’s modulus as a function of compressive strength.....	48
Figure 28: Permeability response as a function of applied pressure.....	64
Figure 29: Percent change in Permeability for various Foam qualities during cyclic loading and unloading.....	65
Figure 30: Average Poisson's Ratio of all samples over both loading and unloading increases with greater foam quality.	66
Figure 31: Average Poisson's Ratio of all samples within each Foam Quality measured across all loading and unloading regimes.	67
Figure 32: Average Young’s modulus for all cement types	69
Figure 33: Variation in Young’s Modulus vs. Applied Pressure for both cycles.....	70
Figure 34: Permeability (34A.), Young's Modulus (34B.), and Poisson's ratio (34C.) of all FCR1 cements over an applied pressure range of 6.5 MPa to 46.0 MPa.....	72

Figure 35: Permeability (35A), Young's Modulus (35B), and Poisson's ratio (35C.) of all FCR2 cements over an applied pressure range of 6.5 MPa to 46.0 MPa.	73
Figure 36: Permeability (36A), Young's Modulus (36B), and Poisson's ratio (36C) of all H-Class Neat cements over an applied pressure range of 6.5 MPa to 46.0 MPa.	74
Figure 37: Static vs. Dynamic Young's Modulus	78
Figure 38: FCR1 - 10% Foam quality Stress - Strain Plot.....	79
Figure 39: FCR1 - 10% Foam quality Stress - Strain Plot.....	80
Figure 40: FCR1 - 10% Foam quality Stress - Strain Plot.....	80
Figure 41: FCR1 - 10% Foam quality Stress - Strain Plot.....	81
Figure 42: FCR1 - 10% Foam quality Stress - Strain Plot.....	81
Figure 43: FCR1 - 20% Foam quality Stress - Strain Plot.....	82
Figure 44: FCR1 - 20% Foam quality Stress - Strain Plot.....	82
Figure 45: FCR1 - 20% Foam quality Stress - Strain Plot.....	83
Figure 46: FCR1 - 20% Foam quality Stress - Strain Plot.....	83
Figure 47: FCR1 - 20% Foam quality Stress - Strain Plot.....	84
Figure 48: FCR1 - 30% Foam quality Stress - Strain Plot.....	84
Figure 49: FCR1 - 30% Foam quality Stress - Strain Plot.....	85
Figure 50: FCR1 - 30% Foam quality Stress - Strain Plot.....	85
Figure 51: FCR1 - 30% Foam quality Stress - Strain Plot.....	86
Figure 52: FCR1 - 30% Foam quality Stress - Strain Plot.....	86
Figure 53: FCR1 - 40% Foam quality Stress - Strain Plot.....	87
Figure 54: FCR1 - 40% Foam quality Stress - Strain Plot.....	87
Figure 55: FCR1 - 40% Foam quality Stress - Strain Plot.....	88

Figure 56: FCR1 - 40% Foam quality Stress - Strain Plot.....	88
Figure 57: FCR1 - 40% Foam quality Stress - Strain Plot.....	89
Figure 58: FCR2 - 10% Foam quality Stress - Strain Plot.....	89
Figure 59: FCR2 - 10% Foam quality Stress - Strain Plot.....	90
Figure 60: FCR2 - 10% Foam quality Stress - Strain Plot.....	90
Figure 61: FCR2 - 10% Foam quality Stress - Strain Plot.....	91
Figure 62: FCR2 - 10% Foam quality Stress - Strain Plot.....	91
Figure 63: FCR2 - 20% Foam quality Stress - Strain Plot.....	92
Figure 64: FCR2 - 20% Foam quality Stress - Strain Plot.....	92
Figure 65: FCR2 - 20% Foam quality Stress - Strain Plot.....	93
Figure 66: FCR2 - 20% Foam quality Stress - Strain Plot.....	93
Figure 67: FCR2 - 20% Foam quality Stress - Strain Plot.....	94
Figure 68: FCR2 - 30% Foam quality Stress - Strain Plot.....	94
Figure 69: FCR2 - 30% Foam quality Stress - Strain Plot.....	95
Figure 70: FCR2 - 30% Foam quality Stress - Strain Plot.....	95
Figure 71: FCR2 - 30% Foam quality Stress - Strain Plot.....	96
Figure 72: FCR2 - 30% Foam quality Stress - Strain Plot.....	96
Figure 73: FCR2 - 40% Foam quality Stress - Strain Plot.....	97
Figure 74: FCR2 - 40% Foam quality Stress - Strain Plot.....	97
Figure 75: FCR2 - 40% Foam quality Stress - Strain Plot.....	98
Figure 76: FCR2 - 40% Foam quality Stress - Strain Plot.....	98
Figure 77: FCR2 - 40% Foam quality Stress - Strain Plot.....	99

LIST OF EQUATIONS

Equation 1: Darcy's Law.....	11
Equation 2: Porosity.....	14
Equation 3: Modulus of Elasticity	16
Equation 4: Stress	16
Equation 5: Strain	16
Equation 6: Poisson's Ratio.....	18
Equation 7: Bulk Density.....	30
Equation 8: Dynamic Young's Modulus.....	57
Equation 9: Dynamic Poisson's Ratio.....	58
Equation 10: Dynamic Shear Modulus	58
Equation 11: Dynamic Bulk Modulus	58
Equation 12: Lamé's First Parameter.....	58
Equation 13: Static and Dynamic Correlation.....	77

PREFACE

Portions of this work were completed as part of National Energy Technology Laboratory (NETL) research for the Department of Energy's Complementary Research Program under Section 999 of the Energy Policy Act of 2005. I wish to acknowledge and thank Dr. Barbara Kutcho, Roy Long (NETL Strategic Center for Natural Gas and Oil) and Elena Melchert (DOE Office of Fossil Energy) for programmatic guidance, direction, and support.

I would like to thank Dr. Dustin Crandall from NETL Morgantown and Erich Zorn from the University of Pittsburgh for manuscript reviews of Chapter 3 and thoughtful discussions on mechanical properties.

I would also like to thank Dr. Bill Harbert, Dr. Igor Haljasmaa, Jim Fazio, and Connor Gieger for their unwavering support and assistance with discussing mechanical properties and testing methods. To the entire Foamed Cement Team at NETL, I would like to extend my immense gratitude and respect. Without the team, this research would have never been possible.

Lastly, I would like to thank my wife for her love and support throughout the process of writing this thesis.

1. INTRODUCTION

The primary function of oil-well cement is to provide casing support and zonal isolation for the life of a well (Thiercelin et al., 1998; Singamshetty, 2004; Iverson et al., 2008). Defined most simply, zonal isolation is the separation or exclusion of fluids along sections of the vertical column that the wellbore occupies. Zonal isolation depends heavily on both the permeability and mechanical behavior of the cement. In addition, the cement must have sufficient strength to secure the casing in the hole and withstand the stress of drilling, perforating, enhanced oil recovery, and hydraulic fracturing. Industry standards require the measurement of mechanical parameters to ensure the integrity of the primary cement job (American Petroleum Institute, 1997)

The use of foamed cement systems for deep-water applications has been increasing and is often the system of choice for shallow hazard mitigation in the Gulf of Mexico (Benge et al., 1996; Fuller, 2010). Foamed cement is a gas-liquid dispersion that is created when a gas, typically nitrogen, is stabilized as microscopic bubbles within the cement slurry (Harms and Febus, 1985). Currently there is little information regarding foamed cement behavior under wellbore conditions. The April 2010 Macondo Prospect oil well blowout and the resulting spill in the Gulf of Mexico demonstrate the importance of foamed cement stability in the safe construction of offshore wells. The Chief Counsel's Report (2011) about the Macondo incident stated: "The root technical cause of the blowout is now clear: The cement that BP and Halliburton pumped to the bottom of the well failed to isolate hydrocarbons in the formation from the wellbore—that is, it did not accomplish

zonal isolation.” Current testing methods are limited to atmospheric conditions. However, it is well known that elevated pressures in the wellbore environment have a profound effect on foamed cement properties (McElfresh, 1982). There is limited understanding of the stability and properties of foamed cement as it is placed in the well and post-placement. Therefore, there is a significant need to test foamed cement under conditions that simulate placement in this environment (De Rozieres, 1991; Ravi et al., 2006). Unstable foams can result in non-cemented sections or channels in the well, enabling gas migration (Kopp et al., 2000). For this reason, foamed cement stability must be known.

Due to the critical importance of cement in zonal isolation of wellbore systems and the complications that arise in high pressure/high temperature (HPHT), deep water, and weak formation environments (Ravi et al., 2006), it is expected that cement will be weakened by pressurization / depressurization processes that are found in these subsurface environments. By understanding some of these processes, researchers can gain some insight as to how cement behaves in a wellbore.

Dynamic modulus experiments were conducted to address the mechanical response to multiple foam qualities under various wellbore pressure conditions using ultra-sonic measurements and the NER AutoLab 1500 at NETL, Pittsburgh. This project will present the mechanical and physical properties of foamed cement that is typically used in deep offshore wells in the Gulf of Mexico. Permeability, porosity, Young’s modulus (E), and Poisson’s ratio (ν) were measured across a range of foam qualities to help determine the elasticity, and ductility of foam cements that are actually used in a well. Four foam qualities were prepared (10%, 20%, 30%, and 40%) according to API RP 10 4-B using Class H cement and industry standard foaming agents.

Although a typical foam quality in a well is somewhere around 15%-20%, a wider range of cement qualities was included for a more comprehensive experimental design.

In addition to dynamic modulus experiments, some static modulus experiments to failure were completed on selected samples. The dynamic estimates of moduli were calculated, and correlate well with previously published workflows for estimating static moduli from dynamic moduli. Dynamic estimates presented in this thesis can thus be used, directly, to estimate static properties.

It is our hope to use the information provided by these results as a baseline for further testing of foamed cements generated under in situ pressures. We conclude that the results of these experiments will aid researchers in predicting the behavior of wellbore cement in a variety of conditions and environments. This information will then allow them to design safer and more effective wellbore foam cements.

This thesis contains 4 chapters outlining our research into how foamed cements' elastic moduli behave under pressure. I apologize for any repetition the reader may find throughout this thesis. Certain ideas and paragraphs have been repeated to give continuity to each of the chapters as a whole. Chapter 1 provides the background, objectives, and methodology used to address the research scope. Chapter 2 presents a correlation of foam quality of atmospheric generated foamed cement with physical and mechanical properties using traditional static tests. Chapter 2 is also the subject of an NETL Technical Report Series (TRS) - one of several being released by NETL on foamed cement research. Some details of Chapter 2 are also available in the Society of Petroleum Engineers (SPE) journal SPE-170298-MS. Chapter 3 describes the dynamic moduli of those same atmospheric generated foamed cements (as presented in Chapter 2) and is currently published as OTC-25776-MS. A high level overview of the project is also available in the January 2015 cover

story of the Journal of Petroleum Technology (JPT). Chapter 4 looks at the differences between static and dynamic testing methods and the relationship between their results.

1.1 FOAM CEMENT

Foamed Cement is a low density material used to fill the annulus (the space between the rock formation and the steel casing) of oil and gas wells (Thiercelin et al., 1998; Nelson and Guillot, 2006). It is created by introducing a gas into a cement slurry that, when combined with chemical stabilizers, creates a stable matrix of microscopic bubbles (Harms and Febus, 1985; Nelson and Guillot, 2006; Kutchko et al., 2014). There are two reasons for using cement in a well. The primary reason for using cement in a well, foamed or conventional is to provide zonal isolation (Thiercelin et al., 1998; Singamshetty, 2004; Iverson et al., 2008) - that is, to prevent fluid/gas migration up the wellhead to the surface and to seal the annulus from permeable or loose rock formations (Iverson et al., 2008). The second reason is to provide support and to help center the steel casing in the well (Bozich et al., 1984; Goodwin K. J., 1997).

Zonal isolation depends primarily on both the permeability and mechanical behavior of the cement (Nelson and Guillot, 2006). When compressive strength is combined with permeability measurements, it is possible to estimate cement's ability to provide zonal isolation and resist attack from formation fluids (Nelson and Guillot, 2006).

1.2 HYPOTHESES, SCIENTIFIC OBJECTIVES AND INTELLECTUAL MERIT

Our research goals are to develop a database of mechanical properties of both foamed cement of different “recipes” and of class-H neat cement that is often used in the oil well cementing operations in the Gulf of Mexico. We will examine these parameters under various simulated wellbore conditions to discern how cement behaves elastically in a well. We will combine and compare this data with static measurements to determine the variations in the static and dynamic moduli of foam cement. Finally, we will compare these results to samples generated in the field by industry collaborators to try and draw a correlation between how cement generated under field conditions vary from those generated in a laboratory environment. This plan will allow us to test the following hypotheses:

(1) We hypothesize that the 30% and 40% foam quality laboratory generated foamed cement will be weakened / destroyed by pressurization / depressurization processes that are found in simulated subsurface environments. To determine this, we plan on subjecting the various foam qualities to cyclic loading and unloading processes and then plotting the data and checking for hysteresis. If the starting values are different from the ending values then it shows some sort of non-elastic deformation, which would ultimately fail to provide zonal isolation in the wellbore.

(2) We hypothesize that the static measurements will have a higher Young’s modulus than the dynamic measurements on both field and laboratory generated cements. By combining and comparing both static and dynamic measurements, we will be able to determine the differences between the two types of measurements. This may then be correlated to preserve rare, expensive field generated samples from unnecessary destructive testing.

(3) We hypothesize that the most significant changes in cement brittleness and ductility will take place in the first sequence of loading and unloading. By conducting cyclic testing and plotting the data points against effective pressure, the resulting data will be able show that the cement is basically unaffected by pressure loading and unloading after an initial maximum effective pressure has been reached. This may prove to be important in that cement already in a well might be able to “seal” itself in the presence of such loading and unloading cycles.

1.3 BACKGROUND

1.3.1 Foamed Cement

Foamed cement is a gas-liquid dispersion that is created when a gas, typically nitrogen but can also include air, is stabilized as microscopic bubbles within the cement slurry (Harms and Febus, 1985; Nelson and Guillot, 2006). The gas volume entrained in the foam cement is referred to as the “foam quality”. The higher the entrained gas content the higher the foam quality, (e.g. 10% foam quality contains 10% nitrogen or air by volume). Foamed cements are low-density cement systems used in formations unable to support the annular hydrostatic pressure of conventional cement slurries (Harlan et al., 2001; Nelson and Guillot, 2006), and their use has been well documented in literature (Harms and Febus, 1985; Thayer et al., 1993; Bengé et al., 1996; Frisch et al., 1999; Kopp et al., 2000; White et al., 2000; Harlan et al., 2001; Bengé and Poole, 2005). Foam cement densities can range from 4 - 18 lbm/gal (.48 to 2.16 g/cc) (SPE International, 2015). More recently, foamed cement use has expanded into regions with high-stress environments, such

as isolating problem formations typical in the Gulf of Mexico (Benge et al., 1996; Judge and Benge, 1998; White et al., 2000; Rae and Lullo, 2004).

There is a common belief in the oil and gas industry that conventional cements, which have higher compressive strengths, are better able to withstand cement sheath fracturing and that the lower compressive strength of foamed cement is a cause for concern. However, the lower compressive strength of foamed cement does not increase the risk for inducing fractures and it is, in fact, able to withstand greater wellbore pressures than conventional cements (Harlan et al., 2001). The entrained air in the cement creates a foamed network within the matrix of the cement, which in turn exhibits a more elastic response, therefore indicating that foamed cement has a lower Young's modulus than conventional cements (Iverson et al., 2008). This is significant because cements with lower Young's moduli are more resistant to the common mechanical stresses associated with well operations (Kopp et al., 2000). In comparison to conventional cement, foamed cement is ductile and will deform when the casing is pressurized (Kopp et al., 2000). As a result, foamed cement has a unique resistance to temperature and pressure-induced stresses and long-term sealing through resistance to cement-sheath stress cracking (Benge et al., 1996).

1.3.2 Factors effecting sheath integrity and zonal isolation.

Goodwin and Crook, (1992) conducted an experiment to evaluate the performance of various cement sheath systems that were subjected to multiple pressure and temperature changes. The study showed that rigid cement sheaths or cement sheaths that exhibit a high Young's modulus are more susceptible to damage caused by pressure and/or temperature changes. They also showed

that the materials with a higher compressive strength provided better casing support but lost the ability to provide zonal isolation at lower internal pressures (Goodwin and Crook, 1992).

Benge et al. (1996) recognized the unique elastic behavior of foamed cement systems and successfully implemented them in the Gulf of Mexico, particularly in HPHT (High Pressure, High Temperature) applications. This experimental work was then followed by mathematical modeling studies of the effect of different stresses on a cement sheath. Thiercelin et al., (1998) applied stress modeling to study the effect of cement sheath mechanical properties, assuming different bonding scenarios. They showed that the integrity of a cement sheath is a function of the set cement's mechanical properties, the geometry of the cased wellbore, and the mechanical properties of the formation rock to which it bonds (Thiercelin et al., 1998). Bosma et al., (1999) simulated the mechanical responses of a cement sheath based on finite element analysis. They modeled plastic deformation, de-bonding, and cracking for cement sheath failure modes and simulated the effect of cement sheath shrinkage and expansion that takes place in the wellbore. They concluded that the failure of a well sealant (cement sheath) is largely the result of in-situ stress conditions, which are dependent on fluctuations in pressure and temperature.

1.3.3 Mechanical Properties of Foam Cement.

As mentioned earlier, there is little understanding of the mechanical properties of set cement in the hydrocarbon industry. There are, however, some data available on foamed cement slurries. Ravi et al., (2006) conducted multiple experiments on various types of foamed slurry to determine the different mechanical properties present. They found, among other things, that compressive strength is not enough to determine the ability of cement to provide zonal isolation. More importantly, they determined that no one parameter (compressive strength, Young's modulus,

Poisson’s ratio, etc.) could explain the behavior of formulations under cyclic loading and unloading.

Iverson et al. (2008) conducted un-confined and confined pressure testing on cement slurries of different compositions (Table 1). They found that neat cements (cement with no additional entrained air or additives) tended to be less elastic and had higher values for the other parameters looked at than the foam or elastomer (Table 1). Of most importance however, were their findings that the addition of additives (foaming agent or elastomer) lowered young’s modulus and also lowered the strength capabilities of the cement (Iverson et al., 2008).

Table 1: Mechanical Properties of multiple variations of Cement Slurries (Iverson et al., 2008)

	Neat	Foam	Elastomer
Modulus (psi)	1.81E+06	8.08E+05	4.91E+05
Comp. Strength (psi)	6851	1052	1350
Tens. Strength (psi)	429	190	218
Poisson's Ratio	0.2	0.151	0.205
Cohesion (psi)	2208	391	540
Friction Angle	24.84	12.49	13.58

1.4 METHODS

1.4.1 Cement slurry/Sample Preparation

The cement slurries were prepared using a base of Class H Portland cement provided by Lafarge with a slurry density of 16.5 lbm/gal (1.97 g/cm³). Class H cement was utilized due to its common use in the Gulf of Mexico. Foamed cement samples were prepared according to API RP 10 4-B using an Ametek (Chandler Engineering) constant speed mixer (model 30-60). Once the base slurry was mixed, it was poured into a stainless steel, screw-top blender with a stacked blade

assembly to provide the proper amount of shear (Galiana et al., 1991). Atmospheric foamed cements contain predefined amounts of air, as a percentage of the total cement volume. One group of H class Neat cement was created to use as a baseline. Two sets of four different foam qualities, 10%, 20%, 30%, and 40% entrained air fractions were mixed using 2 different industry standard foaming agents (provided by industry collaborators). Once mixed, the slurries were poured into 945 ml containers and allowed to cure for 3 days under atmospheric conditions. One-inch diameter cement cores were sub sectioned using a Powermatic variable speed wet drill utilizing a 1-in diamond-tipped core drill bit. The cored samples were then cut to a length of 2-inches and the ends of the samples cleaned using a Struers Secotom-10 wet saw. For consistency, the samples were labeled, weighed, and put in a desiccator to dry. Subsequent measurements of weight were taken until the weight remained consistent over time, thus ensuring the samples were sufficiently dry for gas permeability measurements (Mindess and Young, 1981). All samples were dried at atmospheric pressure and temperature to avoid damaging them by thermally stressing or over desiccating, ensuring quality results (Nelson and Guillot, 2006).

1.4.2 Helium Porosimetry

Sample diameter and length was measured using an electronic caliper and the results recorded digitally. The samples were placed into a Temco, Inc. Helium porosimeter HP 401 (TEMCO, Inc.) using a Smartporosity computer program to determine porosity. The HP 401 is able to measure porosity levels as low as 1% with relative precision.

1.4.3 Nitrogen Permeability

Nitrogen permeability was measured using a constant flow permeameter: Temco UltraPerm 500 Permeameter with a Corelab WinPerm computer program. The permeability was estimated using Darcy's Law (Equation 1):

Equation 1: Darcy's Law

$$K = \frac{Qnl}{S\Delta p}$$

Where n is the viscosity of nitrogen at atmospheric conditions = 0.017631 cP, l is the sample length, and S is the cross-sectional area of the cement sample. Due to gas slippage, a Klinkenberg correction was applied for permeability measurements.

1.4.4 Ultrasonic-waveforms and Velocity measurements

All velocity measurements were made using the New England Research Group (NER) AutoLab 1500 device located at the National Energy and Technology Lab (NETL) of the U.S. Department of Energy (DOE). This device is capable of triaxial compression and temperature control, allowing the user to control the confining, pore, and effective pressures as well as the temperature exposed to the cement samples. In addition, the AutoLab 1500 also has two ultrasonic wave transducers, which generate ultrasonic P and S waves in one end of the core and records the arrival of the waves at the other end. The device also records sampling frequency, wave velocity, and physical characteristics like Young's modulus and Poisson's ratio.

1.5 BROADER IMPACTS

Extensive literature reviews and research has indicated that the mechanical behavior of well cement after being pumped into the annulus is controlled by a number of factors including slurry type, curing time, temperature, pressure, additives, etc. (McElfresh, 1982; Kopp et al., 2000; Ravi et al., 2006). However, there are few examples of experimental research done to these cements after they have been set (Ravi et al., 2006). This research is intended to i) provide researchers with a baseline of values of set foamed cement to then be used to correlate mechanical properties of atmospheric generated cement and field generated cements provided by industry collaborators; ii) help determine the “target window” for foam cement quality based on strength and elastic properties of various types of set foam cements; and iii) act as a stepping off point for a comparison of static and dynamic moduli of similarly fabricated foam cements. The resulting data sets will help give cement researchers a greater comprehension of how the pressure cycles found in a wellbore can affect the mechanical properties of cement and lead to a loss in zonal isolation or compromised cement sheath integrity.

2. FOAMED CEMENTS: CORRELATION OF FOAM QUALITY WITH STRENGTH, PERMEABILITY, AND POROSITY ¹

2.1 INTRODUCTION

The primary function of well cement is to provide casing support and zonal isolation for the life of the well. Industry standards require the measurement of mechanical parameters to ensure the integrity of the primary cement job. This chapter presents the mechanical and physical properties of foamed cement typically used in deep offshore wells in the Gulf of Mexico. Permeability, porosity, compressive strength, Young's modulus (E), and Poisson's ratio (ν) were measured across a range of foam qualities. Four foam qualities were prepared (10%, 20%, 30%, and 40%) according to API RP 10 4-B using Class H cement and industry standard foaming agents. Test results include a modified ASTM C109/C109M relationship correlating different geometries of cement.

In a typical oil and gas well, cement is placed in the annulus between the steel casing and formation rock for both zonal isolation and casing support. Zonal isolation is the prevention of fluids (water, oil, gas) migrating to different zones outside of the casing and is strongly affected by the permeability of the cement sheath (Nelson and Guillot, 2006). Zonal isolation depends heavily on both the permeability and mechanical behavior of the cement (Nelson and Guillot, 2006). When compressive strength is combined with permeability measurements, it is possible to estimate the cement's ability to provide zonal isolation and resist attack from formation fluids

¹ A part of NETL TRS and SPE-170298-MS

(Nelson and Guillot, 2006). Many of the same factors that impact the strength of cement also impact the permeability (Aldrich, 1974). Permeability (K) is the measure of the capacity of a porous medium to allow flow of fluids or gasses. The unit of measurement is commonly presented in millidarcy (mD) (API, 1997). Permeability is an important property of cement in influencing its long-term durability and is vital to the hydro-mechanical behavior of cement (Banthia et al., 2005). Permeability is influenced by porosity and interconnectivity of pores as well as micro-cracks in the cement (Banthia et al., 2005). Porosity (n) is the measure of void space, defined as the ratio of the volume of voids to the total volume, usually expressed as a percentage (Equation 2) (Das et al., 2006):

Equation 2: Porosity

$$n = \frac{V_v}{V}$$

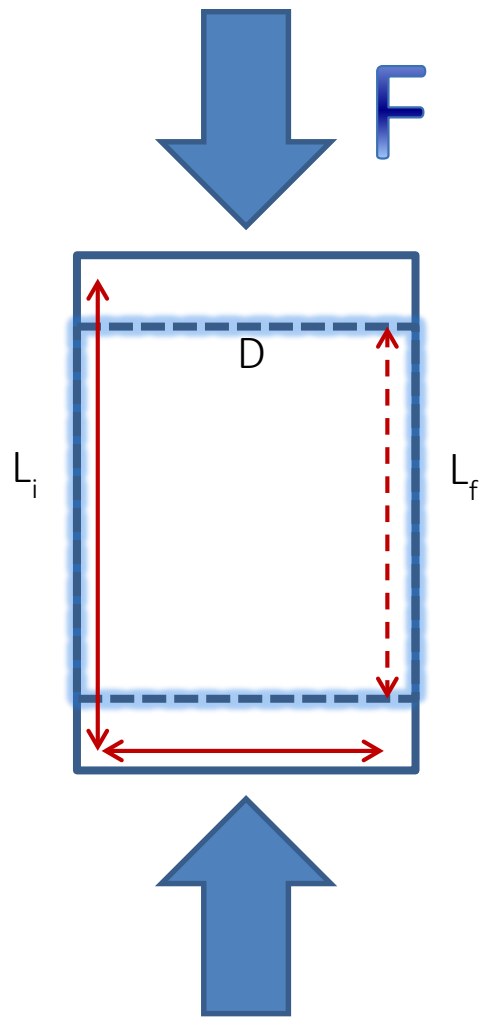
Since pores may or may not be interconnected, there is no guarantee of a correlation between porosity and permeability. Porosity and interconnectivity of cement are controlled by various factors such as the water/cement ratio and the degree of hydration (Banthia et al., 2005). Both porosity and permeability are considered “durability indicators” with regards to cement performance.

Cement must have sufficient strength to secure the casing in the hole and withstand the stress of drilling, perforating, and fracturing (API, 1991 Worldwide Cementing Practices). Cement sheath failure is primarily caused by pressure- or temperature-induced stresses common in typical well operations. Examples of pressure-inducing well operations include casing pressure tests, injecting, stimulating, and producing. Each of these operations can cause the cement sheath to lose its ability to provide zonal isolation (Griffith et al., 2004). Therefore, measuring the mechanical

properties of cement is an important step in predicting cement behavior under applied downhole stresses (Nelson and Guillot, 2006). During laboratory testing, compressive strength values typically range from 500 psi to 2000 psi (3.4 MPa to 13.7 MPa) (Mueller and Eid, 2006).

When measuring strength, a plot of stress versus strain (referred to as a “stress-strain diagram”) is produced. A number of mechanical properties can be deduced from stress-strain diagrams. The ratio of stress to strain in the linear region of the stress-strain diagram is called Young’s modulus, also known as the modulus of elasticity (Craig, Jr., Ed. 2000):

Figure 1: Modulus of Elasticity: The force per unit area required to compress or stretch a certain material.



Equation 3: Modulus of Elasticity

$$E = \frac{\sigma}{\epsilon}$$

Where E = Young's modulus, σ = stress, and ϵ = strain. Stress and strain are defined as:

Equation 4: Stress

$$\sigma = F/A$$

Equation 5: Strain

$$\epsilon = (L_i - L_f)/L_f$$

Where F = force, A = area, L_i = initial length, and L_f = final length.

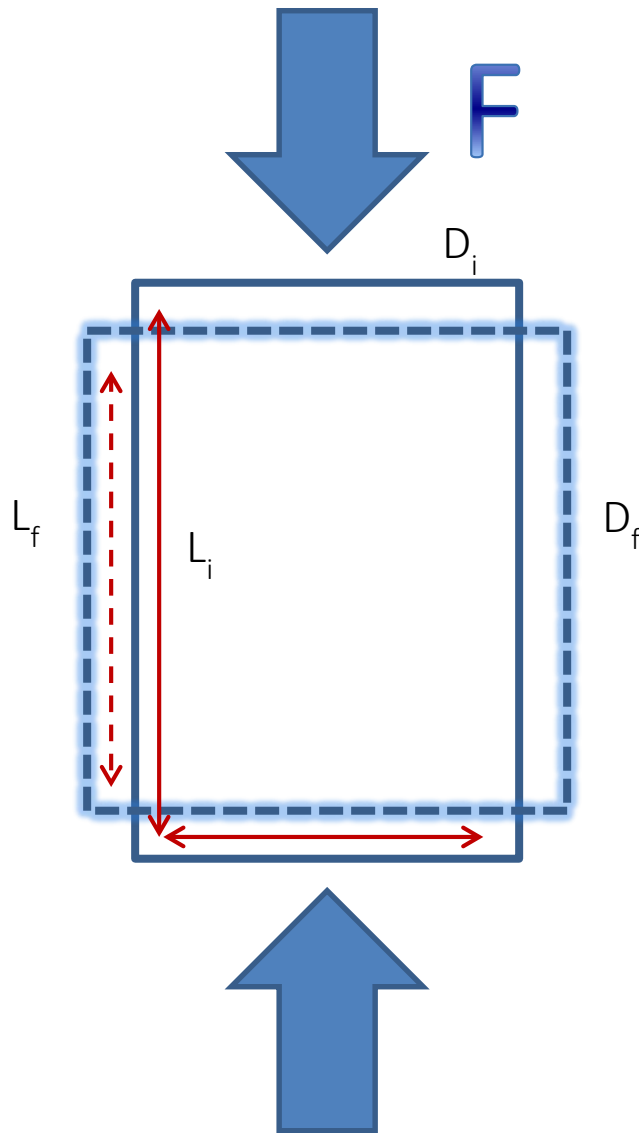
Young's modulus is a measure of the stiffness of a material: How brittle or ductile a material is. That is to say, the force per unit area required to compress or stretch a certain material. Higher Young's modulus indicates a more brittle material whereas lower Young's modulus describes more ductile materials. Young's modulus can be used to predict the elongation or compression of a material (Craig, Jr., Ed. 2000). Young's modulus can be derived by a variety of methods including ultrasonic (dynamic) and compressional (static) testing (Mueller et al., 2004). Young's moduli of some common materials are presented in Table 2.

Table 2: Young's moduli of various materials (Nelson and Guillot, 2006 – modified after Table 8.1)

Material	Young' Modulus (psi)	Young's Modulus (GPa)
Aluminum	10×10^6	69
Copper	16×10^6	110
Steel	30×10^6	207
Oilwell Cement	$0.14 - 1.4 \times 10^6$	1-10
Polyethylene	$14 - 200 \times 10^3$	97-1379
Rubber	$0.6 - 11 \times 10^3$	4-76

During the compression of a material in one direction, expansion may occur perpendicular to the direction of the compression. This occurrence is known as the Poisson effect and is measured by Poisson's ratio. Poisson's ratio is the negative ratio of transverse to axial strain (Craig, Jr., Ed. 2000):

Figure 2: Deformation measured by Poisson's Ratio



Equation 6: Poisson's Ratio

$$\nu = \frac{-\epsilon_t}{\epsilon_l}$$

Where ν = Poisson's ratio, ϵ_t = transverse strain, and ϵ_l = longitudinal or axial strain.

Most isotropic materials have Poisson’s ratio values ranging between 0.0 and 0.5. The less compressible the material, the higher the Poisson’s ratio – a material with a Poisson’s ratio of 0.5 is considered incompressible. Conventional cements have a Poisson’s ratio of about 0.15 (Nelson and Guillot, 2006). Mueller et al. cited a Poisson’s ratio value for oil well cement at 0.12 (Mueller et al., 2004). Typical Poisson’s ratios of common materials are shown in Table 3.

Table 3: Poisson’s ratio of various materials (www.EngineeringToolBox.com; Nelson and Guillot 2006; Mueller et al., 2004)

Material	Poisson’s Ratio
Aluminum	0.32 – 0.35
Copper	0.355
Steel	0.265 – 0.305
Oilwell Cement	0.12 – 0.15
Concrete	0.1 – 0.2
Rubber	0.48 – ~0.5

2.2 FOAMED CEMENT

Foamed cement is a gas-liquid dispersion that is created when a gas, typically nitrogen, is stabilized as microscopic bubbles within the cement slurry (Harms and Febus, 1985; Nelson and Guillot, 2006). The gas volume entrained in the foam cement is referred to as the “foam quality”. The higher the foam quality, the higher the entrained gas content (e.g. 20% foam quality contains 20% nitrogen or air by volume). Foamed cements are ultralow-density cement systems used in formations unable to support the annular hydrostatic pressure of conventional cement slurries (Harlan et al., 2001; Nelson and Guillot, 2006). The use of foamed cement for its lightweight density is well documented in literature (Harms and Febus, 1985; Thayer et al., 1993; Bengel et al.,

1996; Frisch et al., 1999; Kopp et al., 2000; White et al., 2000; Harlan et al., 2001; Bengel and Poole, 2005). More recently, foamed cement use has expanded into regions with high-stress environments, for example, isolating problem formations typical in the Gulf of Mexico (Bengel et al., 1996; Judge and Bengel, 1998; White et al., 2000; Rae and Lullo, 2004).

There is a misconception that conventional cements, with their higher compressive strengths, are better able to withstand cement sheath fracturing and that the lower compressive strength of foamed cement is a cause for concern. However, the lower compressive strength of foamed cement does not increase the risk for inducing fractures and it is, in fact, able to withstand greater wellbore pressures than conventional cements (Harlan et al., 2001). The entrained air in the cement creates a foamed network within the matrix of the cement, which in turn exhibits a more elastic response – foamed cement has a lower Young’s modulus than conventional cements (Iverson et al., 2008). This is significant because cement with lower Young’s moduli is more resistant to the common mechanical stresses associated with well operations (Kopp et al., 2000). In comparison to conventional cement, foamed cement is ductile and will deform when the casing is pressurized (Kopp et al., 2000). As a result, foamed cement has a unique resistance to temperature and pressure-induced stresses and long-term sealing through resistance to cement-sheath stress cracking (Bengel et al., 1996; White et al., 2000). For example, the mechanical properties of foamed cement make it ideal for use in hydraulic-fracturing operations (Harlan et al., 2001).

In this chapter, permeability, porosity, and mechanical properties (compressive strength, Young’s modulus, and Poisson’s ratio) are presented for two sets of foamed cement recipes and one neat cement mixed under atmospheric conditions using a standard testing method (API, 2004). Four foam qualities (10, 20, 30, and 40%) of each foamed cement recipe were correlated to provide

a better understanding of how foam quality impacts the physical properties of the cement. Bubble size distributions were previously studied by CT image and data analysis for each foamed cement system and provide further understanding of the impact that the gas distribution has on overall cement stability (Kutchko et al., 2013).

2.3 MATERIALS AND METHODS

2.3.1 Sample Preparation

All cement samples were prepared using a base slurry of Class H Portland cement (Lafarge, Joppa, IL) with a slurry density of 16.5 lbm/gal (1.97 g/cm³). The foamed cement represents systems commonly used in offshore wells in the Gulf of Mexico. Foamed cement samples were prepared according to API recommended practices 104-B using an Ametek (Chandler engineering) constant speed mixer (model 30-60). The cement slurry was then poured into a stainless steel, screw top blender with a stacked blade assembly. Four foam qualities (10%, 20%, 30%, and 40%) were mixed using two different industry standard foaming agents and stabilizers.

- A neat cement using Class H and water mixed to a density of 16.4 lbm/gal (1.97 g/cm³)
- Foamed cement mixed using Class H cement with a base slurry of 16.4 lbm/gal to generate four foam qualities: 10%, 20%, 30%, and 40% using industry surfactant #1 (Recipe 1)
- Foamed cement mixed using Class H cement a base slurry of 16.4 lbm/gal to generate four foam qualities: 10%, 20%, 30%, and 40% using industry surfactant #2 and stabilizer (Recipe 2)

Once mixed, the slurries were cured for approximately 3 days under atmospheric conditions. One-inch diameter cement cores were sub sectioned using a Powermatic variable speed wet drill using a 1” diamond tipped core drill bit. The cored samples were next cut to a length of 2 inches and the ends of the samples were cleaned using a Struers Secotom-10 wet saw. The samples were then labeled, weighed, and allowed to dry at ambient temperature. Subsequent measurements of weight were taken until it was clear that the samples were sufficiently dry for gas permeability measurement (Mindess and Young, 1981). All samples were dried at atmospheric pressure and temperature to avoid damaging them by thermally stressing or over desiccating (Nelson and Guillot, 2006).

2.3.2 Porosity and Permeability Measurements

Sample diameter and length were measured using an electronic caliper and the results were recorded. The samples were placed into a Temco, Inc. Helium porosimeter HP 401 (TEMCO, Inc.) using a Smartporosity computer program to determine porosity (Figure 3). The HP 401 is able to measure porosity as low as 1% with reasonable precision. Nitrogen permeability was measured using a constant flow permeater: Temco UltraPerm 500 Permeameter with a Corelab WinPerm computer program (Figure 4). The permeability was estimated using Darcy’s Law (Equation 1):

$$K = \frac{Qnl}{S\Delta p}$$

Where n is the viscosity of nitrogen at atmospheric conditions = 0.017631 cP, l is the sample length, and S is the cross-sectional area of the cement core. An average of eight porosity and permeability measurements was determined for each cement sample.

Figure 3: Temco, Inc. Helium porosimeter HP 401 (TEMCO, Inc.)

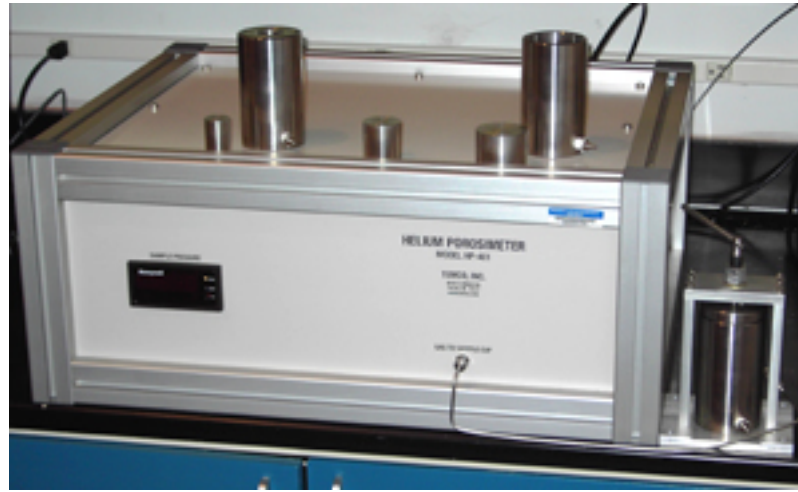


Figure 4: Temco UltraPerm 500 Permeameter



2.3.3 Effect of Variable Conditions on Cement Permeability

Three Class H neat cement samples were cured at 50 °C to determine the effect of temperature on cement permeability. The permeability of Class H neat cement samples was also measured under a confining pressure of 1000 psi and 2500 psi (6.8 MPa and 17.2 MPa) to determine the effects of

pressure. However, no measurable difference was observed and those results are not included in this report.

2.3.4 Strength Measurements – Comparisons of sample geometries

The standard test method for compressive strength (ASTM C109/C109M) requires the use of 2-inch cubes. However, in many situations in cement research different geometries are needed; for example, 1-inch rods were required for the permeability and porosity measurements. Therefore we investigated whether geometries smaller than the ASTM 2-inch cubes can be used to reliably determine changes in compressive strength of test cement samples. Four cement geometries were compared, including 1/2-inch round rods, 1-inch round rods, 1-inch cubes, and the ASTM 2-inch cubes. A total of 13 batches were mixed consisting of seven different initial cement densities (4 duplicates were used for validation of the sample mixing process). The samples were prepared using Class H cement to obtain different compressive strengths ranging from strong to very weak by varying the initial cement slurry density from 11.9 to 16.45 lbm/gal (1.43 – 1.97 g/cm³). All cements were mixed using a Waring blender as per API Recommended Practice 10B, poured into the appropriate mold, and cured in a humid chamber for 7 days prior to compressive strength testing using a modified Forney compression load frame capable of maintaining very low load rates and measuring stress at low applied pressures. Prior to the strength testing, the 1/2- and 1-inch rods were sawn to a length of 1- and 2-inches (respectively).

2.3.5 Strength Measurements – Foamed Cements

Four Class H foamed cements (foam qualities: 10, 20, 30, 40%) using two different surfactants were tested using uniaxial compression testing. Five samples of each cement system were tested to create statistical reliability within the data sets. Five samples of Class H neat cement were also tested as a baseline comparison. The following parameters were collected: Peak strength, axial stress, axial strain, and radial strain (Young's modulus and Poisson's ratio). Young's modulus and Poisson's ratio were measured in compression.

2.4 RESULTS

2.4.1 Effects of hydration age and temperature on Porosity and Permeability

In order to test sample control and integrity as well as determine effects due to hydration beyond 7 days, permeability and porosity measurements were performed on Class H neat cement every 7 days over a period of 28 days (Figure 5 - Figure 6). During the 28-day time period there were no significant changes in permeability: The average measurements ranged from 0.25 to 0.28 mD. In addition, there was little sample variability as noted by the small standard deviations. Porosity appeared to increase slightly; however, the increase was not significant ($\phi = 15.2$ to 20.5). Temperature had a significant effect on permeability, decreasing the value from an average of 0.3 mD at 21 °C to 0.03 mD at 50 °C (Figure 7).

Figure 5: Permeability measurements of Class H neat cement over a period of 28 days. Error bars represent standard deviation.

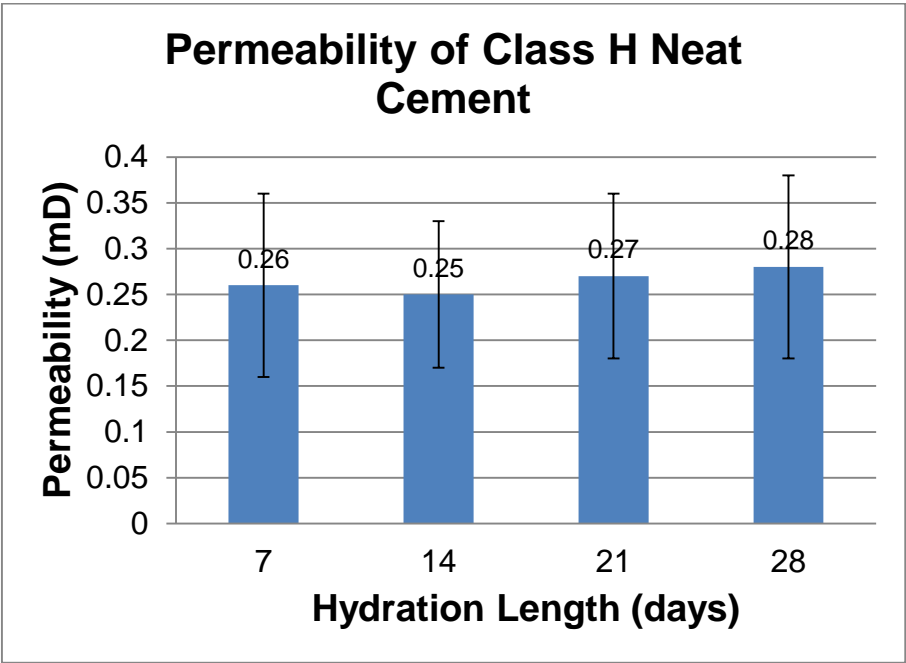


Figure 6: Porosity measurements of Class H neat cement over a period of 28 days. Error bars represent standard deviation.

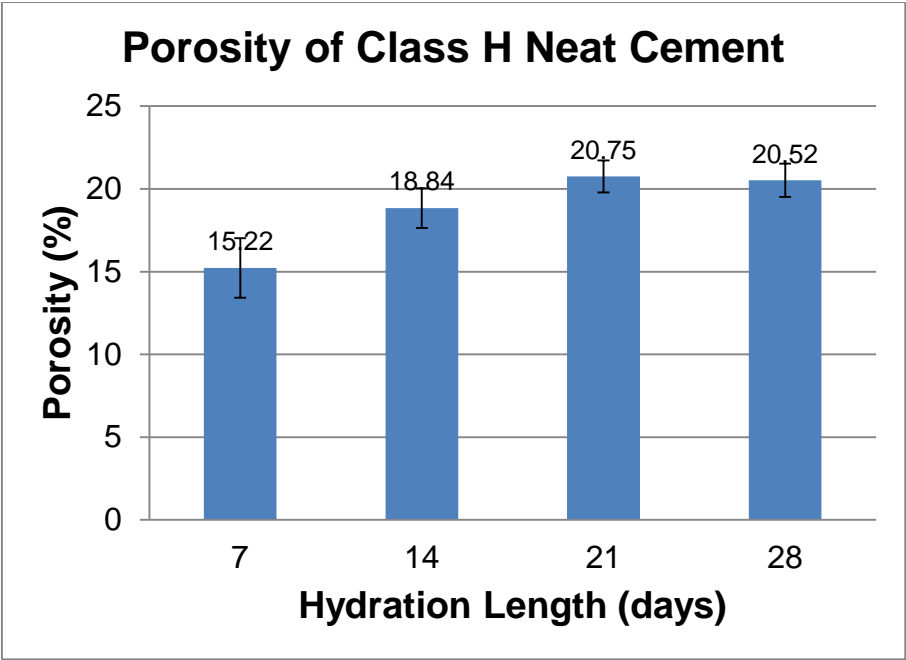
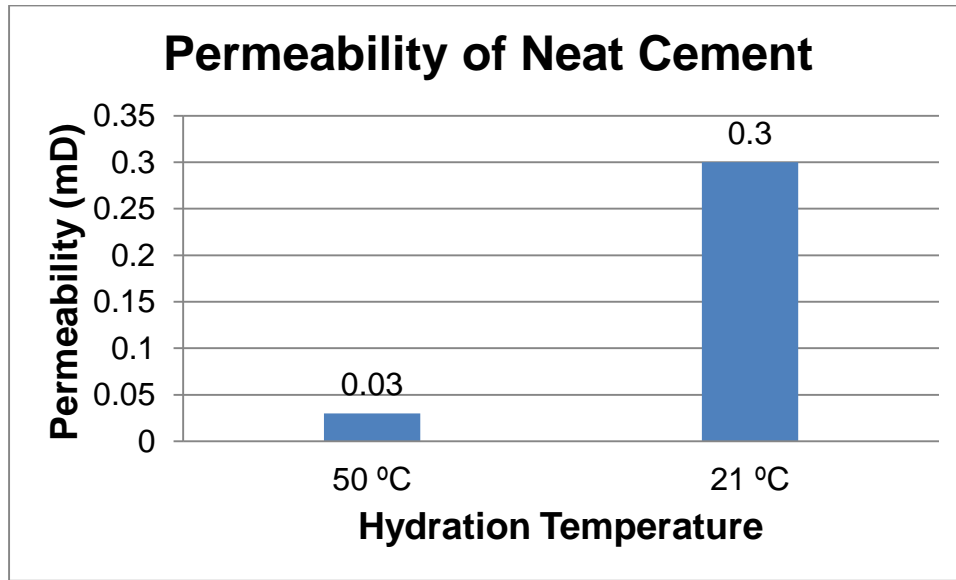


Figure 7: The impact of hydration temperature on permeability.



2.4.2 Strength Measurements – Comparisons of sample geometries

The compressive strength measurements of the 2-inch cubes of varying initial cement slurry densities can be seen in Figure 8. As expected, compressive strength increased with increasing slurry density. Figures 9 - 11 show the compressive strength comparisons of the cement test sample geometries. The various cement mixes using the 2-inch cubes yielded load results ranging from ca. 5 to 100 kN, and a range of stress values from ca. 3 to 40 MPa. When the standard 2-inch cube results were plotted against the other geometries, strong linear correlation coefficients ($R^2 > 0.98$) for both the stress and load results were observed.

Figure 8: The compressive strength of the different slurry densities

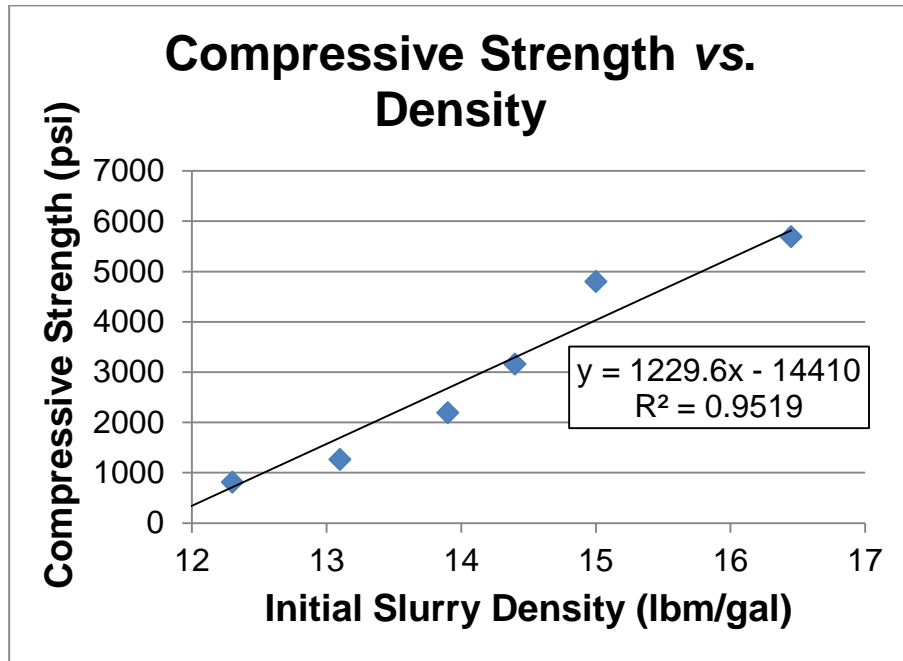


Figure 9: Compressive Strength Comparisons of the 0.5-inch cylinder vs. the standard ASTM 2 inch cube

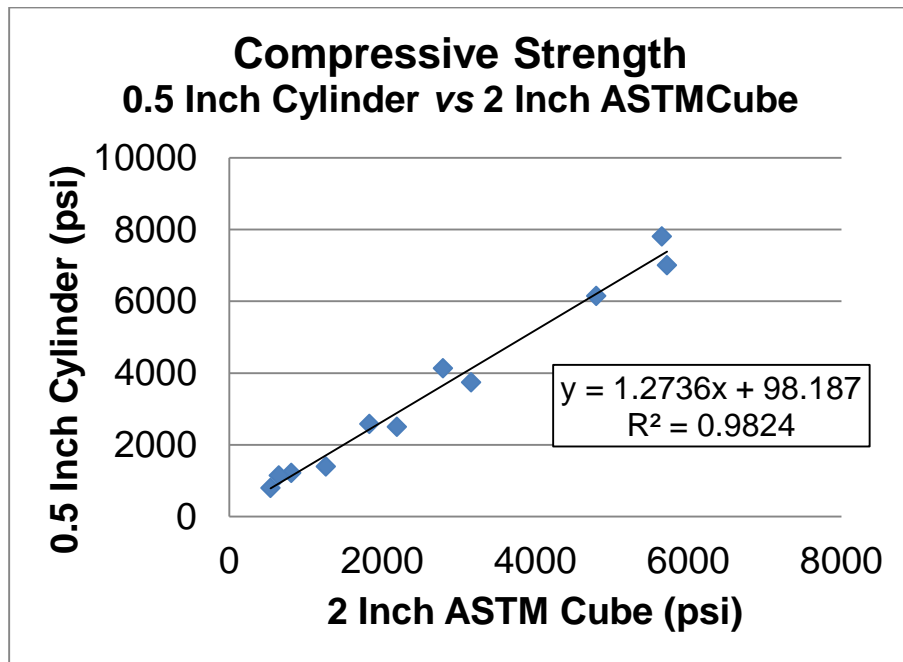


Figure 10: Compressive Strength Comparisons of the 1-inch cylinder vs. the standard ASTM 2 inch cube.

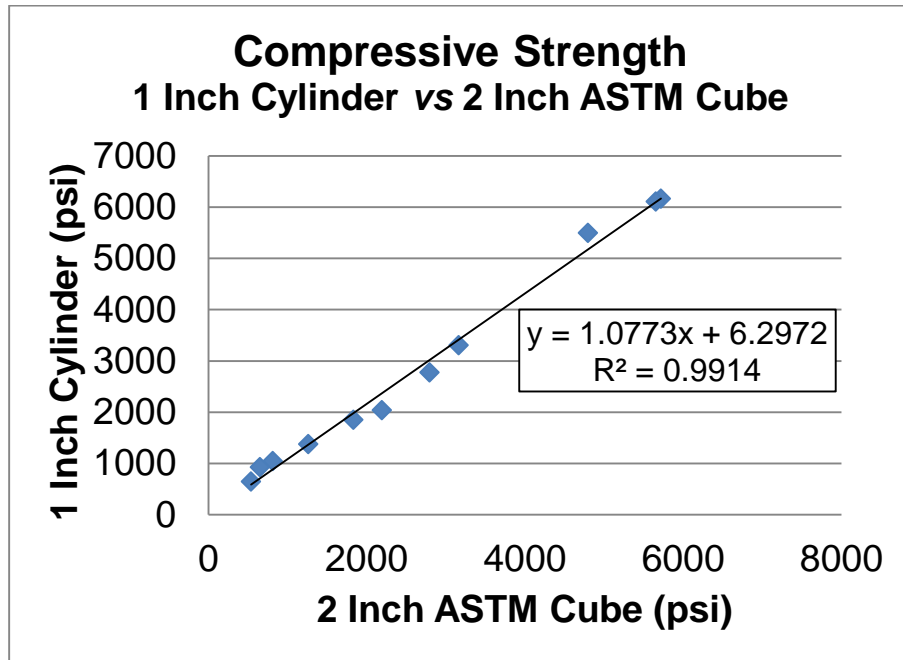
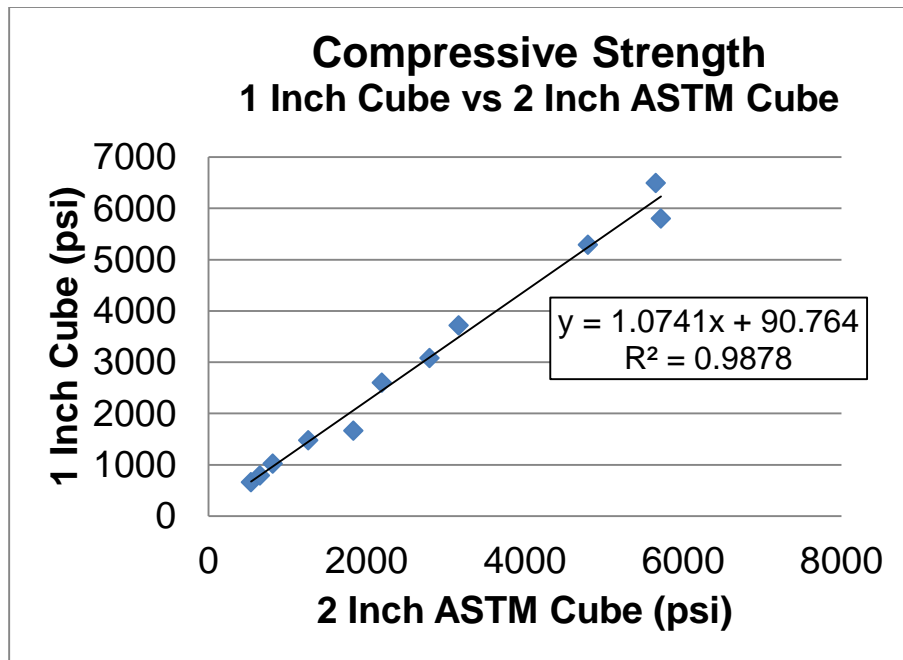


Figure 11: Compressive Strength Comparisons of the 1-inch cube vs. the standard ASTM 2 inch cube



2.4.3 Correlations between Foam Quality and Permeability, Porosity, Mechanical

Properties

To test the accuracy of CT-derived image data, the experimentally determined porosity of the cement samples was compared to porosity data derived from CT images (Figure 12). The correlation between the experimental gas fraction and the measured CT air volume was remarkably good. For 10 and 20% entrained air cements, the calculated porosity values were within 1% of experimental gas volume percentages. For the higher 30 and 40% foam quality cements, the measured porosities overestimated the air percentage, with the highest mismatch recorded for the low-resolution scan of 40% foam quality cement, where the CT scan calculated porosity was 46.2%. Predictably, the higher resolution scans provided a more accurate estimate of entrained air. Bulk average density of the set cement was measured on a subset of representative samples (Figure 13). In order to calculate average bulk density of a cylindrical sample we use the following formula (Equation 7):

Equation 7: Bulk Density

$$\rho = \frac{m}{V}$$

Where m = mass of sample, V = volume of the sample. As expected, density decreases with increasing foam quality.

Figure 12: Comparison of CT-derived porosity to foam quality, with the dashed line denoting a linear relationship with slope = 1. Results from low and high-resolution scans are included

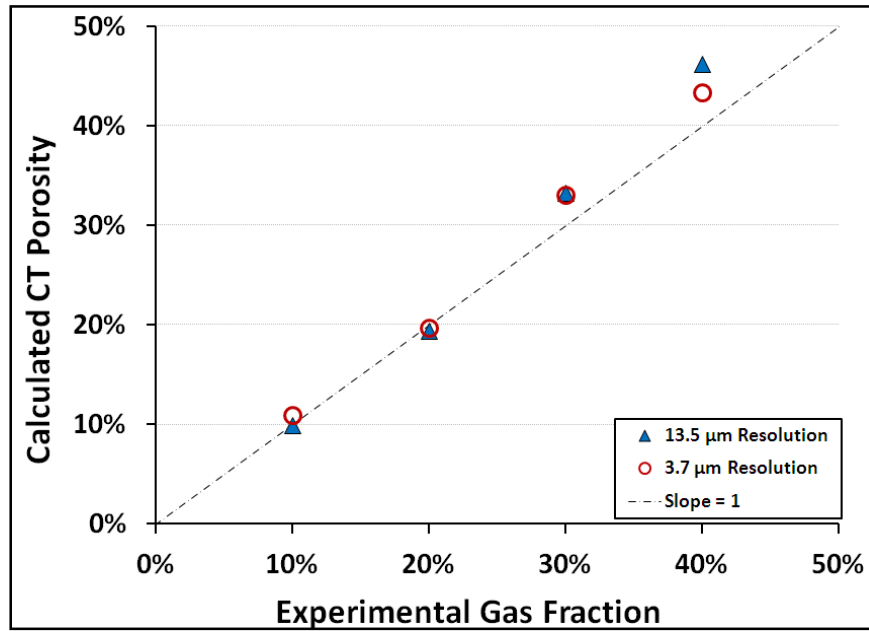
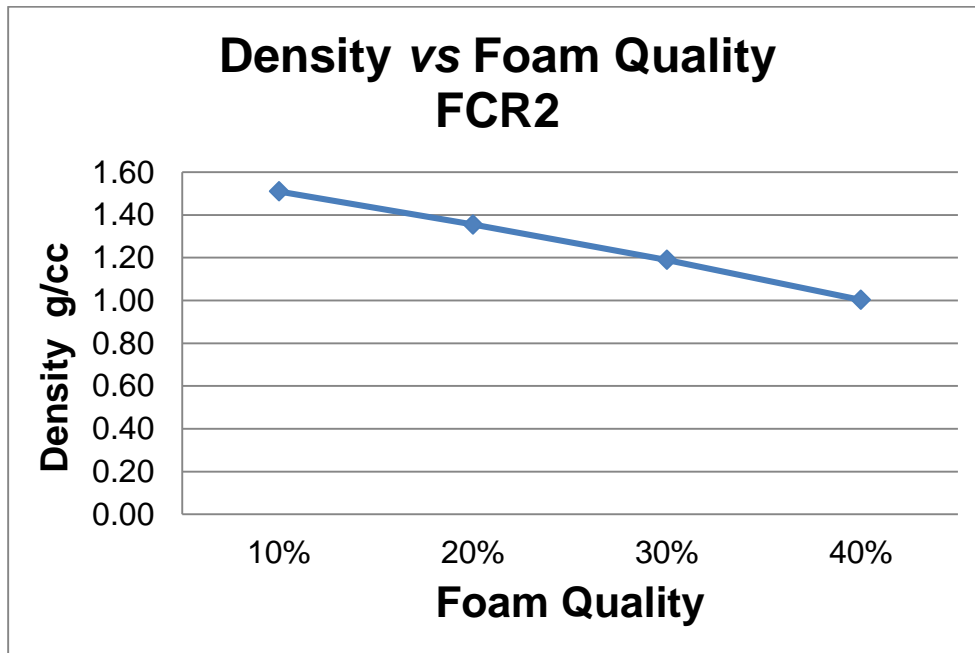


Figure 13: Comparison of foam quality and the bulk average density. Measurements were taken from a representative subset of foamed cement samples. 1g/cc \approx 8.35 lbm/gal



2.4.4 Permeability and Porosity

Porosity and permeability measurements were taken of two different foamed cement systems (FCR1 and FCR2) mixed at four foam qualities (10%, 20%, 30%, and 40%). 2D slices of reconstructed CT scans of each foam quality can be seen in both Figure 14 and Figure 15 (Kutchko, et al., 2013). All measurements are compared to neat cement as a baseline. The compiled properties for all nine cement mixes can be seen in Table 4.

Figure 14: 2D slices of reconstructed 3.7 μm resolution CT scans taken of the 0.6 cm diameter sub-samples of FCR1 with a foam quality of 10%, 20%, 30%, and 40%, from left to right.

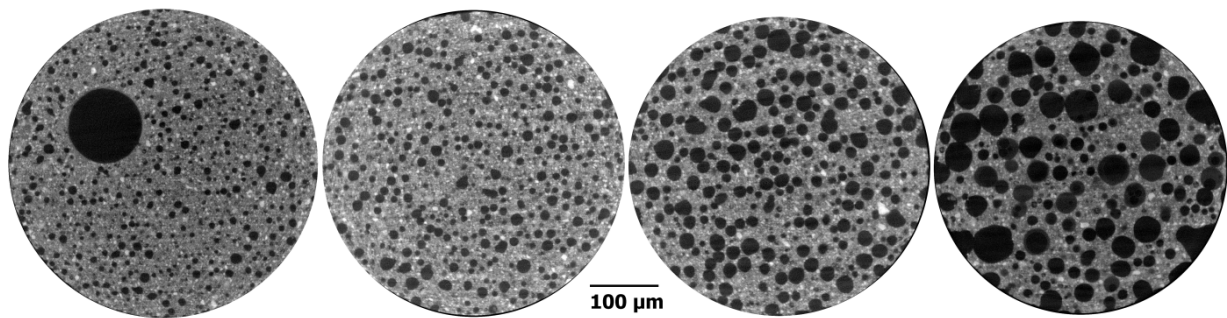


Figure 15: 2-D slices of reconstructed 3.9 μm resolution CT scans taken of the 0.6 cm diameter sub-samples of FCR2 with a foam quality of 10%, 20%, 30%, and 40%, from left to right.

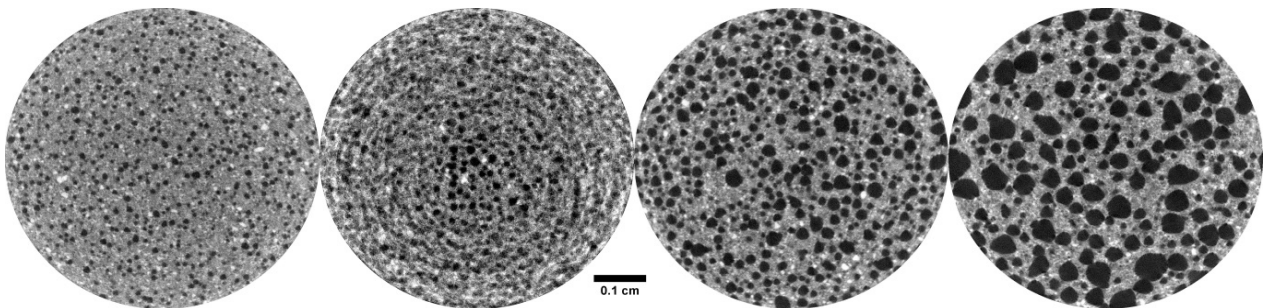


Table 4: Measured properties of the cement samples.

	Neat	10% FCR1	20% FCR1	30% FCR1	40% FCR1	10% FCR2	20% FCR2	30% FCR2	40% FCR2
Permeability (mD)	0.3 ±0.0	0.1 ±0.0	0.3 ±0.1	1.7 ±0.7	40.8 ±18.9	0.2 ±0.0	1.8 ±0.2	5.3 ±0.2	18.9 ±3.4
Porosity	27.6	38.8	44.4	53.8	63.1	40.3	45.1	51.4	58.9
Compressive Strength (psi)	4850	4303	3459	2211	1284	4405	3607	2717	1617
Compressive Strength (MPa)	33.4	29.6	23.8	15.2	8.8	30.3	24.8	18.7	11.1
Young's Modulus (psi)	804636	748178	585961	436483	310089	520178	463178	432482	431482
Young's Modulus (MPa)	5547.7	5158.5	4040	3009.4	2137.9	3586.5	3193.5	2981.8	2974.9
Poisson's Ratio	0.11	0.125	0.101	0.108	0.106	0.11	0.106	0.108	0.107

Permeability and porosity increased with foam quality. The permeability values of the 10% and 20% foamed cement systems were well within range of neat cement (FCR1-10% $K = 0.1$ mD, FCR1-20% $K = 0.3$ mD; FCR2-10% $K = 0.2$ mD, FCR2-20% $K = 1.8$ mD) (Figure 16). However, the permeability increased dramatically for the 40% foam quality in both systems (FCR1-40% $K = 40.8 \pm 18.9$ mD; FCR2-40% $K = 18.9 \pm 3.4$ mD). In addition to having a significantly higher permeability, measurements of FCR1-40% were extremely variable. This could likely be because FCR2 was mixed using a stabilizer whereas FCR1 was not. Plots of the porosity measurements show a steady increase corresponding with increasing foam quality (Figure 17). Plots of permeability versus porosity exhibited a nonlinear, exponential increase (Figure 18).

Figure 16: Permeability measurements of foamed cement system 1(a.) and 2 (b.) (FCR1 and FCR2) showing the dramatic increase in permeability above foam quality of 30%. Error bars represent standard deviation.

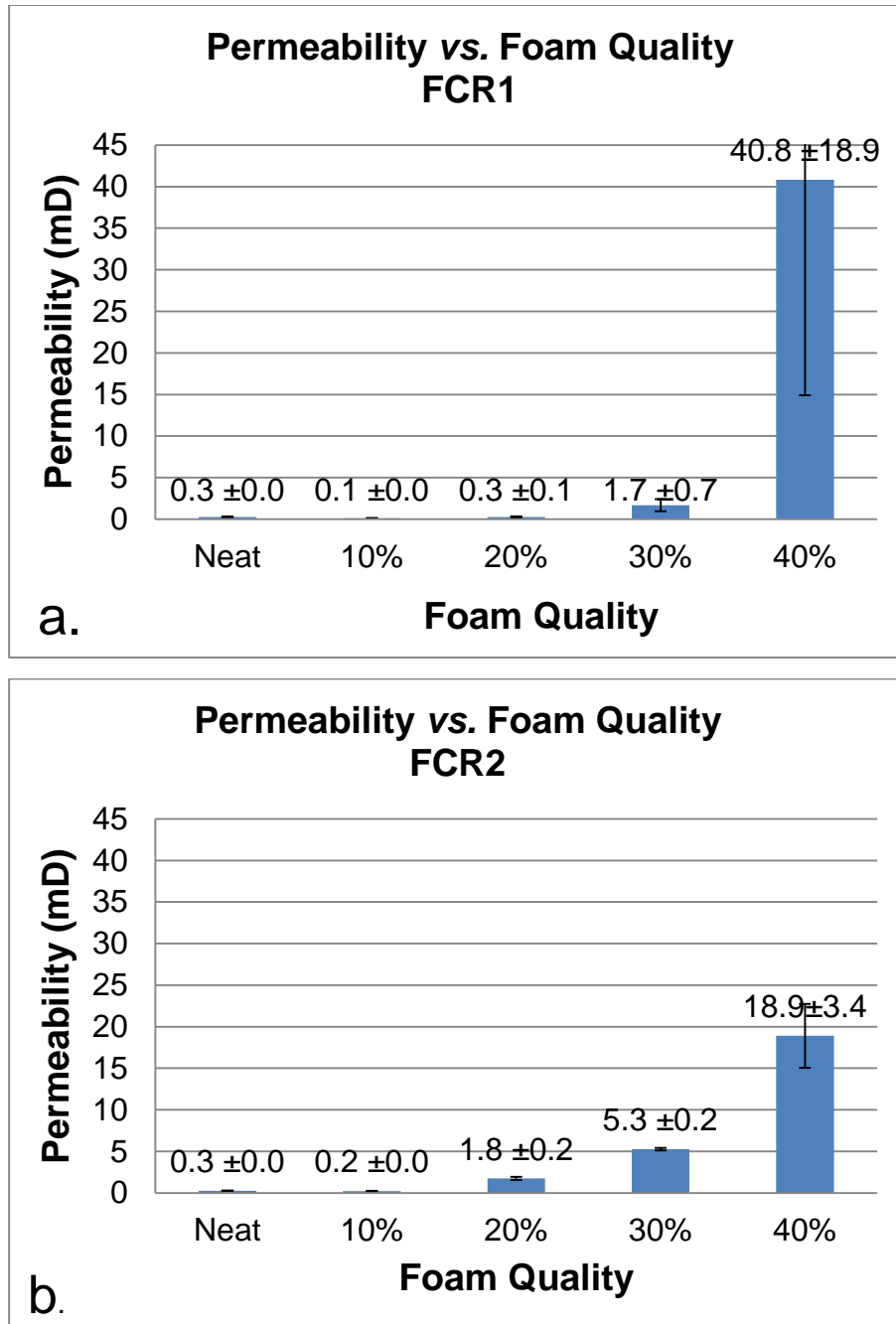


Figure 17: Porosity measurements of foamed cement system 1(a.) and 2(b.): (FCR1 and FCR2)

showing a steady increase as foam quality increases.

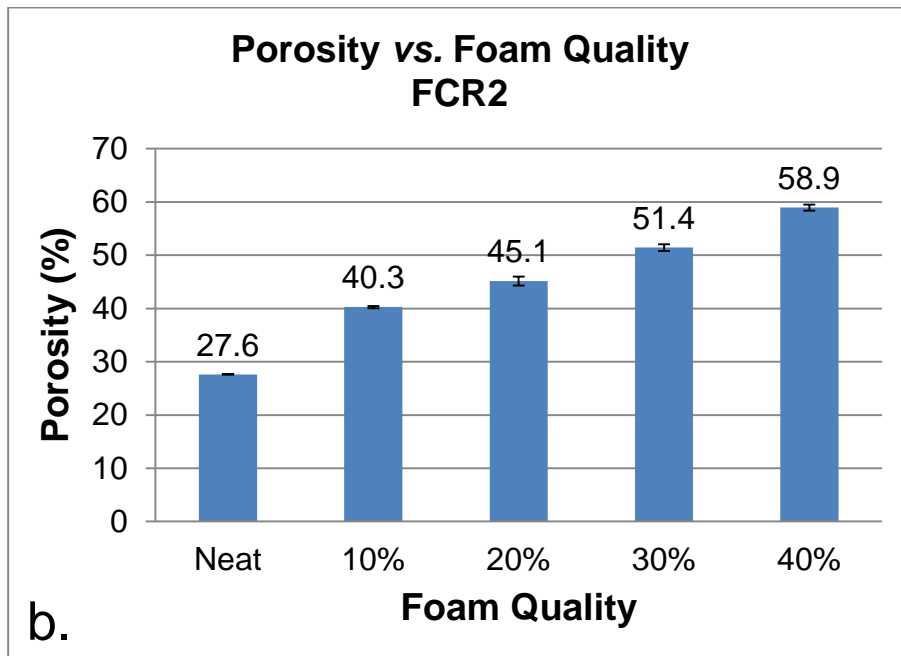
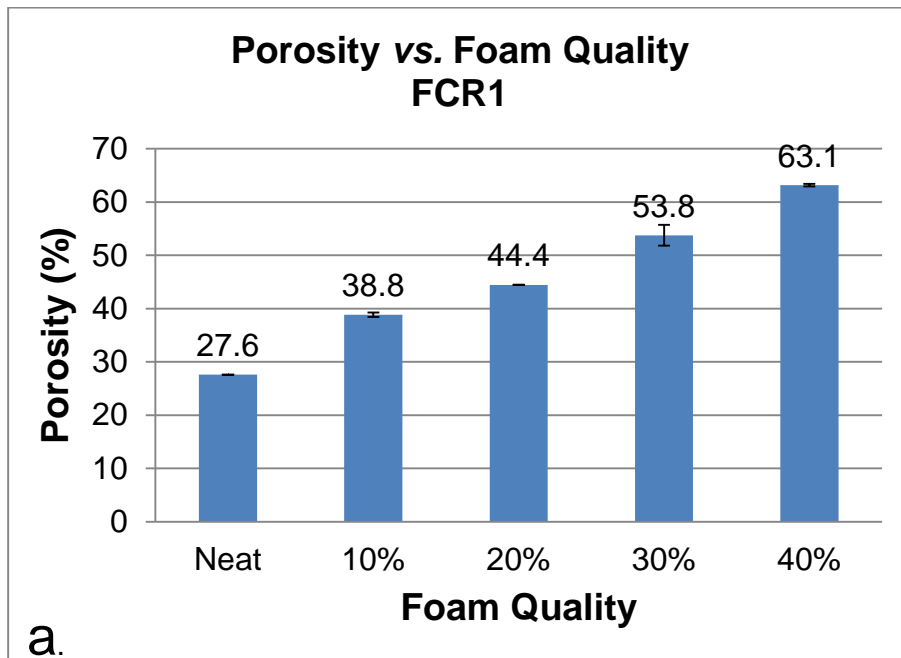
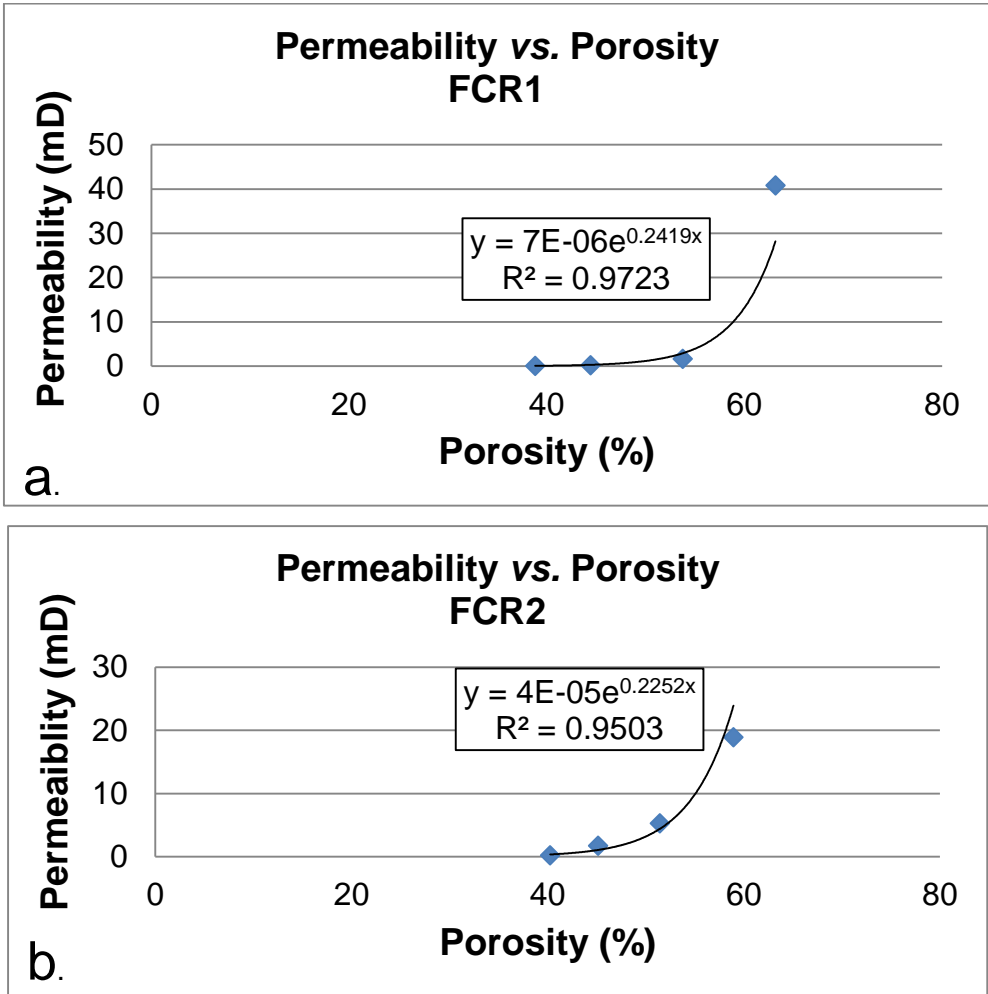


Figure 18: Plots of permeability versus porosity measurements of foamed cement system 1(a.) and 2(b.): (FCR1 and FCR2).



2.4.5 Mechanical Properties

Mechanical properties for the neat cement and all 8 foamed cements are shown in Table 3. Strength is observed to decrease with increasing foam quality. Class H neat cement had an average compressive strength of 4850 psi (33.4 MPa). The compressive strength values for the foamed cements were successively lower and appear to follow a linear relationship. There is a significant

difference in strength from the neat (4850 psi) to the 40% FCR1 (1284 psi) (33.4 MPa and 8.8 MPa respectively). The 40% FCR1 decreases from the neat by approximately 73%. The decrease in strength between the neat and the 40% FCR2 (1617 psi) (11.1 MPa) is similar, decreasing by approximately 66%. However, the difference between the neat cement and the 10% FCR1 and FCR2 is only ~11% and ~9% respectively. Increasing the foam quality to 20% decreases the strength by ~29% - 26% from the neat cement.

Young's modulus followed a similar trend and also appears to decrease in a linear fashion (Figure 20). Young's modulus decreases by approximately 61% from the neat cement (8.05×10^5 psi) (5550 MPa) to the 40% FCR1 (3.1×10^5 psi) (2137 MPa)(Figure 20a). The FCR2 decreased in value by ~46% from the neat to the 40% foam quality (Figure 20b). While the decrease from the neat to the 40% foam quality was less for the FCR2 cement mix, it was greater when the difference was measured from the neat to the 10% foam quality. The decrease in Young's modulus from the neat cement to the 10% FCR1 was ~7% whereas the decrease to the 10% FCR2 foamed cement mix was ~35%.

Poisson's ratio is consistent for all foam qualities and is similar to that of the neat cement (Figure 21). Poisson's ratio consistently stayed in the 0.11 – 0.12 range across the range of cement mixes. Stress-strain diagrams of the foamed cement mechanical tests are provided in Appendix A.

Figure 19: Compressive Strength as a function of foam quality

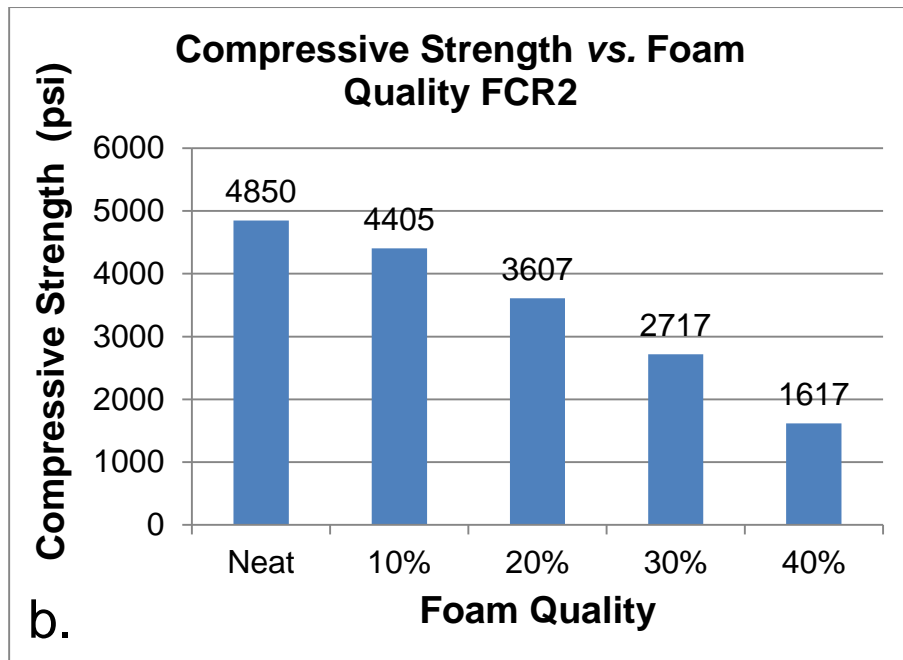
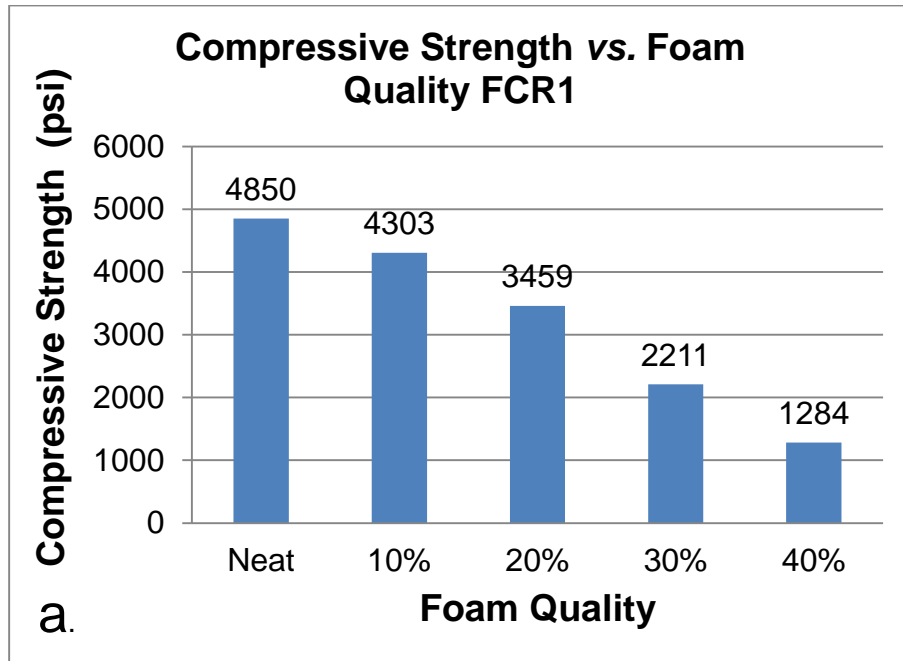


Figure 20: Young's Modulus as a function of foam quality.

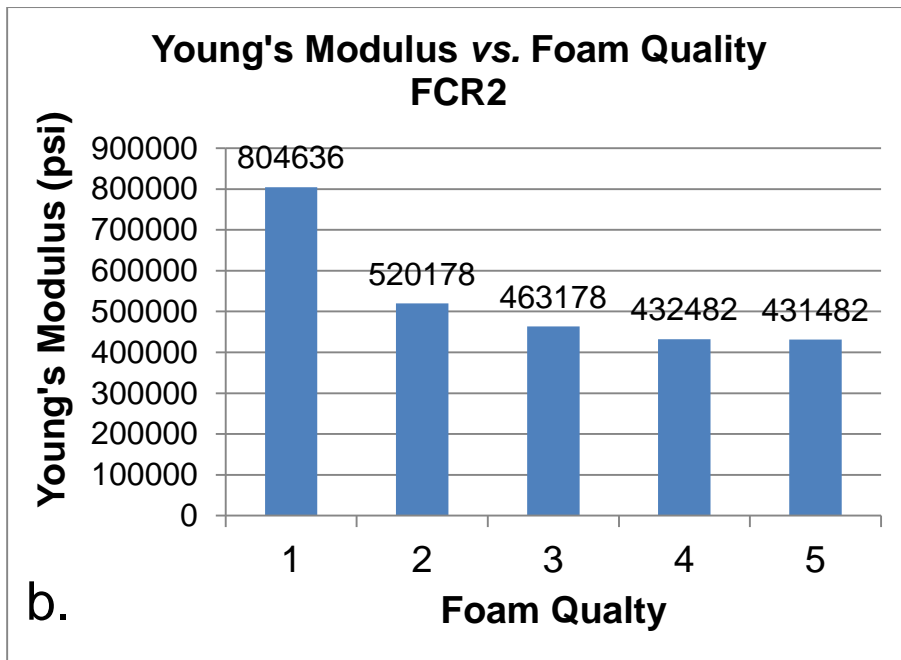
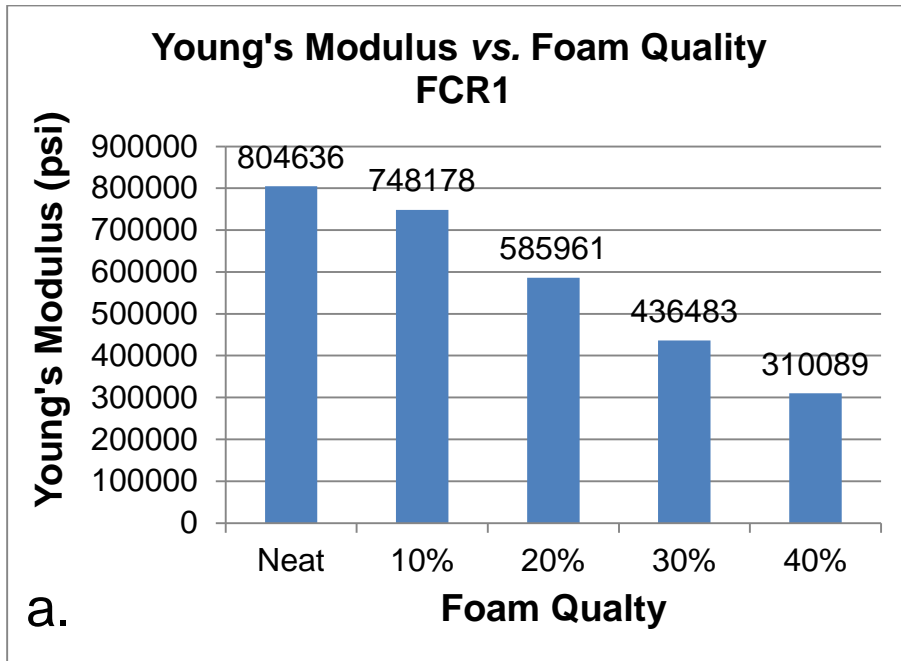
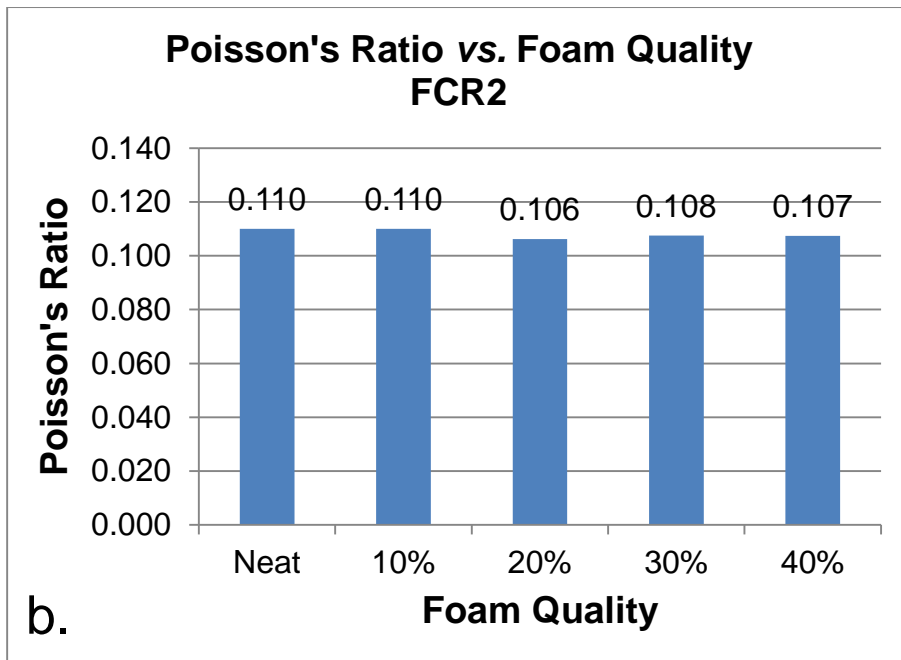
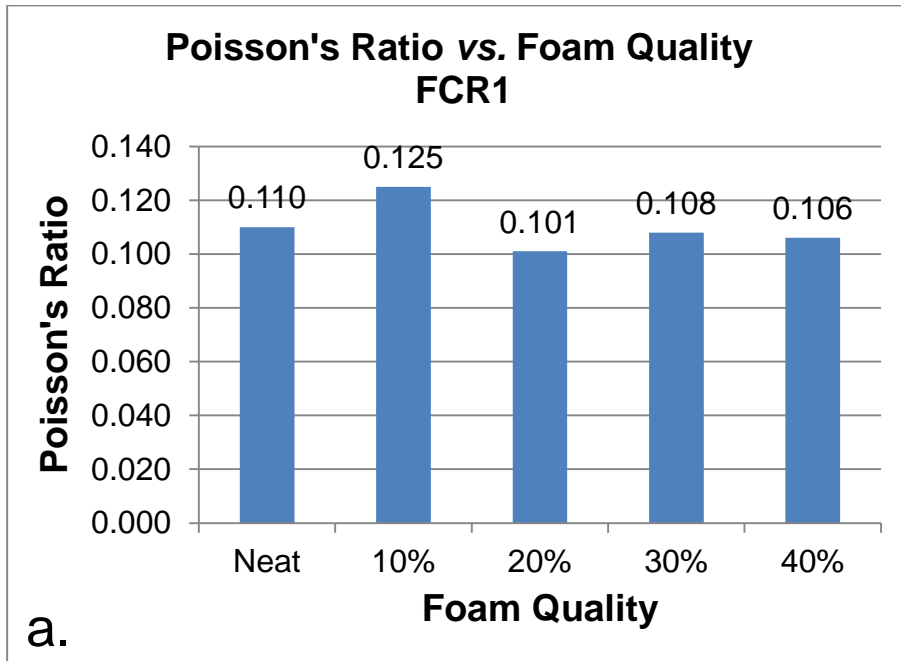


Figure 21: Poisson's Ratio as a function of foam quality.



2.4.6 Strength Permeability and Porosity Relationship

Compressive strength appears to have a logarithmic correlation with permeability (Figure 22). The value for the 40% foam quality mix is an apparent outlier with an average compressive strength around 1284 psi (8.8 MPa) (Figure 22a). This outlier likely represents the lack of stability of the cement at a 40% foam quality. Strength dropped with increasing porosity – given the correlation between porosity and foam quality, this is expected (Figure 23). Both foamed cement mixes exhibited a linear relationship between compressive strength and porosity. The linear relationship of FCR2 with respect to these parameters is remarkably good with a correlation coefficient of .999 (Figure 22).

Figure 22: Compressive strength as a function of permeability.

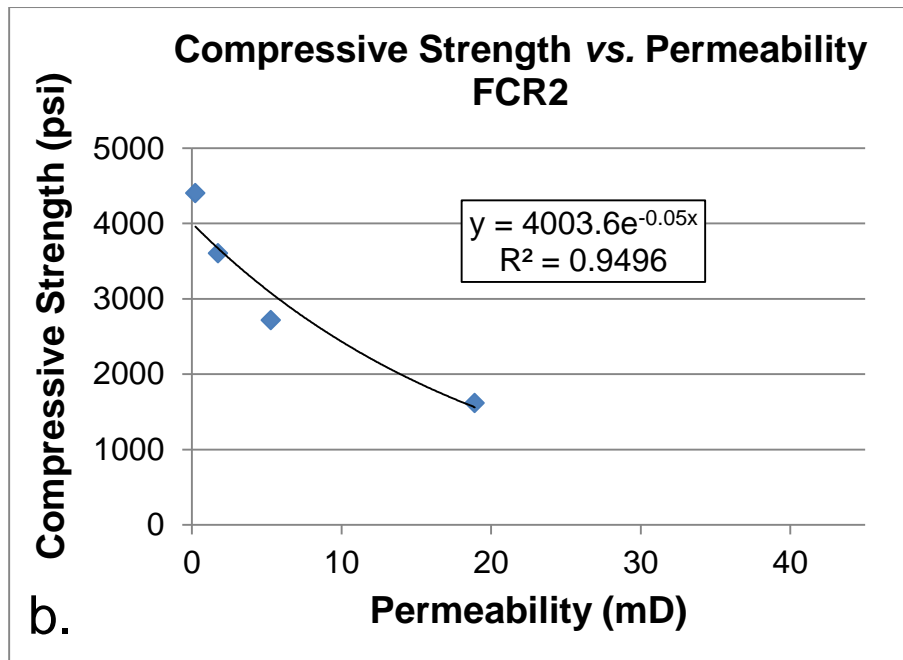
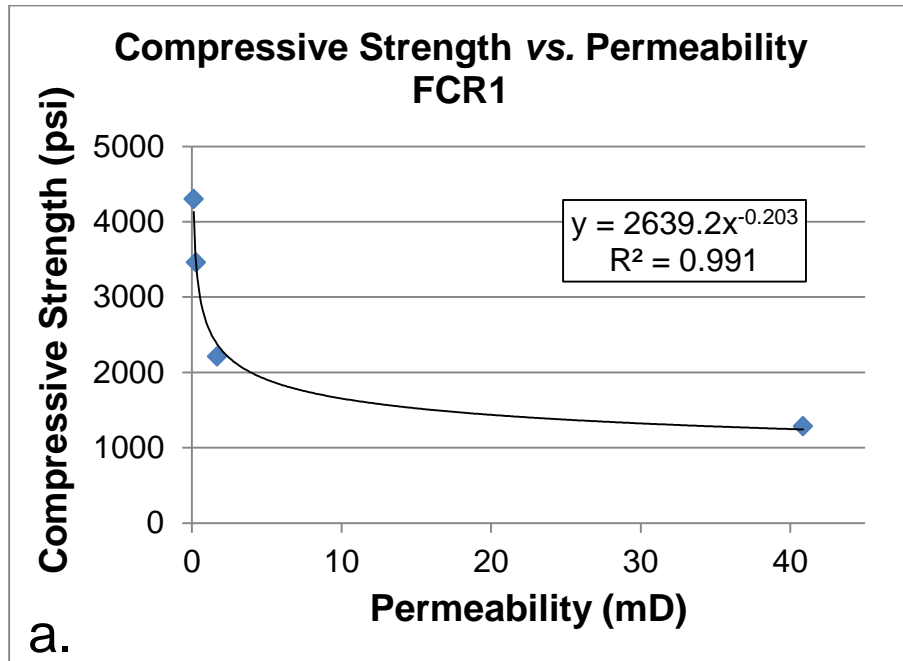
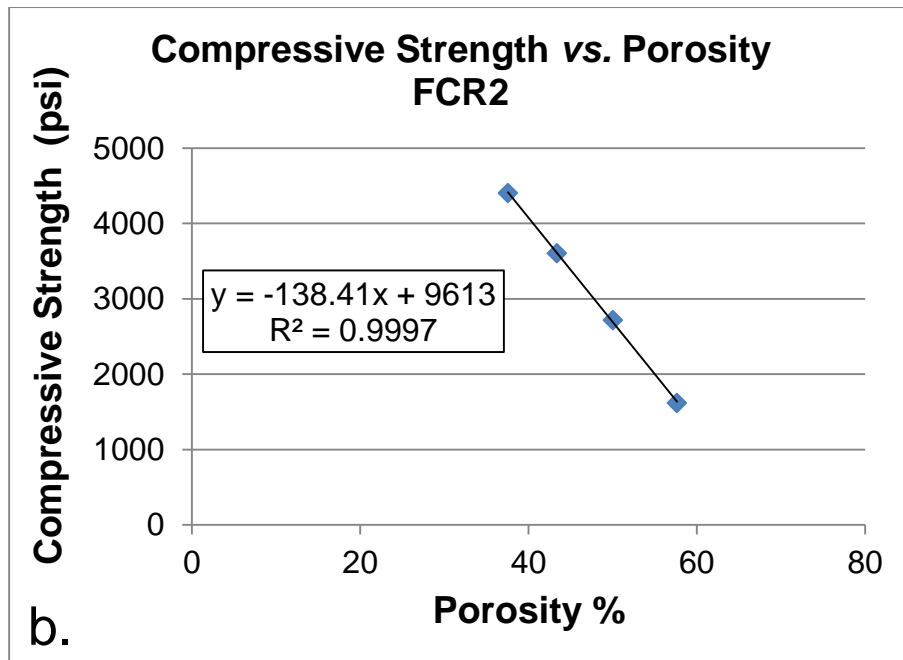
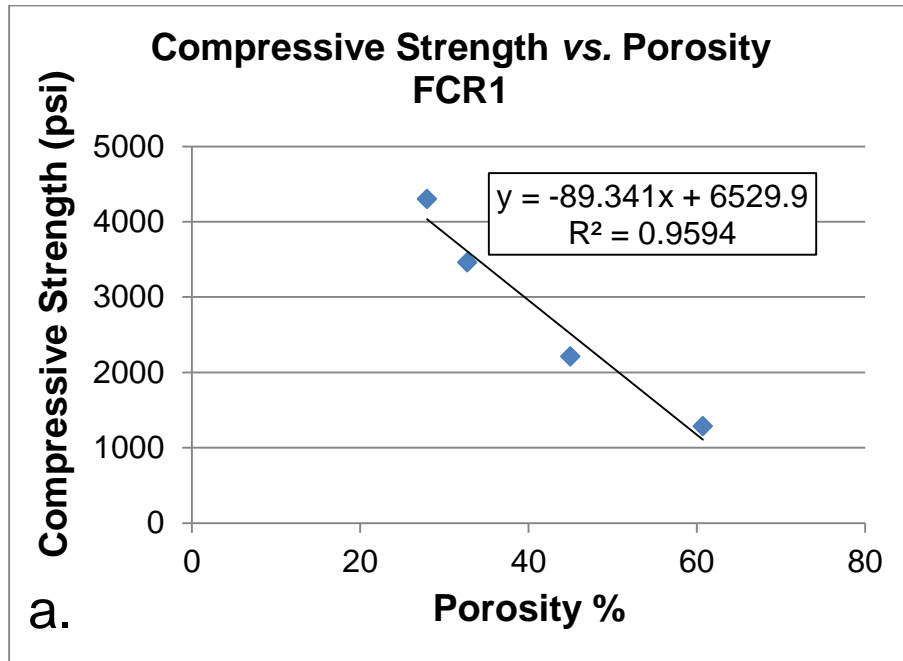


Figure 23: Compressive strength as a function of porosity.



2.4.7 Modulus of elasticity (Young's Modulus vs. Porosity, and Permeability)

The relationship between Young's modulus and porosity appears to be in the form of a power law (Figure 24). Young's modulus appears to have a logarithmic correlation with permeability (Figure 25). The outliers at 40% likely represent the lack of stability of the 40% foam quality.

Figure 24: Young's modulus as a function of porosity.

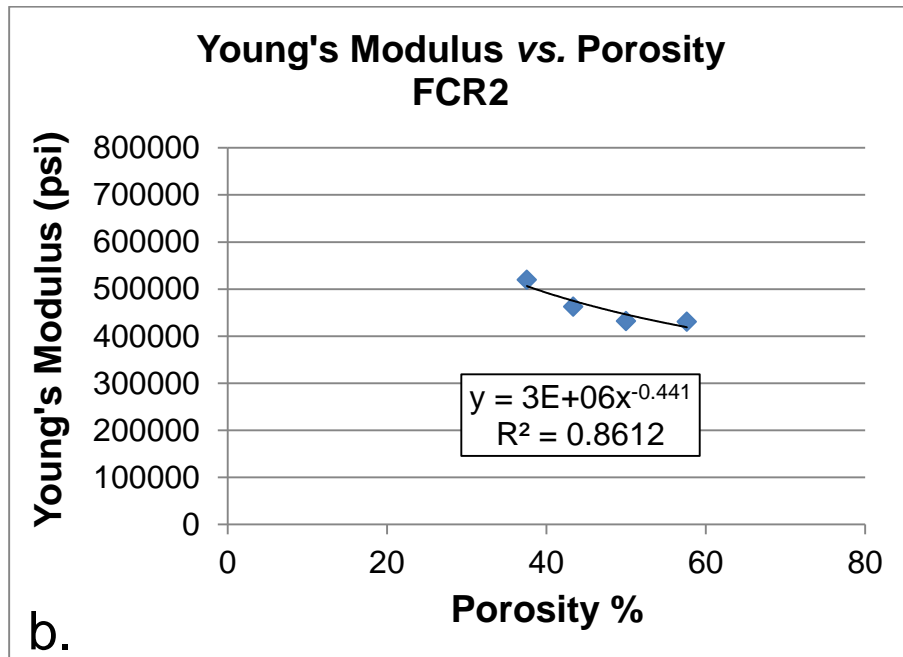
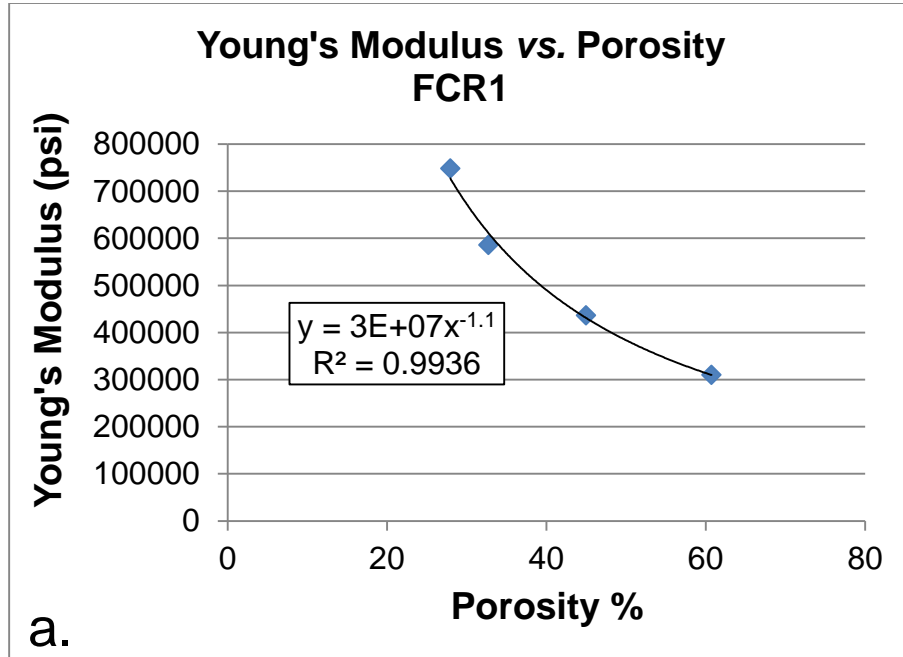
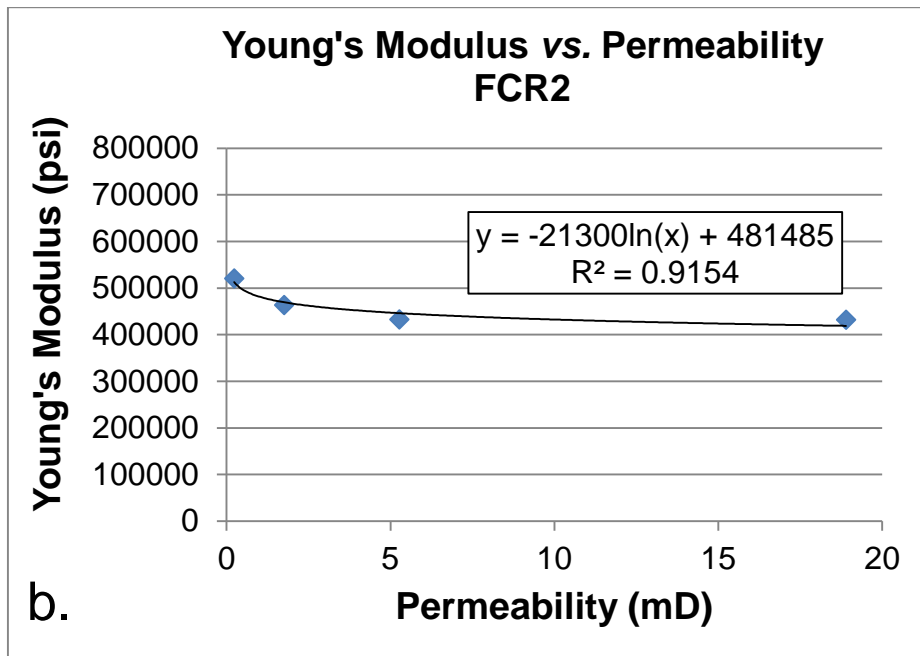
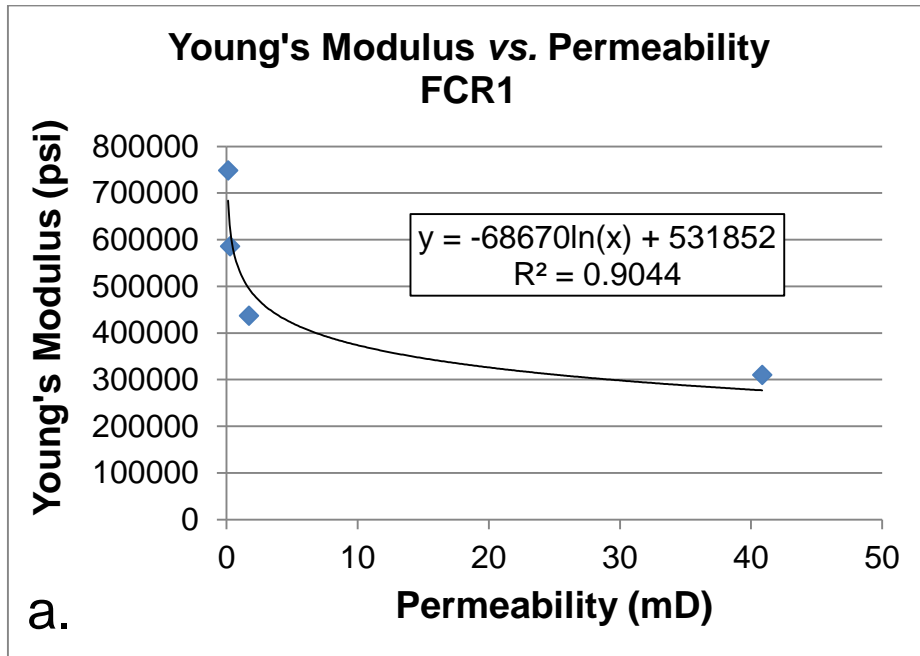


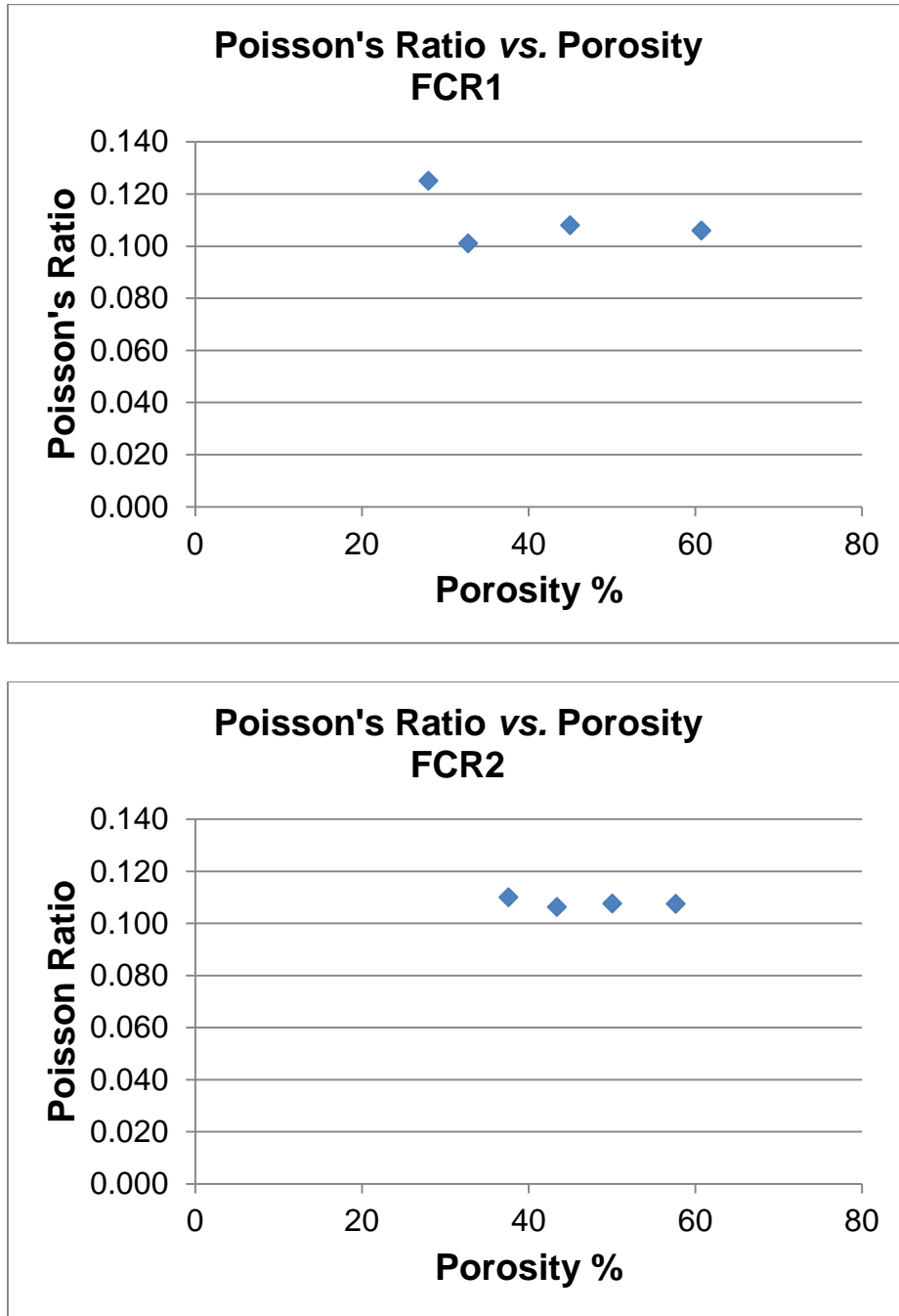
Figure 25: Young's modulus as a function of permeability.



2.4.8 Poisson's Ratio vs. Porosity, Permeability

The influence of porosity on Poisson ratio appears inconclusive (Figure 26).

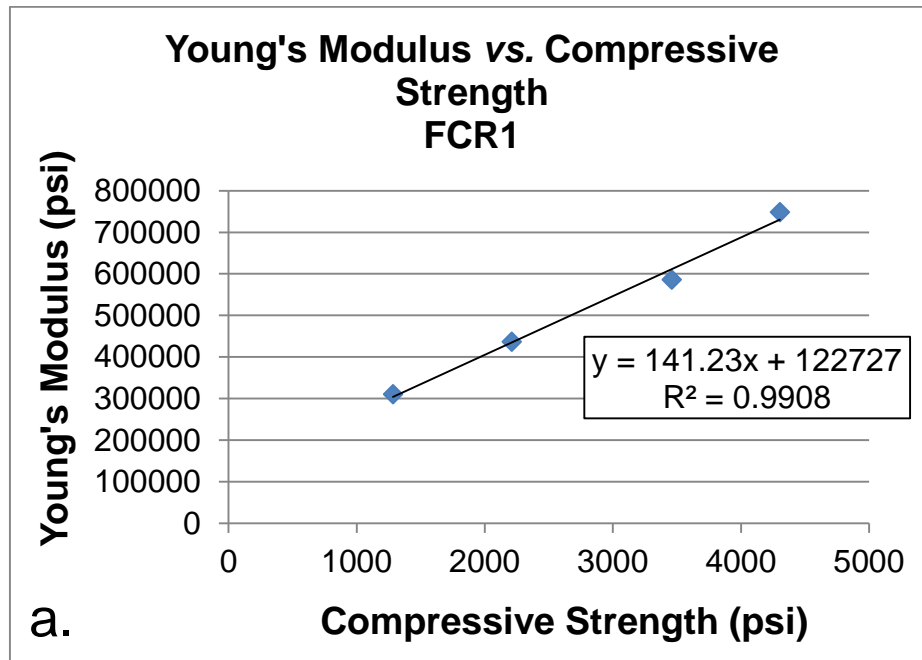
Figure 26: Poisson's ratio as a function of porosity.

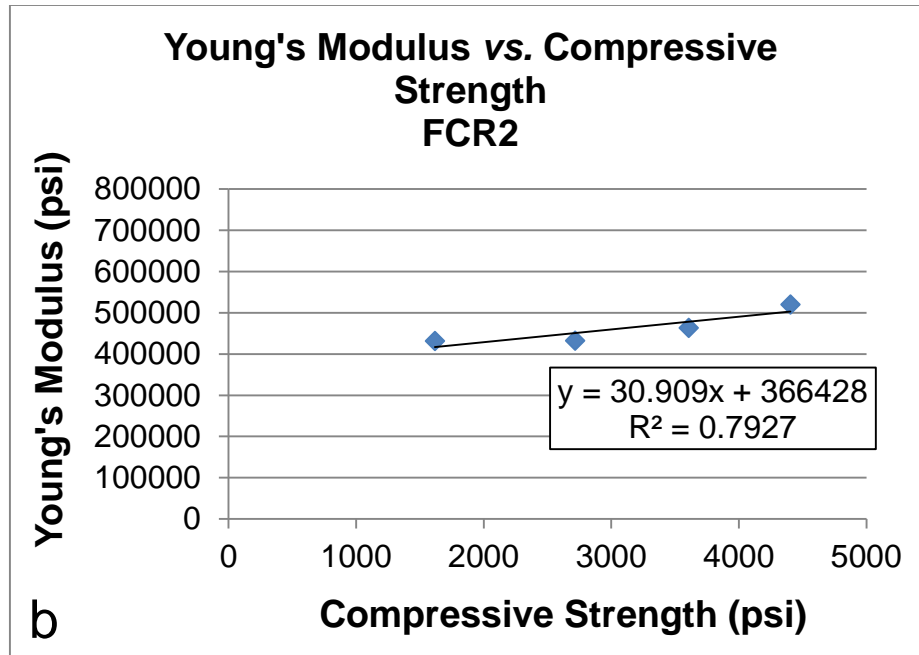


2.4.9 Young's Modulus vs. Compressive strength relation

With FCR1, the impact on compressive strength is shown as a linear relationship (Figure 27a). However, the correlations for FCR2 are not as clear (Figure 27b). This may be due to the different chemicals added to this “recipe” that change the behavior of the cement.

Figure 27: Young's modulus as a function of compressive strength.





2.5 DISCUSSION

The increase in porosity with foam quality is as expected per the definition of foam quality. Permeability of 10% and 20% FCR1 foam quality practically does not appreciably change compared to the neat cement permeability. This may be a good indication that bubbles formed have rather small size and that little to no coalescence takes place; therefore the permeability is still determined mostly by the matrix (as for the neat cement). Some minor change in permeability could be caused by the fact that foaming agent may somewhat alter the forming cement matrix. Starting from 30% FCR1, permeability appreciably increases (more than three times) compared to 10% and 20% FCR1 foam quality. This likely indicates the beginning of bubble coalescing. Finally, for 40% FCR1 foam quality, the change in permeability increases by more than an order of magnitude. This may mean that coalesced bubbles predominantly determine permeability. It is important to know that typically, in a well, a foam quality of 15 – 25% is desired because of difficulties in providing zonal isolation for foams of higher qualities.

FCR2 measurements show a different behavior compared to FCR1. In particular, appreciable permeability growth starts already for 20% FCR2 foam quality (about 4 times higher compared to neat cement). The 30% FCR2 foam quality continues the same trend and exceeds permeability of neat cement by about an order of magnitude. Difference in permeability between FCR1 and FCR2 of the same quality gives birth to the hypothesis about different bubble size distribution (BSD). This is because the only difference between the 20% FCR1 and 20% FCR2 is the addition of a stabilizer.

The primary goal of foaming is to decrease the density of cement, while leaving the permeability unchanged. From this perspective, 10% and to some extent 20% foam cements fit the goal. Plots of permeability versus porosity exhibited a nonlinear, exponential increase showing the rapid decline in stability beyond the 30% foam quality (Figure 18a. &b.). However, measurements of the cements cured under pressure may give dramatically different results. Therefore, the above conclusions should be considered only as a base line for future investigations. Given the significant impact of hydration temperature on permeability (Figure 7) these permeability measurements might be considered to be higher than they would be in a wellbore environment.

The results of the geometry tests demonstrate that valid compressive strength data can be obtained with cement geometries as small as 1/2-inch diameter rods. This is significant because smaller samples are often more convenient to use in reactor studies than the standard ASTM 2-inch cubes.

The addition of air (as a light-weight additive) resulted in lower Young's modulus and compressive strength (with increasing foam quality). The lower Young's moduli values are consistent with more ductile cement as seen in Iverson et al. (2008). The consistency of the Poisson's ratio values attest to the uniformity of foamed cement to systematic deformation.

The most significant finding is an observed upper/lower limit to foam quality that is guided by the mechanical/physical properties. The foam quality should not be too low because it will not exhibit the mechanical benefits as shown by the Young's modulus values. The foam quality also shouldn't be too high as it still needs to provide zonal isolation. The cutoff for these values is determined by the specific needs of the wellbore and the environment in which the cement is placed.

Given the success of the atmospheric-generated foamed cement work, the next step is to apply this methodology to field-generated and pressure-generated foamed cements. A correlation

between atmospheric-, field-, and pressure-generated foamed cement systems is desired to improve an understanding of the physical properties of foamed cement under wellbore conditions. This correlation will aid in a better understanding of the effects that foam cement production, transport downhole, and delivery to the wellbore annulus have on the overall sealing process. Ultimately, this research will provide researchers, regulators, and industry the knowledge to ensure the safe operation and integrity of wells in which foamed cements are used.

3. AN ASSESSMENT OF THE DYNAMIC MODULUS OF ATMOSPHERICALLY GENERATED FOAM CEMENTS²

3.1 INTRODUCTION AND LITERATURE REVIEW

The objective of this chapter is to evaluate the dynamic moduli of atmospheric generated foamed cements at varying foam qualities routinely used for zonal isolation during well construction. Mechanical properties of the hardened foamed cement samples, such as Young's modulus (YM) and Poisson's ratio (PR) were obtained as a function of cyclic confining pressure ranging from 12 - 52 MPa (1,740 – 7,540-psi). The dynamic parameters were derived from ultrasonic velocity measurements, while permeability was measured using the transient method. Stepwise loading and unloading schedules were conducted to test the permeability and mechanical properties of the foamed cement at simulated wellbore conditions. Applied pressures varied between 6.5 MPa (943 psi) to 46.5 MPa (6,744 psi) in 4 MPa (580 psi) increments in two full up/down cycles. At every increment during these cycles, ultrasonic compressional (P) fast shear (S1), and slow shear (S2) wave velocities were measured, as well as the samples' response to the upstream sine pressure wave approximately 0.5 MPa in amplitude. From the sonic velocity data the dynamic moduli including YM and PR were calculated, while the sample's response to the pressure wave was used for permeability calculations. Multiple observations of both neat and foamed samples reveal variations in YM as well as changes in the other properties and characteristics. Differences were observed between the foam qualities, depending on the parameter being assessed. This information

² Published as OTC-25776-MS

should enable design contingencies and allow for more resilient designs of foamed cements when used during well construction. In addition, industry can use these results as a baseline for comparison with previous, current, or future work including recently acquired field-generated foamed cement samples (Kutchko et al., 2014).

Foamed cement is obtained in the process of curing a gas-liquid dispersion that is created when a gas is stabilized as microscopic bubbles within cement slurry (Harms and Febus, 1985; Nelson and Guillot, 2006). Foamed cements are typically low-density cement systems used in formations that are not able to support the annular hydrostatic pressure of conventional cement slurries (Harlan et al., 2001; Nelson and Guillot, 2006). The use of foamed cement for its lightweight density has been well documented (Harms and Febus, 1985; Kopp et al., 2000; Harlan et al., 2001; Bengue and Poole, 2005). Other applications of foamed cement expanded into regions with high-stress environments, for example, isolating problem formations typical in the Gulf of Mexico (Benge et al., 1996).

There is a common belief that conventional cements withstand cement sheath fracturing because of their higher compressive strengths and that the lower compressive strength of foamed cement is a cause for concern. However, the lower compressive strength of foamed cements does not increase the risk for inducing fractures and it is able to withstand greater wellbore stresses than conventional cements (Harlan et al., 2001). The entrained gas phase in the cement creates a foamed network within the cement's matrix. This foamed network exhibits a more elastic response, indicating that foamed cements have a lower YM than conventional cements (Iverson et al., 2008). This is significant because cement with a lower YM is more resistant to the mechanical strain typically associated with well operations (Kopp et al., 2000). In comparison to conventional cement, foamed cement is ductile and has the tendency to flex when the casing is pressurized

(Kopp et al., 2000). As a result, foamed cement has a unique resistance to temperature and pressure-induced stresses as well as long-term zonal isolation capabilities through resistance to in-situ stresses affecting the cement-sheath integrity (Benge et al., 1996).

Previous work (Goodwin and Crook, 1992) evaluated the performance of cement sheath systems under varying pressure and temperature environments. The study showed that cement sheaths that exhibit a high YM are more susceptible to damage caused by pressure and/or temperature changes or cycles over time. This work also showed that the materials with a higher compressive strength provided better casing support but lost the ability to provide zonal isolation at lower internal pressures (Goodwin and Crook, 1992).

This experimental work was then complemented with mathematical modeling leading to studies on the effect of different stresses on cement sheath integrity. One study involved analytical procedures to study the effect of cement sheath mechanical properties, and their relationship with varying pressure loads, temperatures, and rock formation properties (Thiercelin et al., 1998). Another study simulated the mechanical responses of a cement sheath based on a finite element numerical analysis. This study modeled plastic deformation, de-bonding, and cracking for cement sheath failure modes while incorporating the effect of cement sheath shrinkage/expansion that takes place in the wellbore (Bosma et al., 1999).

There is a need for more comprehensive research regarding the mechanical properties of set cement in the oil and gas industry. Previous work (Ravi et al., 2007) included multiple experiments on three types of foamed slurries to determine the various mechanical properties. This work concluded that compressive strength is not enough to determine a foamed cement's ability to provide zonal isolation. More importantly, it was determined that no one parameter (compressive

strength, YM, PR, etc.) can explain the behavior of any of the varying cement sheaths under cyclic loading and unloading (Ravi et al., 2007). Another study (Iverson et al., 2008) involved unconfined and confined pressure testing on cement slurries of different compositions. The findings indicated that neat cements tended to be less elastic than cements with performance improving additives (i.e. gas to create foamed cements). One interesting result of this study was that the addition of performance additives (i.e. gas, foaming agents, and elastomers) lowered YM and overall strength capabilities (Iverson et al., 2008) but enabled a more resilient design suitable for long-term zonal isolation.

In this chapter I report on dynamic moduli experiments conducted to address the mechanical response of set (hardened) foam cements under various wellbore pressure conditions utilizing the NER AutoLab 1500 at the United States Department of Energy – National Energy Technology Laboratory (NETL) in Pittsburgh, Pennsylvania. These results represent the mechanical properties of atmospherically generated foamed cement typically used in deep offshore wells in the Gulf of Mexico. Permeability, P-wave, and S-wave velocities were measured across a range of applied pressures on various foam qualities to determine the mechanical properties of these foam cement designs. Using API Class H cement as a base, industry-standard foaming agents were incorporated to create three foam qualities (10%, 20%, 30). Although a typical cement foam quality in a deep-water well is typically somewhere around 15%-25%, this study attempts to observe any significant differences across a slightly wider range.

This study should help provide researchers with a more in-depth understanding of the mechanical properties of atmospherically generated foam cement during cyclic loading and unloading. With the results presented here, we now have a foundation for future foam cement

research, particularly with foam cements generated under wellbore pressures (Kutchko et al. 2014). Our work will also provide a baseline for future predictive modeling of foamed cements in actual wellbore conditions.

3.2 MATERIALS AND METHODS

3.2.1 Cement Slurry and Sample Preparation

Neat API Class H- Portland cement samples were mixed according to industry recommended practice API-RP-10B2 (API, 2004) at a slurry density of 16.5 lbm/gal (1.97 g/cm³) and a water to cement mass ratio (W/C) of 38% (0.38). The Class H cement was used in this study as it is more commonly used for foamed cement applications in the Gulf of Mexico. The cement slurry was then poured into 1-inch inner diameter plastic tube molds, sealed, and allowed to cure for 3 days at atmospheric pressure and temperature. The cement was removed from the molds and cut to roughly 2 inches in length with a wet saw then placed in a Nitrogen desiccator for drying.

3.2.3 Foamed Cements

The foamed cement samples were mixed according to industry recommended practice API RP 10B-4. The same base design described above was used to generate all of the foamed cement samples. Two different industry standard foaming agents (Provided by industry collaborators) were used to generate foam cements: Foamed Cement Recipe 1 (FCR1) which required the addition of a foaming agent only and Foamed Cement Recipe 2 (FCR2) which included the

addition of a different foaming agent and stabilizer. Every recipe was added and mixed with three different foam qualities (10%, 20%, and 30%), providing in total, six different types of foam cement. Once mixed, the slurries were poured into 945 ml containers and allowed to cure for 3 days under atmospheric conditions. One-inch diameter cement cores were sub sectioned using a Powermatic variable speed wet drill fitted with a 1-in diamond-tipped core drill bit. The cored samples were then cut to a length of approximately 2 inches and the ends of the samples cleaned using a wet saw. For consistency, the samples were labeled, weighed, and put in a desiccator to dry.

3.2.4 Ultrasonic-Waveforms, Velocity and Permeability Measurements

All velocity and permeability measurements were made using an AutoLab 1500 device (New England Research, Inc.) located at NETL. This device is capable of creating a wide range of both lithostatic (confining) pressures and pore pressures inside the sample in order to simulate realistic underground conditions in the process of measurements. The AutoLab 1500 also has an ultrasonic system which generates ultrasonic pressure and shear pulses (P and S waves) at one end of the core and records the response at the other end.

YM and PR values are determined from shear and compressional wave velocities using Equation 8 and Equation 9 where E = Young's Modulus, ρ = Bulk density, V_s = Shear wave velocity, V_p = Compression wave velocity, ν = Poisson's Ratio (Murayama, Kobayashi, and Jen, 2013).

Equation 8: Dynamic Young's Modulus

$$E = \frac{\rho V_s^2 (3V_p^2 - 4V_s^2)}{V_p^2 - V_s^2}$$

Equation 9: Dynamic Poisson's Ratio

$$\nu = \frac{1 - 2(V_S/V_P)^2}{2[1 - (V_S/V_P)^2]}$$

Additionally, shear modulus (μ), bulk modulus (K), and the first Lamé' parameter (λ) were calculated using equations (10-12) below (De Beer and Maina, 2008). The averages from these calculations and their standard deviations can be found in Table 5.

Equation 10: Dynamic Shear Modulus

$$\mu = \rho V_S^2$$

Equation 11: Dynamic Bulk Modulus

$$K = \rho \left(V_P^2 - \frac{4}{3} V_S^2 \right)$$

Equation 12: Lamé' First Parameter

$$\lambda = K - \frac{2}{3} \mu$$

Table 5: Dynamic Moduli calculated from equations 10-12

Sample	Shear modulus (μ)						Bulk Mod (K) (GPa)						Lamé' First Parameter (λ)					
	μ initial	Std. Dev.	μ end first cycle	Std. Dev.	μ end second cycle	Std. Dev.	K initial	Std. Dev.	K end first cycle	Std. Dev.	K end second cycle	Std. Dev.	λ initial	Std. Dev.	λ end first cycle	Std. Dev.	λ end second cycle	Std. Dev.
H-Class Neat	4.701	0.798	4.661	0.800	4.640	0.804	5.881	1.010	5.746	1.006	5.694	1.027	2.747	0.479	2.639	0.477	2.601	0.496
FCR1-10%	4.111	0.305	4.052	0.295	4.031	0.299	5.056	0.061	4.836	0.080	4.772	0.129	2.315	0.237	2.135	0.258	2.085	0.322
FCR2-10%	3.985	0.076	3.929	0.084	-----	-----	4.783	0.462	4.960	0.644	-----	-----	2.126	0.351	2.340	0.505	-----	-----
FCR1-20%	3.364	0.036	3.338	0.010	3.324	0.010	4.561	0.064	4.483	0.042	4.420	0.017	2.318	0.040	2.257	0.044	2.204	0.011
FCR2-20%	3.045	0.127	3.134	0.334	3.212	0.475	3.813	0.264	3.934	0.106	4.003	0.314	1.783	0.348	1.845	0.158	1.862	0.031
FCR1-30%	2.260	0.045	2.198	0.015	2.245	0.064	3.089	0.036	2.986	0.015	3.013	0.117	1.583	0.006	1.521	0.004	1.517	0.075
FCR2-30%	2.297	0.014	2.357	0.004	2.337	0.003	3.114	0.020	3.209	0.033	3.149	0.038	1.583	0.030	1.638	0.030	1.591	0.035

* All values reported in this table are averages of multiple sample runs on the NER AutoLab 1500
 ** FCR2-10% was only subjected to a single pressure cycle
 *** n=3 for all Cement Categories except for 30% Foam Qualities. For FCR1-30% and FCR2-30% n=2

Permeability values of the samples were calculated by using the transient method. The samples were saturated with argon gas at approximately 5.5 MPa (798 psi). A 6-period, low frequency (<1Hz), low amplitude (about 0.5MPa) sine wave pore pressure pulse was induced to the upstream end of the sample. This periodic upstream pressure variation causes certain temporal pressure response in a fixed volume downstream of the sample. Based on this pressure response, the permeability can be determined. An in-depth description of the transient method can be found in other literature (Siriwardane et al., 2009).

3.3 RESULTS

A total of 19 cement samples of various types were subjected to cyclic pressure variations. Average YM, PR, permeability, and the respective standard deviations for each are presented in Table 6.

Table 6: Young's Modulus, Poisson's ratio, and Permeability recorded by AutoLab 1500

Sample	Young's Modulus (E) (GPa)						Poisson's Ratio (ν)						Permeability (μ D)					
	<i>E</i> initial	Std. Dev.	<i>E</i> end first cycle	Std. Dev.	<i>E</i> end second cycle	Std. Dev.	ν Initial	Std. Dev.	ν end first cycle	Std. Dev.	ν end second cycle	Std. Dev.	Initial Perm	Std. Dev.	Perm end first cycle	Std. Dev.	Perm end second cycle	Std. Dev.
H-Class Neat	11.140	1.894	11.010	1.895	10.950	1.911	0.180	0.002	0.180	0.004	0.180	0.005	670.580	246.190	587.500	208.781	588.790	208.356
FCR1-10%	9.693	0.548	9.490	0.511	9.420	0.483	0.180	0.020	0.173	0.022	0.170	0.026	267.006	47.577	226.702	36.317	220.048	22.756
FCR2-10%	9.347	0.312	9.307	0.380	-----	-----	0.172	0.017	0.184	0.024	-----	-----	337.477	25.295	237.603	16.053	-----	-----
FCR1-20%	8.100	0.093	8.023	0.021	7.973	0.025	0.204	0.001	0.202	0.002	0.199	0.000	452.877	29.641	267.752	18.881	253.808	18.673
FCR2-20%	7.200	0.124	7.420	0.652	7.597	1.009	0.183	0.029	0.186	0.021	0.185	0.017	1777.303	208.427	600.205	273.862	529.839	276.813
FCR1-30%	5.450	0.105	5.295	0.035	5.395	0.165	0.206	0.002	0.205	0.001	0.202	0.002	2213.090	554.680	448.772	70.688	346.884	44.165
FCR2-30%	5.530	0.118	5.680	0.016	5.620	0.016	0.204	0.002	0.205	0.002	0.203	0.002	4618.505	59.061	740.973	67.548	738.542	15.922

* All values reported in this table are averages of multiple sample runs on the NER AutoLab 1500

** FCR2-10% was only subjected to a single pressure cycle

*** n=3 for all Cement Categories except for 30% Foam Qualities. For FCR1-30% and FCR2-30% n=2

3.3.1 Neat Cement

Average initial PR for the neat cement samples was 0.18 at the end of both the first and second pressure cycle. The average YM, however, decreased with each pressure cycle, from an initial value of 11.40 GPa (1.65×10^6 psi) to 11.01 GPa (1.60×10^6 psi) after the first cycle and to 10.95 GPa (1.59×10^6) after the second cycle. Average permeability values varied from an initial value of 670.58 μD (0.671 mD), to a post-first cycle value of 587.50 μD (0.588 mD), but practically did not change after the second pressure cycle, 588.79 μD (0.589 mD) (Table 6).

3.3.2 Foam Quality 10%

The 10% foam quality cements exhibited a higher initial YM than the other foamed cements in the study, but lower than the neat cements. Average initial YM values of FCR1 are 9.69 GPa (1.41×10^6 psi) and the initial FCR2 values average 9.35 GPa (1.36×10^6 psi). On average, after the initial pressure cycle, the YM for FCR1 dropped 0.2 GPa (1.40×10^6 psi), and after the second pressure cycle dropped 0.07 GPa (1.39×10^6 psi). For FCR2, the average YM dropped roughly 0.04 GPa (1.35×10^6 psi) as seen in (Table 6). A second pressure cycle was not run on the FCR2 10% foam quality samples.

Average initial PR values range between 0.18 and 0.17 for both foamed cement systems (FCR1 and FCR2). During both pressure cycles, Poisson ratio values did not change significantly, and were similar to those of neat cement (Table 6).

The starting average permeability value for FCR1 was 267.01 μD (0.267 mD). After the first pressure cycle, the value decreased to 226.70 μD (0.227 mD). By the end of the second pressure cycle, the permeability value had decreased even further to 220.05 μD (0.220 mD). The

values for FCR2 were slightly different. Average initial permeability was 337.48 μD (0.337 mD) and decreased to 237.60 μD (0.238 mD) after the first pressure cycle.

3.3.3 Foam Quality 20%

The 20% foam quality cements exhibited a lower initial YM than both the 10% foamed and the neat cements. Average initial YM value of FCR1 is 8.10 GPa (1.17×10^6 psi) and the initial FCR2 average is 7.20 GPa (1.04×10^6 psi). On average, after the initial pressure cycle, the YM for FCR1 decreased 0.08 GPa (1.16×10^6 psi), and after the second pressure cycle it decreased 0.05 GPa (1.15×10^6 psi) as seen in (Table 6). For FCR2, the average YM increased 0.22 GPa (1.08×10^6 psi) after the first pressure cycle, and increased again by 0.18 GPa (1.10×10^6 psi) after the second cycle as seen in (Table 6).

The average initial PR values range between 0.20 for FCR1 and 0.18 for FCR2. During both pressure cycles, FCR1, on average, stayed the same value at 0.20. FCR2 also stayed relatively the same at 0.185 as seen in (Table 6).

The initial average permeability value for FCR1 was 452.88 μD (0.453 mD). After the first pressure cycle, the value decreased to 267.75 μD (0.268 mD). By the end of the second pressure cycle, the permeability value had decreased even further to 253.81 μD (0.254 mD). The initial permeability values for FCR2 varied from FCR1. The average initial permeability was 1777.3 μD (1.77 mD) and decreased to 600.21 μD (0.600 mD) after the first pressure cycle. At the conclusion of the second cycle, the permeability of FCR2 decreased further to 529.84 μD (Table 6).

3.3.4 Foam Quality 30%

The 30% foam quality cements displayed the lowest initial YM of all of the cement systems. FCR1 averaged 5.45 GPa and FCR2 averaged 5.53 GPa. After the first pressure cycle, FCR1 decreased 0.15 GPa, and increased 0.10 GPa after the second cycle. FCR2 had an initial average YM of 5.53 GPa. This value increased by 0.13 GPa after the first cycle and decreased 0.20 GPa at the conclusion of the second cycle (Table 6).

The average initial PR values range between 0.21 for FCR1 and 0.20 for FCR2. During both pressure cycles, FCR1, on average, stayed the same value at 0.20 while FCR2 also stayed roughly the same at ending the test with a PR of 0.20.

The starting average permeability value for FCR1 was 2213.09 μD . After the first pressure cycle, the value decreases to 448.77 μD . By the end of the second pressure cycle, the permeability of FCR1 had decreased even further to 346.88 μD . The values for FCR2 were higher. The average initial permeability for FCR2 was 4618.51 μD and decreased to 740.97 μD after the first pressure cycle. At the conclusion of the second cycle, the permeability for FCR2 averaged 738.54 μD (0.530 mD) as seen in (Table 6).

3.4 DISCUSSION

3.4.1 Permeability

For the permeability measurements, we focused on changes in permeability during loading and unloading, as well as the varying response of permeability to the pressure cycling for respective

foam qualities. Each cement foam quality is observed to have a unique permeability response to pressure cycles. The permeability of the neat cement is generally less sensitive to pressure cycles, whereas the permeability for the 30% foam quality cement undergoes great change during the first loading cycle (Figure 28d). This indicates that most deformation occurs during the first pressure loading. The insignificant change of permeability during the second pressure cycle also indicates an irreversible change to the pore structure in the cement (Figure 28d).

In our experiments we observed that 20% foam quality cements generally have a smaller permeability change during the first loading, but similar full cycle response, with little permeability recovery after initial loading (Figure 28c.). This trend is similar for 10% foam quality and neat cement, indicating that with lower quality, permeability is less sensitive to pressure cycling, and returns closer to initial values (Figure 28a. & 28b.). These permeability trends for each quality are consistent across multiple samples.

Larger permeability values are observed with increasing foam quality, with the exception of the neat cement, which has permeability values higher than the 10% cements for all samples in the study (Table 6). The increased levels of permeability found in the higher quality foamed cements is likely to be a result of more interconnected pore throats that come with the inclusion of more entrained air.

Greater change in permeability after initial loading is observed with increasing foam quality (Figure 28). There is a greater change in 30% foam quality cements compared to the 20% cements and greater in the 20% cements compared to the 10% or neat cements (Figure 29). The permeability decrease is greater during initial loading for the higher foam-quality cements and higher for all cements during initial loading than on subsequent loading (Table 6). After loading

the cements with 52 MPa (7,541 psi) confining pressure and then unloading them, cements with lower foam quality still have lower permeability than cements with higher foam quality.

It should be noted that there exists a significant difference in permeability values between foam cement recipes. On average, as foam quality increases, a larger difference in permeability is observed between recipes. FCR1 is consistently observed to have lower permeability values than FCR2. This phenomenon may be a result of the additives used in the FCR, indicating that the recipes used in cement design can play a large role in the physical properties.

Figure 28: Permeability response as a function of applied pressure.

: 28a. H-class Neat Cement sample #7054. 28b. FCR1-10% sample #7081. 28c. FCR2-20% sample #0109.

28d. FCR2-30% sample #5297

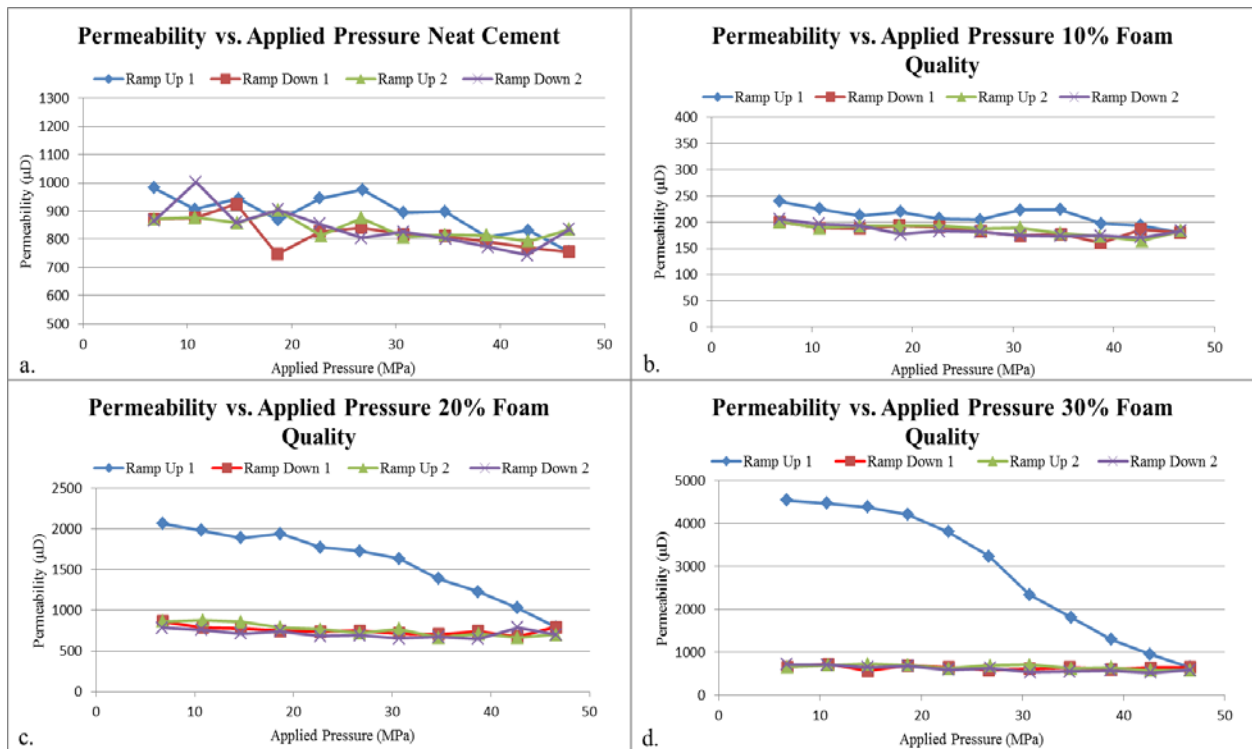
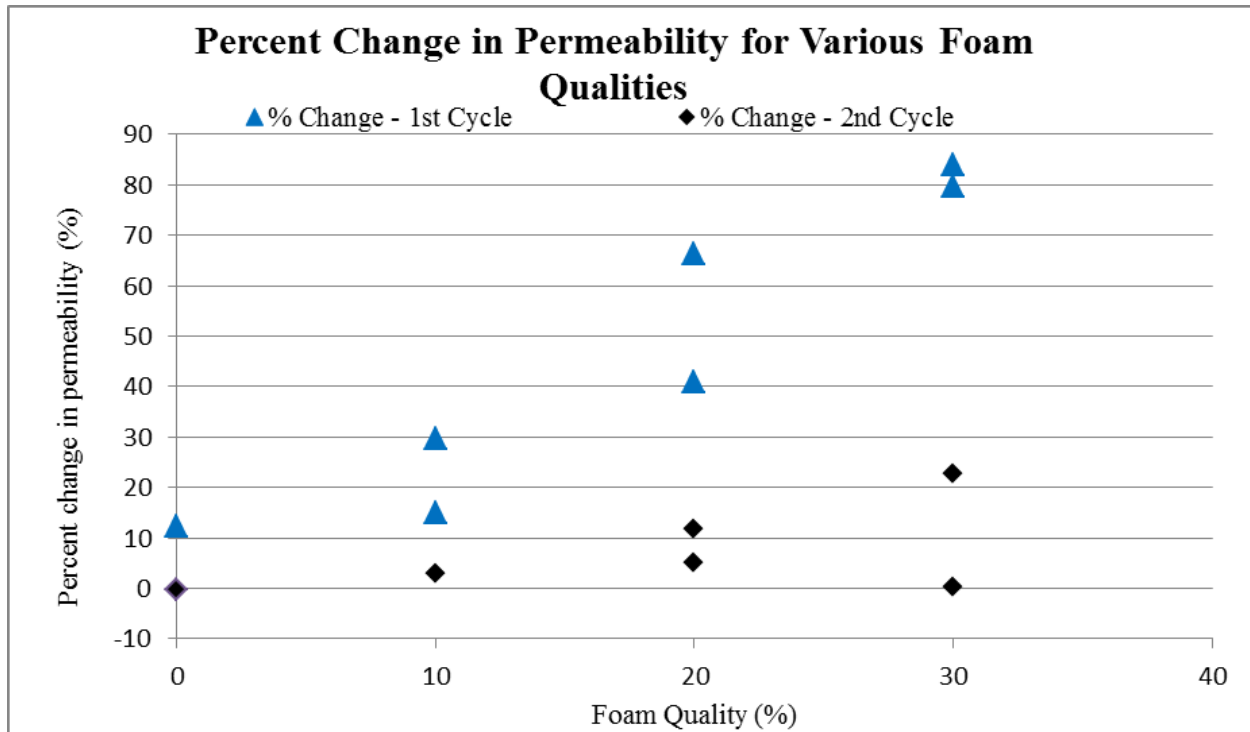


Figure 29: Percent change in Permeability for various Foam qualities during cyclic loading and unloading



3.4.2 Poisson’s Ratio

Previous studies (McDaniel et al. 2014) have reported PR values ranging from 0.23-0.32 for cements using a Class H base with various recipes. Reddy et al., (2007) presented dynamic PR values for foamed cements of different qualities (0-25%) that ranged between 0.17-0.23. The results of our study showed an average initial PR value ranging from 0.17-0.20, which follows closely with previous dynamic test results (Reddy et al., 2007). It is possible that the results reported in the McDaniel study are significantly different than our own due to the variation in the cement system compositions.

The PR data exhibited limited variation throughout pressure cycles compared to the changes in permeability and YM. However when comparing PR as a function of foam quality, we observed that the values increase with foam quality, although neat cement and 10% show similar PR values (Figure 30 and Figure 31). This trend can be significant for design optimization due to the idea that an increase in PR can lead to a decrease in compressibility, which, in turn, allows the cement to play a better role in long term cement sheath integrity (Le Roy-DeLange et al., 2000).

Figure 30: Average Poisson's Ratio of all samples over both loading and unloading increases with greater foam quality.

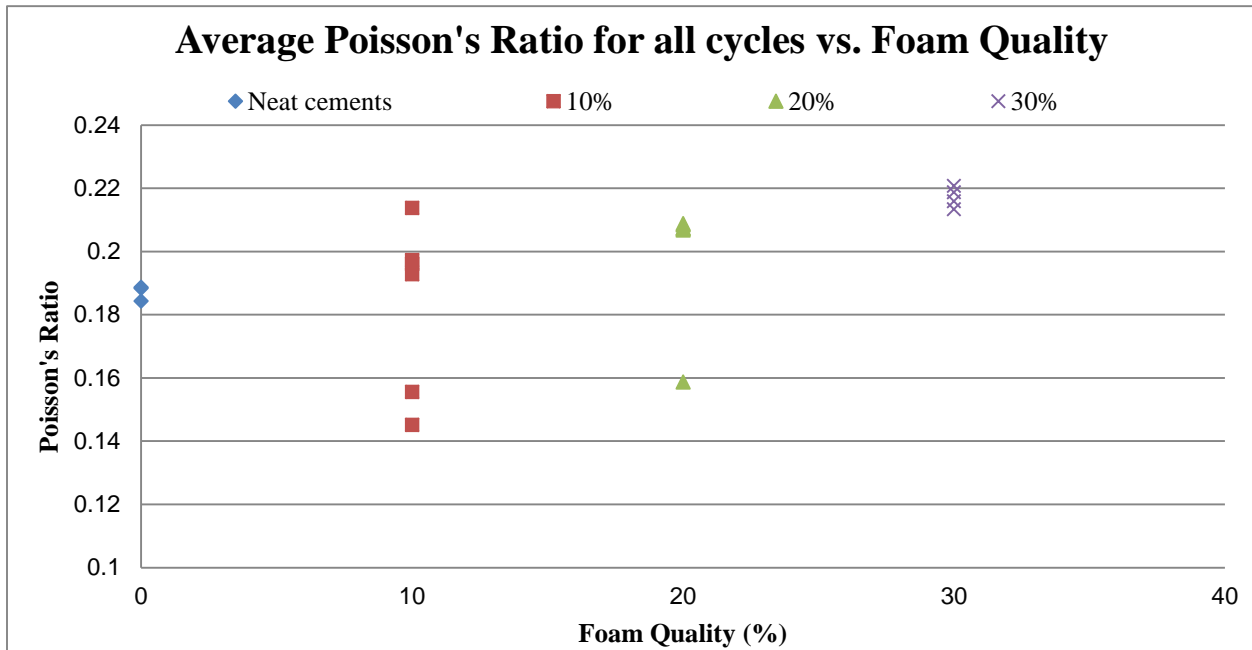
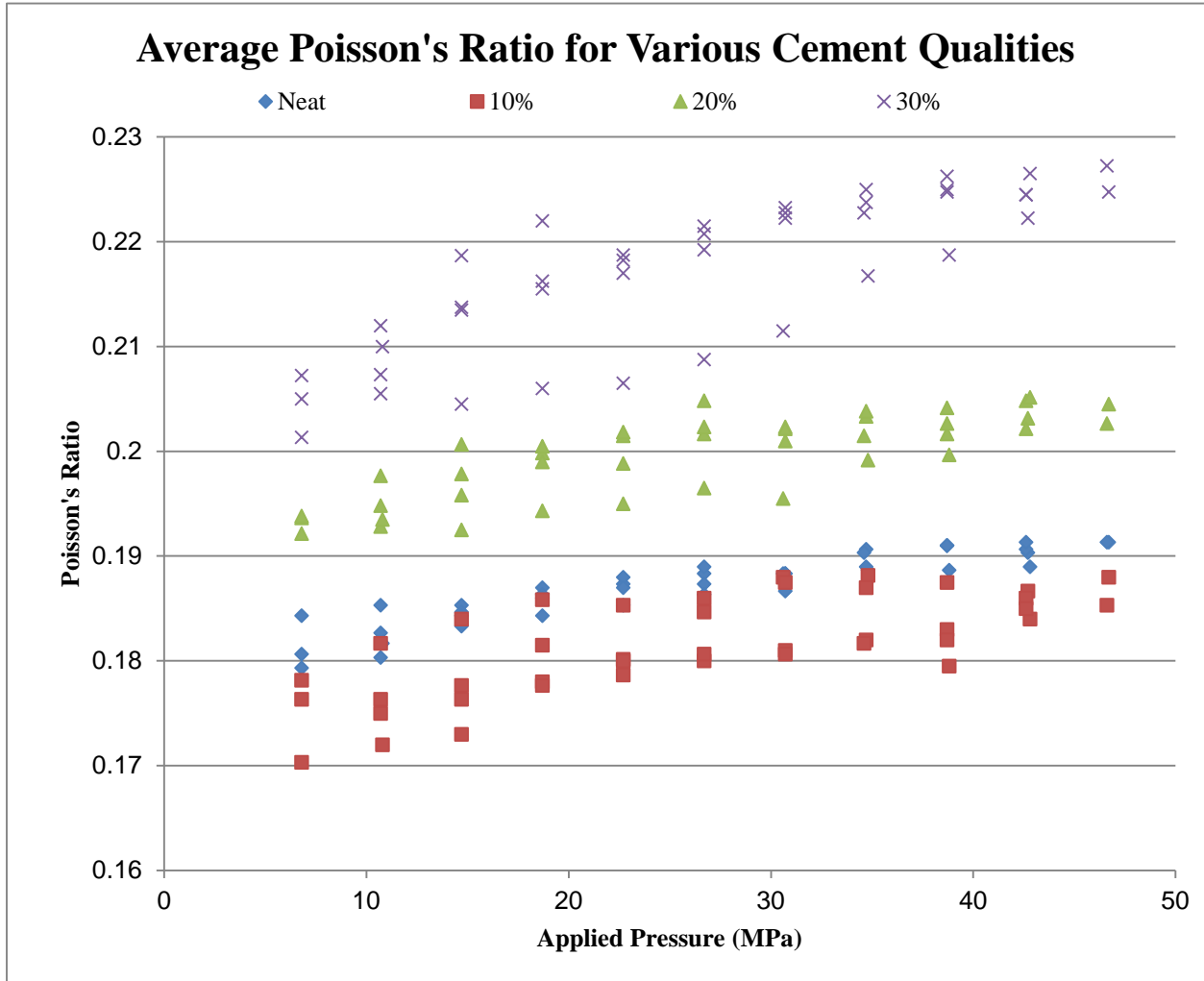


Figure 31: Average Poisson's Ratio of all samples within each Foam Quality measured across all loading and unloading regimes.



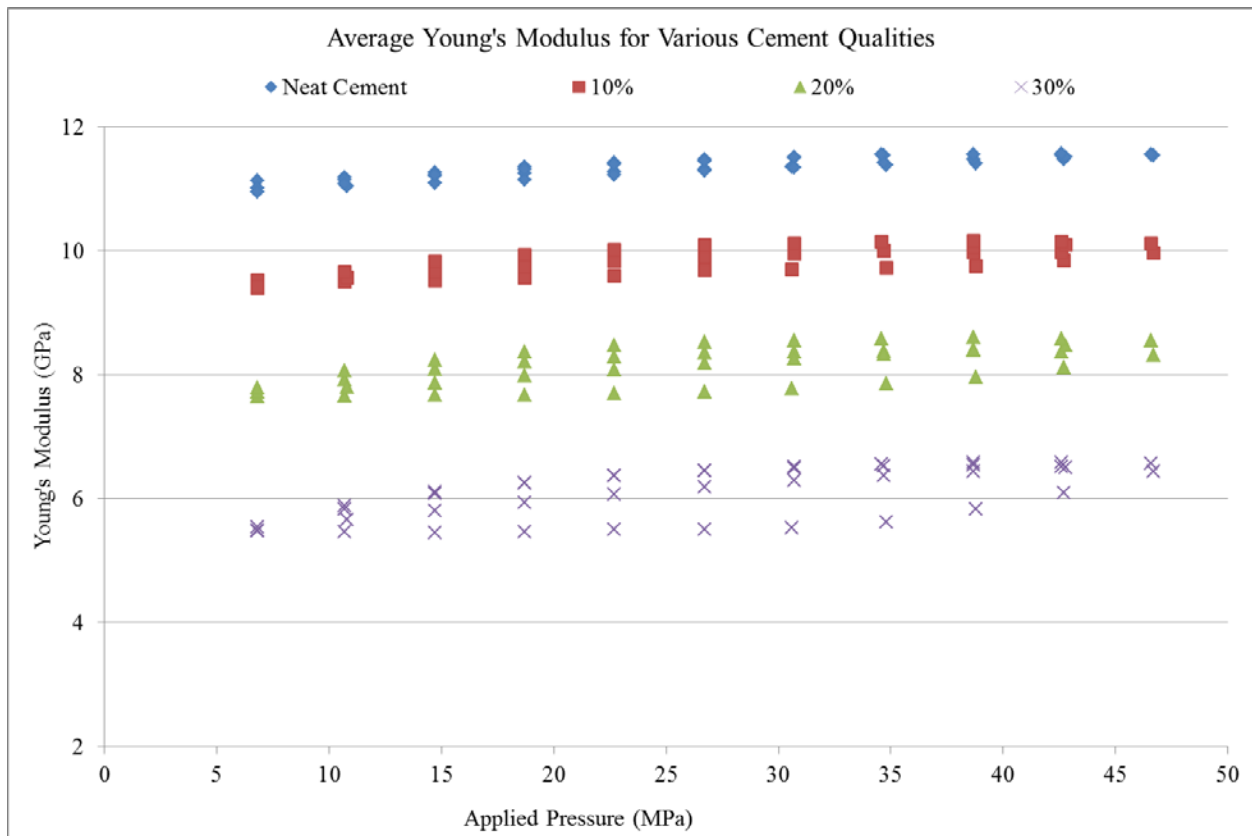
3.4.3 Young's Modulus

McDaniel et al. (2014) reported YM values of Class H cements that varied between 5.2 GPa-11.3 GPa (7.54×10^5 to 1.63×10^6 psi). Reddy et al., (2007) presented dynamic YM values for foamed cements of different qualities (0-25%) that ranged between 12.41 GPa - 19.99 GPa (1.8×10^6 to 2.90×10^6 psi). Our results showed average YM values ranging from 5.5 GPa (7.97×10^5 psi) for the 30% foam quality cements to 11.1 GPa (1.6×10^6 psi) for the Neat cements. These results are similar

to those previously reported providing greater confidence in the results and methods. However, it is interesting to note that the YM results from this work were the most similar to those found in McDaniel et al. (2000), yet the PR values were slightly lower which could be due to analytical methods.

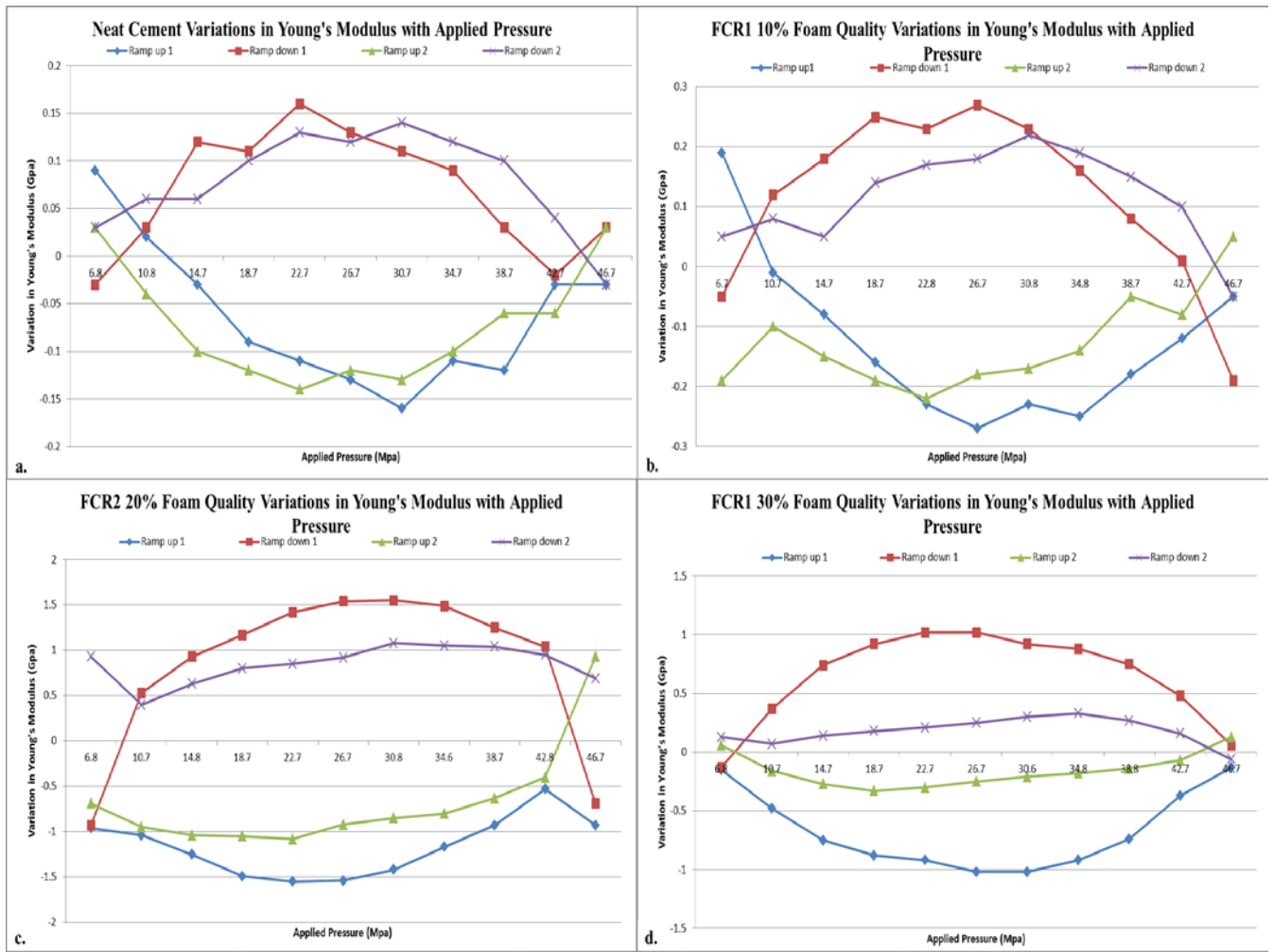
When analyzing the data, there were two main observations seen regarding YM. (1) As foam quality increases, the YM over the entire pressure regime decreases (Figure 32). This implies that at comparable pressures, cements of higher foam quality display more elastic response than those of lower foam qualities. (2) As each sample undergoes pressure cycling, the YM changes for an individual sample in a consistent pattern (Figure 32). As applied pressure increases, the YM increases. From the loading to unloading within one pressure cycle, varying degrees of change in the YM are observed for different foam qualities.

Figure 32: Average Young's modulus for all cement types. Figure shows that an increase in foam quality results in the lowering of Young's modulus (increased elasticity).



This phenomenon can be observed in the variance of YM (Figure 33). Greater variance between the loading and unloading for the first cycle compared with the second cycle is observed with higher foam qualities. The variation in YM approaches values closer to zero during the second pressure cycle for the 20% and 30% foamed cements, while the 10% foam and neat cements show similar variance between the two cycles (Figure 33). This suggests that for higher foam qualities, cements are undergoing a greater amount of inelastic deformation during loading of the first cycle. The lower amount of variation in the lower foam quality cements and neat cements indicates a less severe inelastic deformation, allowing for similar responses from the first and second cycle.

Figure 33: Variation in Young's Modulus vs. Applied Pressure for both cycles. These results display variance for one individual sample of each quality, not averages for each quality.



3.5 CONCLUSIONS

In our experiments we observed that permeability is permanently altered with pressure cycling of the cement. The permeability decreases for all cement systems following loading, which may indicate a closing of connected pore throats in the cement matrix. Because the cements show no drastic increase in permeability during the pressure cycling, there is no reason to believe that

connected fractures occurred in the cement due to the applied pressure suggesting cement framework coherence and stability. We observed that Young's Modulus (YM) decreases as foam quality increases. We interpret this observation to be the result of having more entrained air in the cement framework structure is allowing the cement framework to undergo more physical change. This variation in YM is especially observed for the first loading of the cement systems. After this initial loading the cement displays a lack of ability to return to its initial state. We also observed that Poisson's ratio (PR) is generally unaffected by pressure cycling although it tends to increase slightly with an increase in foam quality. The greatest mechanical changes occur during the first pressure cycle, and less for the second based on observations of YM and Permeability. Experiments utilizing a greater number of pressure cycles may provide insight into how many pressure cycles it takes for the cement to be completely invariable in its mechanical properties as a function of applied pressure.

3.6 LESSONS LEARNED AND FUTURE WORK

The cement samples used in this study were of a significant age (roughly 2 years old), at the time of dynamic moduli testing. Cured cements of a younger age may give different results; however, the goal was to test the mechanical properties of multiple set cements and their ability to maintain long-term zonal isolation when affected by different pressure cycles that can be found in a wellbore before, during, and after production. Figures 34, 35, and 36 show the results of these tests and are defined by their cement design type (i.e., FCR1, FCR2, and H-class neat cement, respectively).

Figure 34: Permeability (34A.), Young's Modulus (34B.), and Poisson's ratio (34C.) of all FCR1 cements over an applied pressure range of 6.5 MPa to 46.0 MPa.

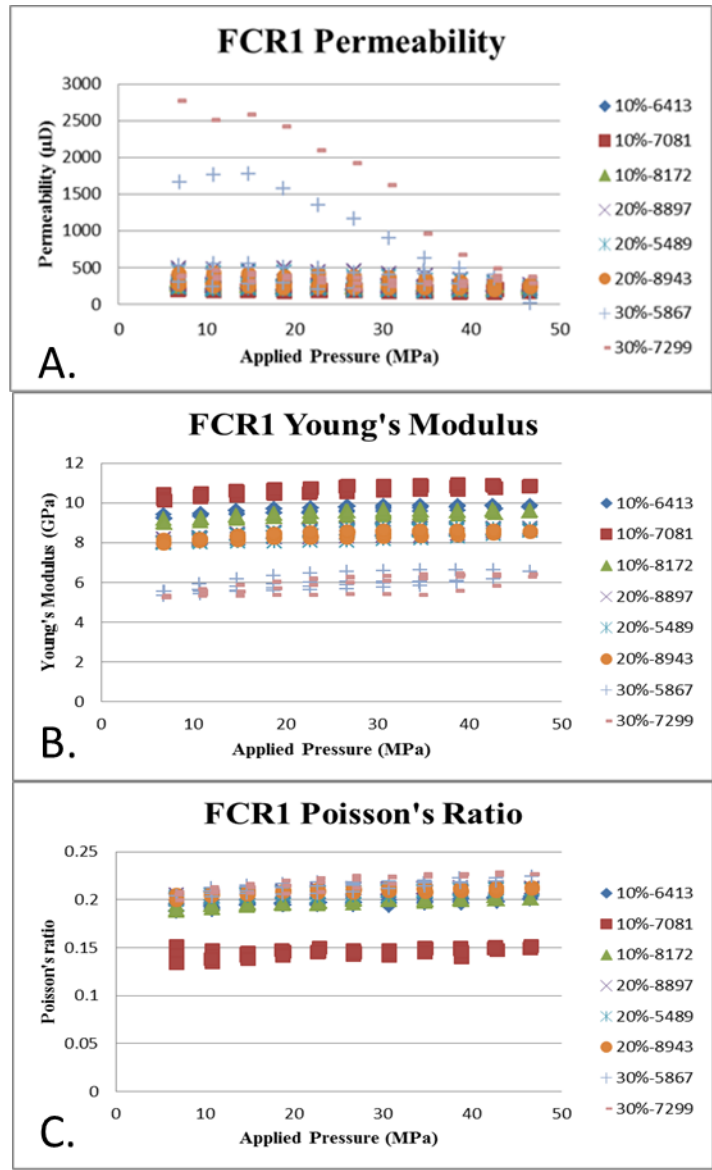
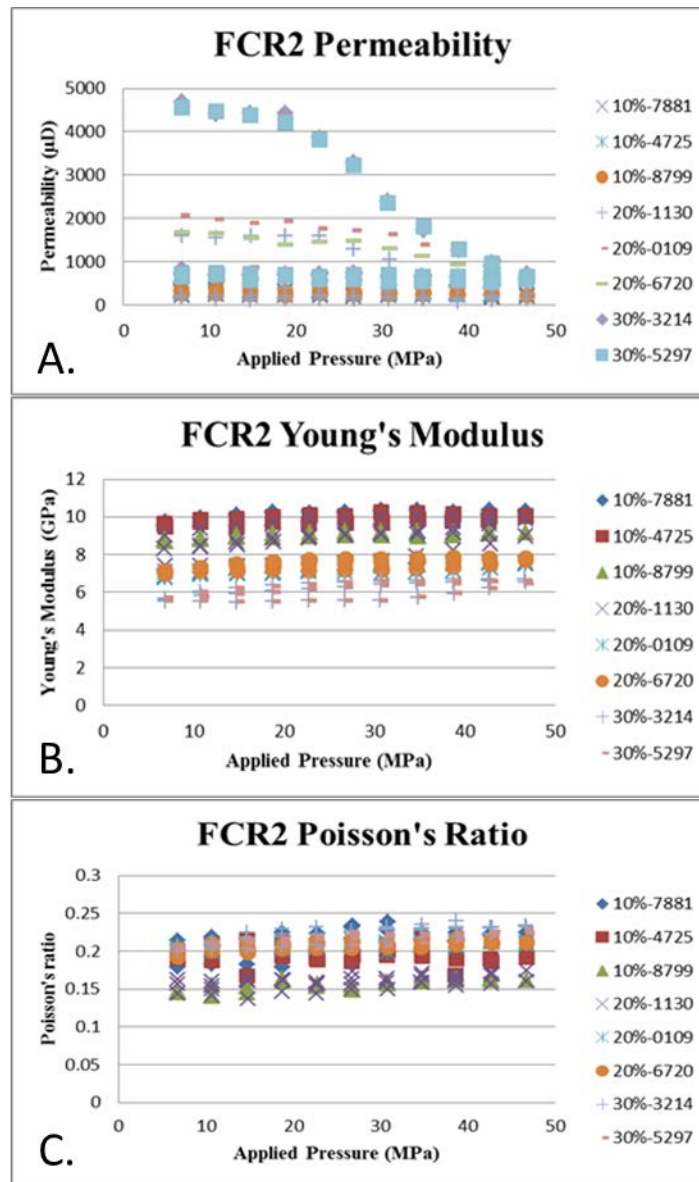
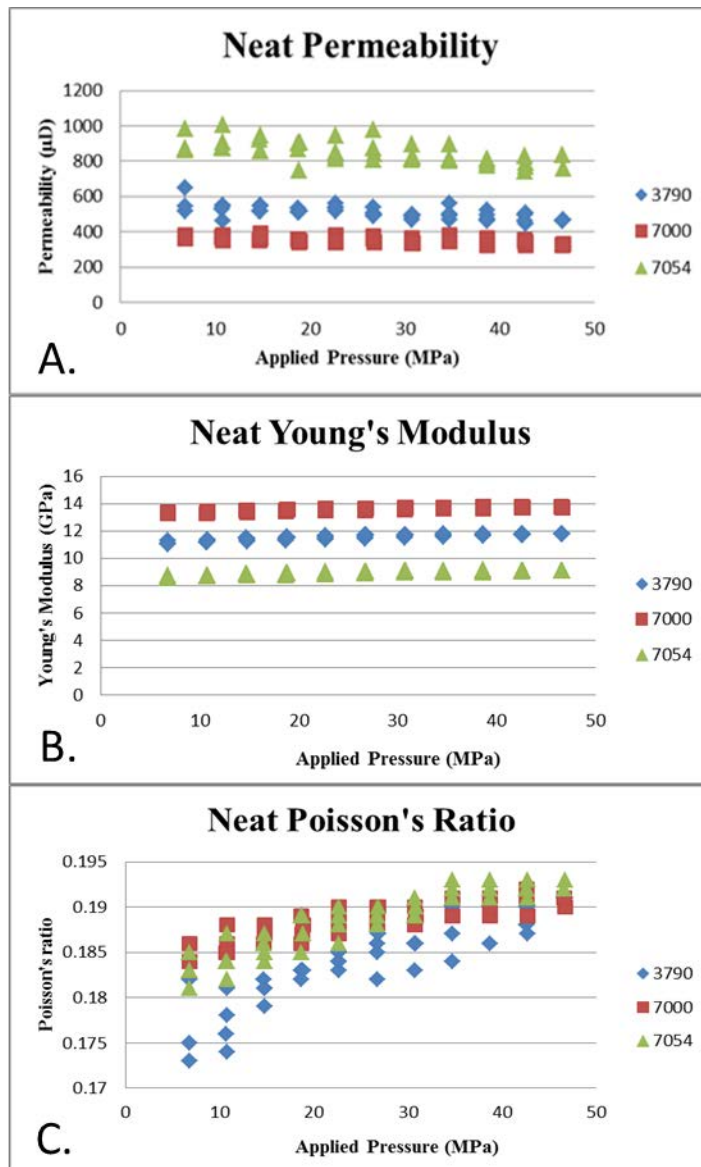


Figure 35: Permeability (35A), Young's Modulus (35B), and Poisson's ratio (35C.) of all FCR2 cements over an applied pressure range of 6.5 MPa to 46.0 MPa.



The group of FCR2 10% cements were not run at multiple cycles in the AutoLab 1500. The samples were depressurized, removed from the containment system and ultimately deformed; therefore we could not run them for a second cycle with confidence in the results.

Figure 36: Permeability (36A), Young's Modulus (36B), and Poisson's ratio (36C) of all H-Class Neat cements over an applied pressure range of 6.5 MPa to 46.0 MPa.



In the future, it is our goal to subject cements generated in the field (Kutchko et al. 2014) to similar dynamic and static testing. From this evaluation, a correlation between the laboratory cements and those from the field may be able to be deduced. If a correlation exists, it will then be possible for industry to have a better understanding of how the cement in a well may actually

behave mechanically; thus improving the overall design methodologies for foamed cement applications.

4. COMPARITIVE ANALYSIS OF STATIC AND DYNAMIC YOUNG'S MODULUS

4.1 STATIC VS. DYNAMIC MECHANICAL PROPERTIES

Static moduli are often used in wellbore stability and in-situ stress applications to evaluate the possibility of breakouts, elevated pore pressure, and to gain insight into tectonic stress distribution (Zimmer, 2003). As mentioned in Chapter 2, a compressive strength test can be conducted and a stress strain diagram can be utilized to determine Young's Modulus and Poisson's Ratio. Static moduli are measured under a relatively slow loading of material and the examination of the physical deformation of this material in response to these loading forces. It is important to remember that deformation measured statically includes both the solid material and the void spaces in a porous medium.

In Chapter 3, compressional and shear wave velocities were used to determine Young's Modulus and Poisson's ratio. These are considered dynamic mechanical properties in reference to the short time duration of the associated deformation as well as the low magnitude of the stresses applied. Dynamic moduli are commonly measured in core samples and can be inferred from well logs. Such dynamic measurements in rock are referred to as linear elastic and usually are thought to be stiffened by material filling pore spaces, because these pore filling materials do not have adequate time to respond to the brief deformation being applied to the sample. This can lead to a systematic difference between static and dynamic moduli for the same material. It is therefore generally accepted that the differences between the two testing methods are caused by the many contributions of inelastic mechanisms at quasi-static and dynamic moduli loading as a function of

strain rate and energy, and that appropriate comparison of the two is only possible under the same conditions (Mashinsky, 2003).

4.2 CORRELATION BETWEEN STATIC AND DYNAMIC MEASUREMENTS

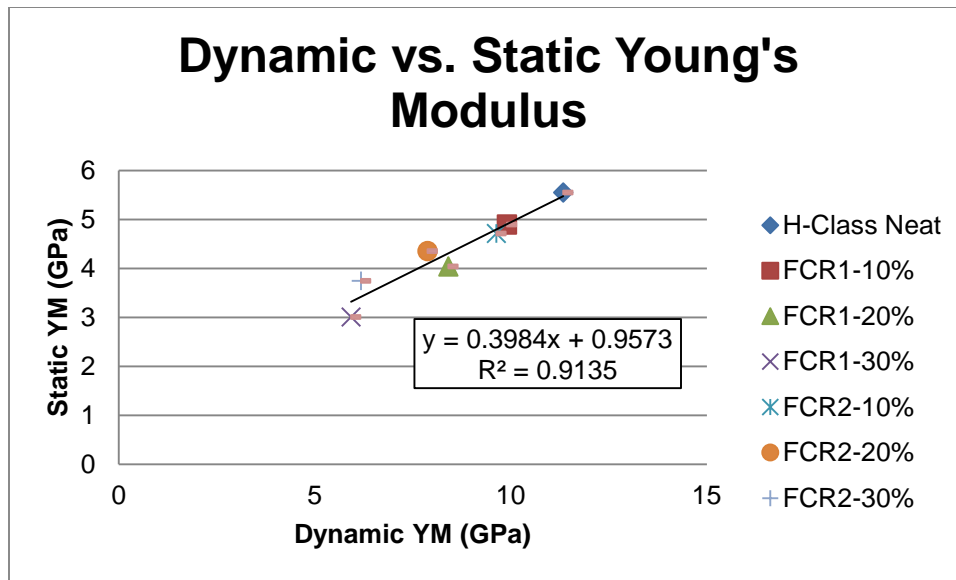
There is a significant amount of evidence available demonstrating that the two methods of measurements do not always coincide. Relationships describing the differences between static and dynamic measurements have been made for specific sets of materials, but there is not one accurate method of correlating for all materials (Coon, 1968; van Heerden, 1987; Morales et al., 1993). In general, the values of both static and dynamic measurements are plotted for a particular type of material and then a numerical relationship can be determined. Research exists from different material groups that show both linear and non-linear relationships between static and dynamic moduli.

The correlation between the static and dynamic Young's Modulus data presented in this thesis can be described by a linear relationship similar to that used by Starzec (1999). Individual comparisons between the dynamic YM and static YM for each foam quality yielded a relationship that was consistent for all cement foam qualities (Figure 37). This relationship was obtained by linear regression analysis of static and dynamic moduli. A line of best fit was determined for the data of the cement samples used in this study. The best fit line leads to Equation 13 with a coefficient of determination (R^2) of 0.9135. This allows accurate prediction of either type of moduli, static or dynamic, given one of these two sets of measurements for this material.

Equation 13: Static and Dynamic Correlation

$$E_{Static} = (0.3984 * E_{Dynamic}) + 0.9573$$

Figure 37: Static vs. Dynamic Young's Modulus



Our results show almost a 1:2 relationship between static and dynamic measurements. This result isn't always seen in the literature because the relationships found for different materials vary widely. For example, crystalline rocks studied by Starzec (1999) show a correlation equation of $E_{\text{Static}} = (0.48 * E_{\text{Dynamic}} - 3.26)$, while the British Testing standard BS8110 has a correlation equation of $E_{\text{Static}} = (1.25 * E_{\text{Dynamic}} - 19)$ for high strength concrete. Future research on a wider variety of foam cements may reinforce the relationship seen between our static and dynamic measurements.

APPENDIX A:

FOAMED CEMENT STRESS STRAIN DIAGRAMS

FCR1 10%

Figure 38: FCR1 - 10% Foam quality Stress - Strain Plot

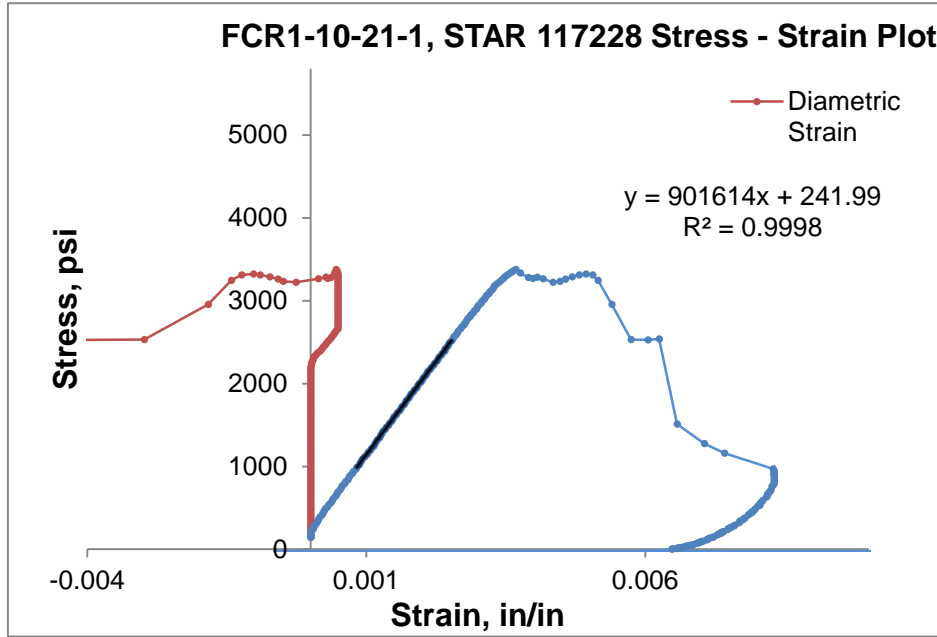


Figure 39: FCR1 - 10% Foam quality Stress - Strain Plot

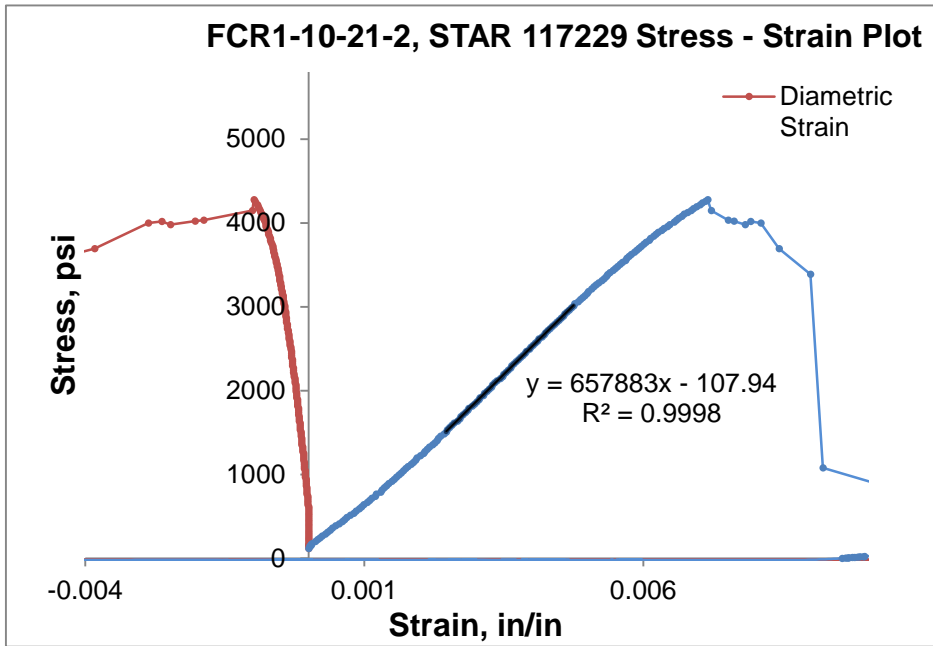


Figure 40: FCR1 - 10% Foam quality Stress - Strain Plot

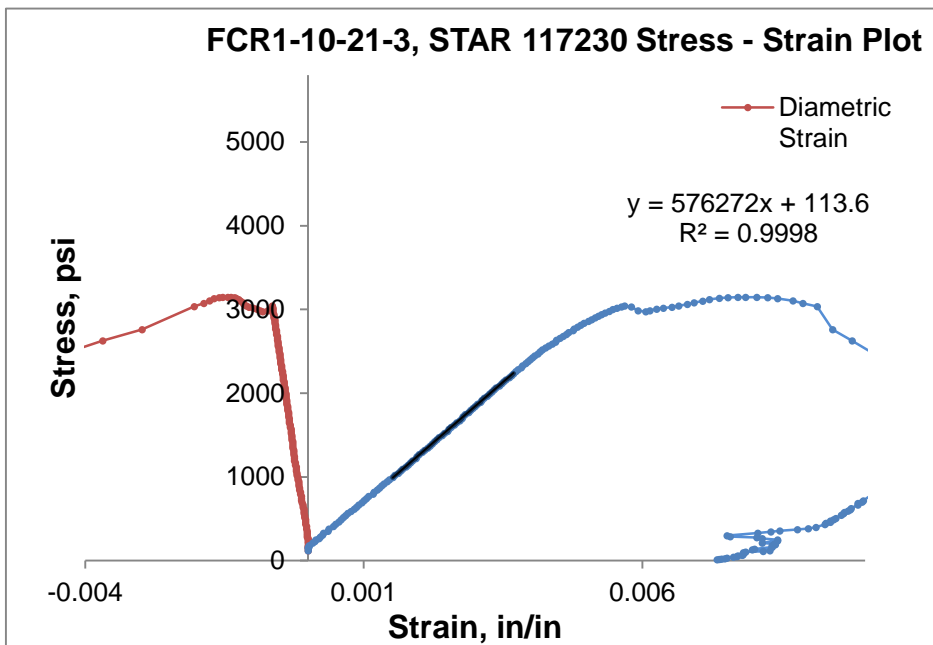


Figure 41: FCR1 - 10% Foam quality Stress - Strain Plot

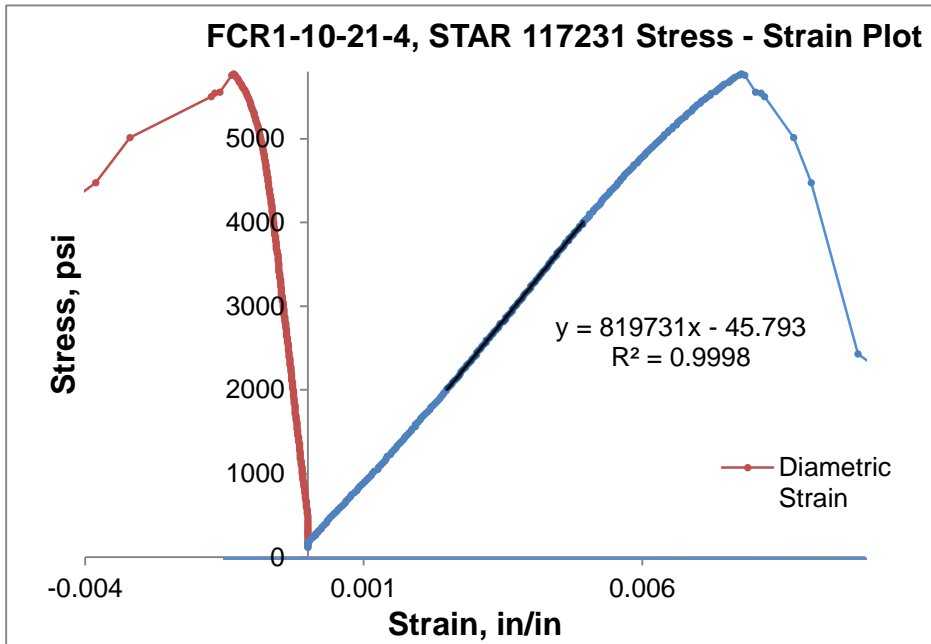
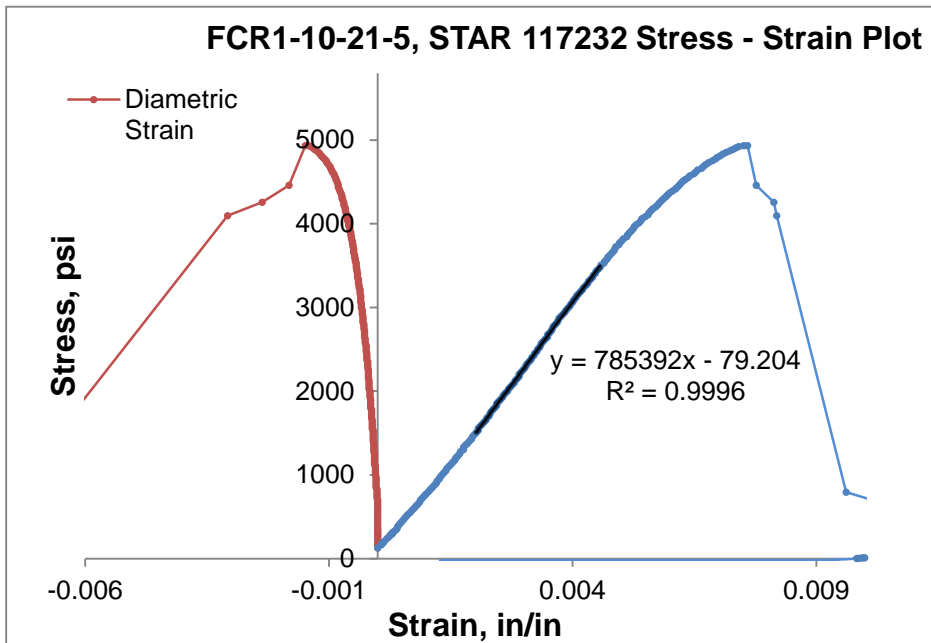


Figure 42: FCR1 - 10% Foam quality Stress - Strain Plot



FCR1 20%

Figure 43: FCR1 - 20% Foam quality Stress - Strain Plot

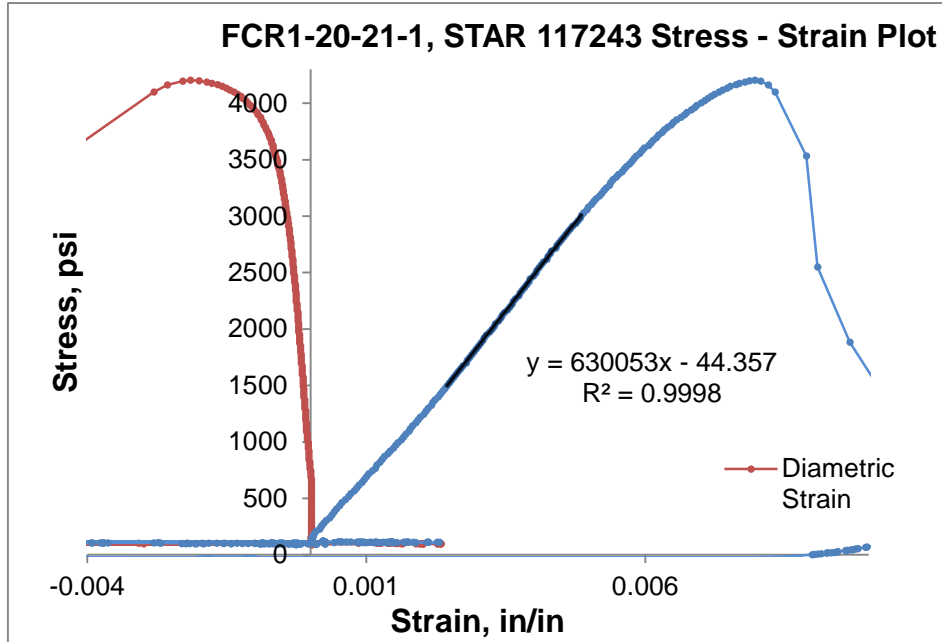


Figure 44: FCR1 - 20% Foam quality Stress - Strain Plot

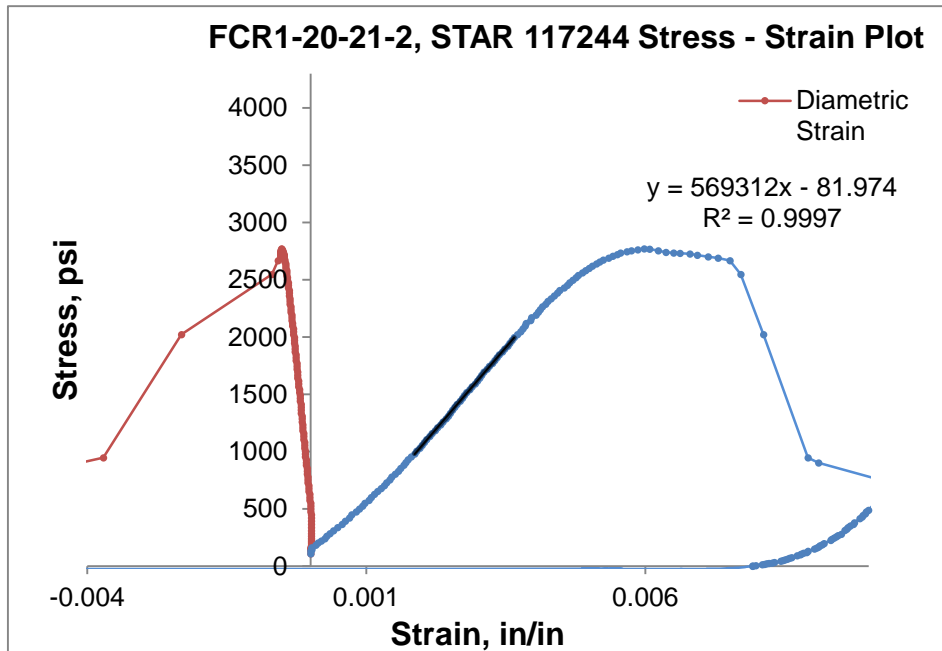


Figure 45: FCR1 - 20% Foam quality Stress - Strain Plot

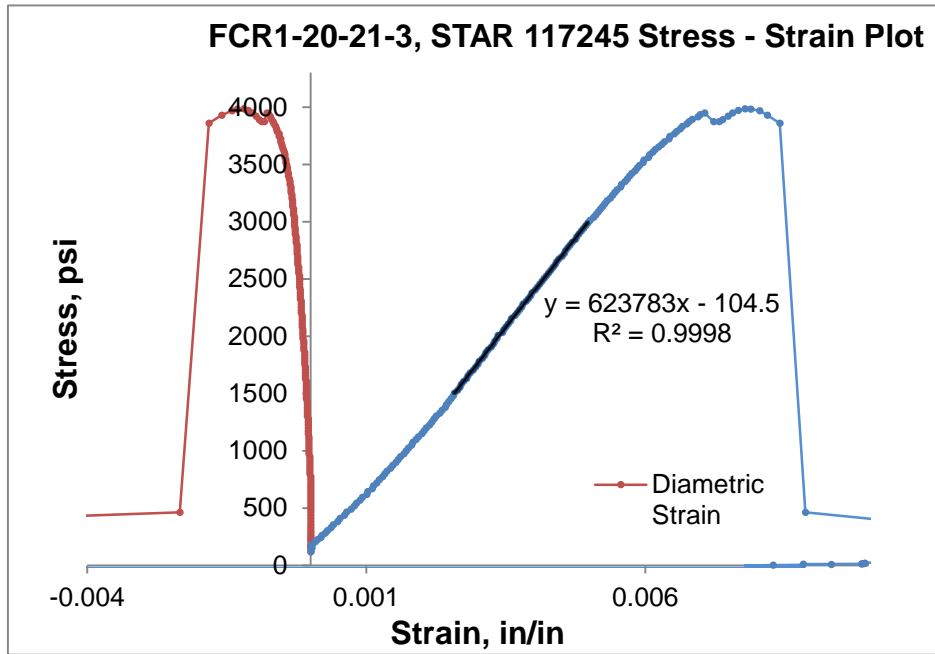


Figure 46: FCR1 - 20% Foam quality Stress - Strain Plot

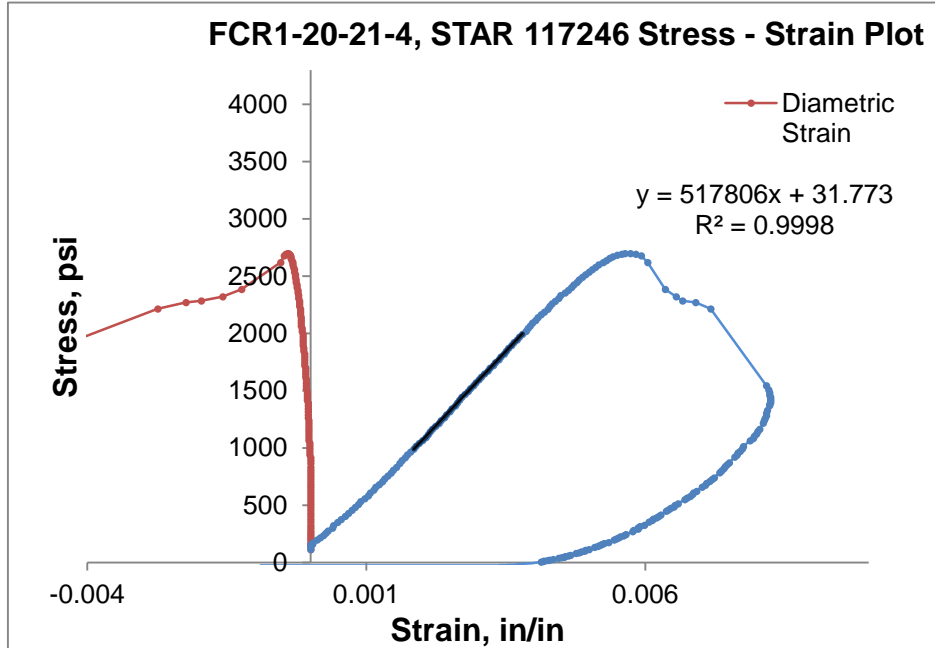
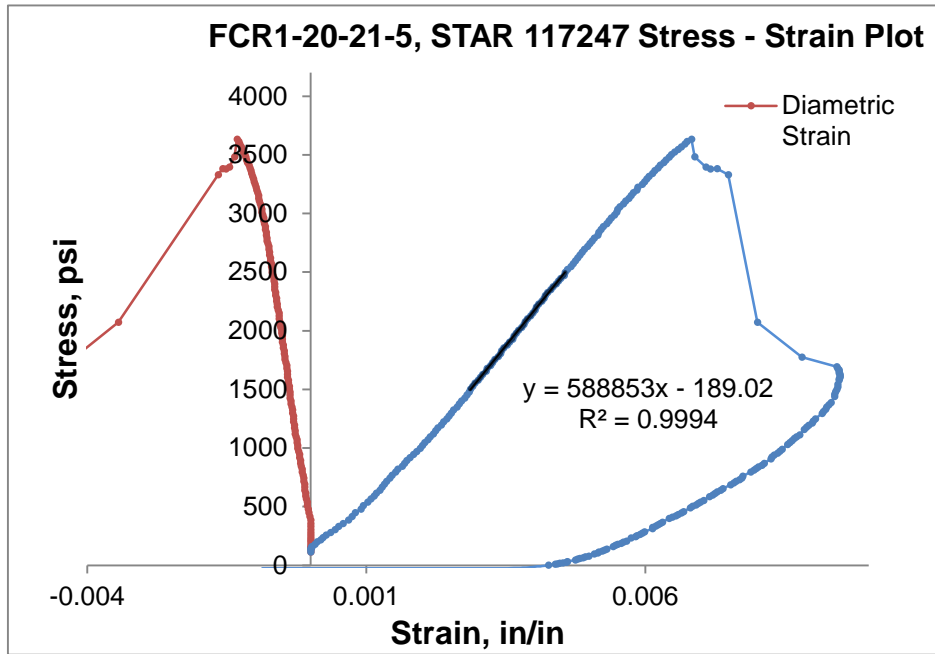


Figure 47: FCR1 - 20% Foam quality Stress - Strain Plot



FCR1 30%

Figure 48: FCR1 - 30% Foam quality Stress - Strain Plot

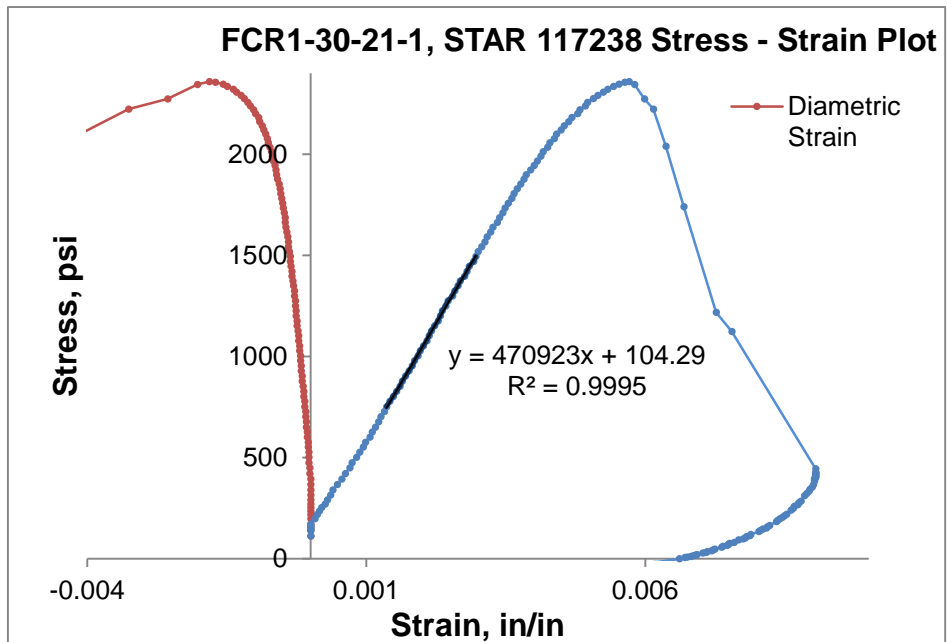


Figure 49: FCR1 - 30% Foam quality Stress - Strain Plot

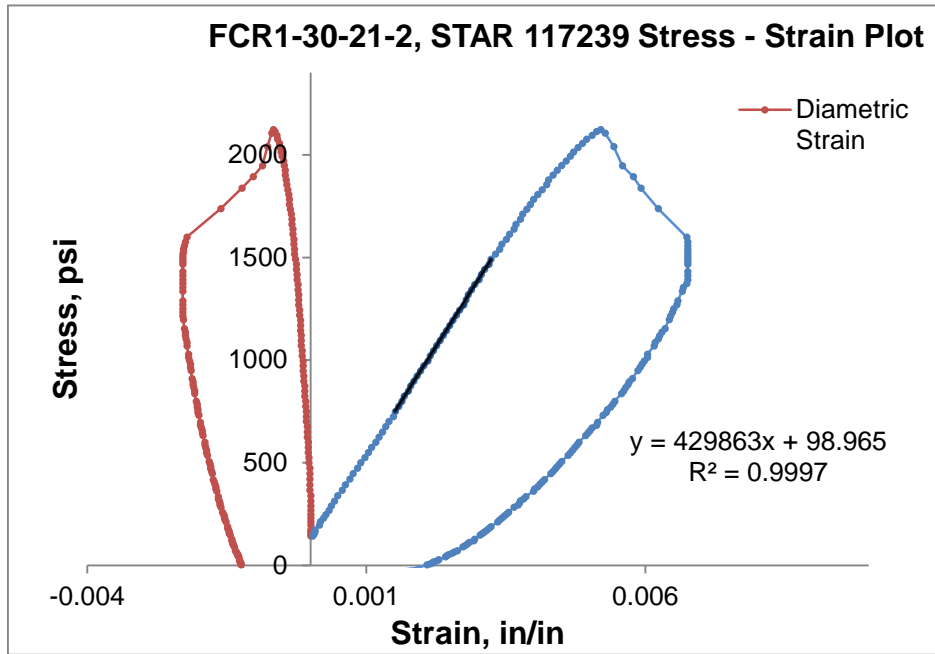


Figure 50: FCR1 - 30% Foam quality Stress - Strain Plot

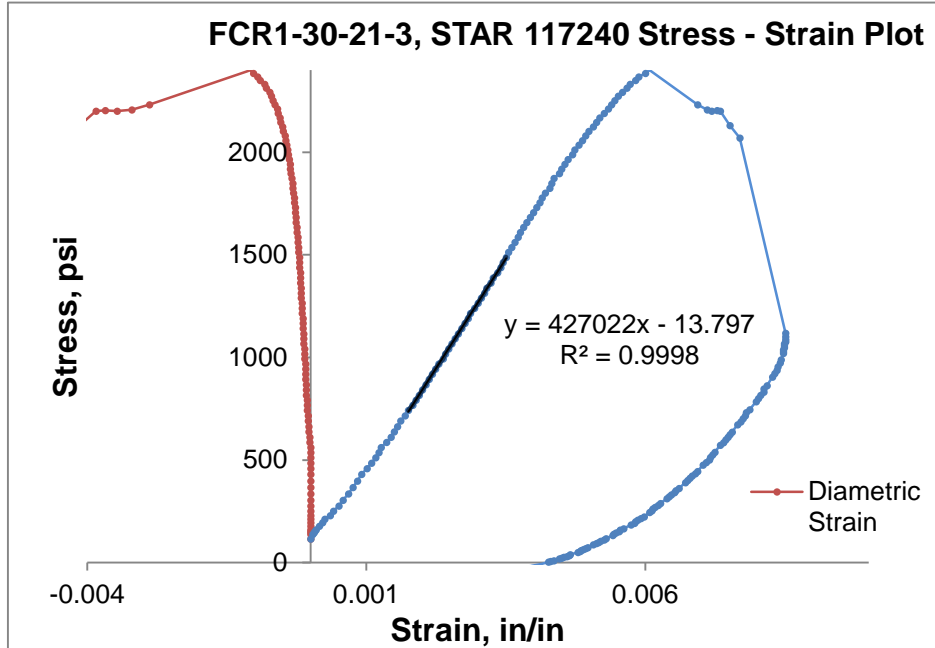


Figure 51: FCR1 - 30% Foam quality Stress - Strain Plot

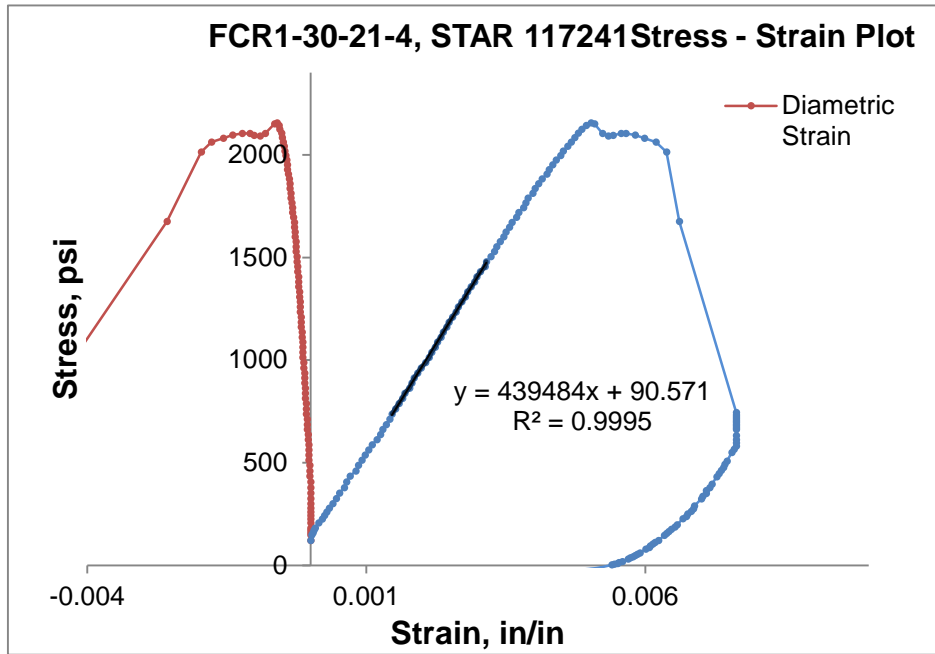
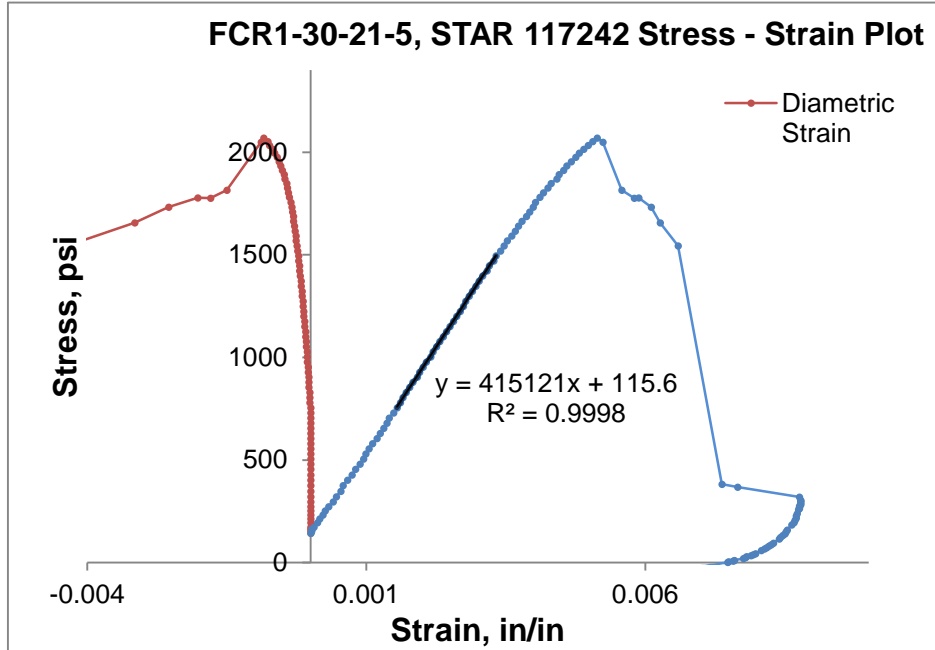


Figure 52: FCR1 - 30% Foam quality Stress - Strain Plot



FCR1 40%

Figure 53: FCR1 - 40% Foam quality Stress - Strain Plot

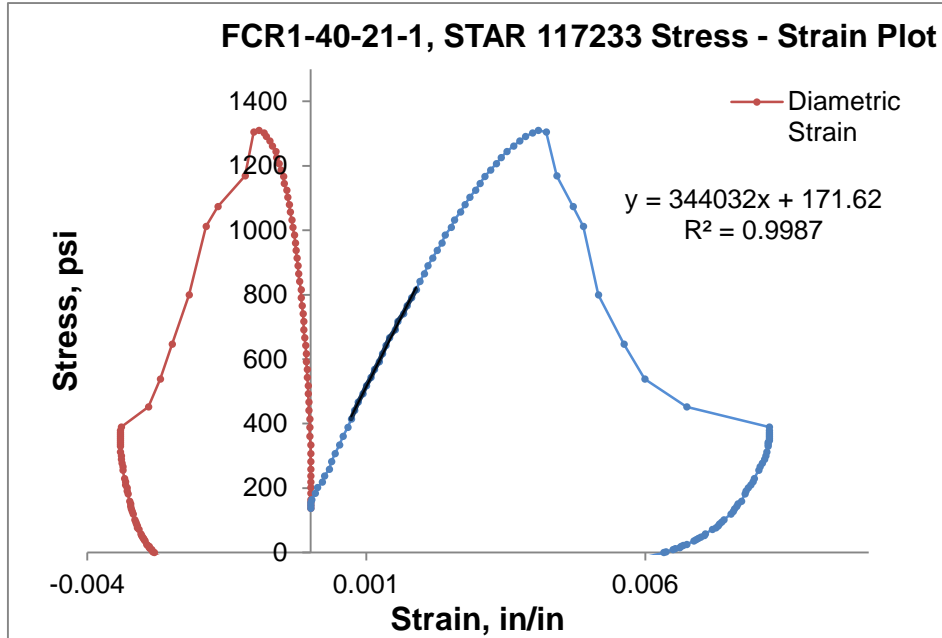


Figure 54: FCR1 - 40% Foam quality Stress - Strain Plot

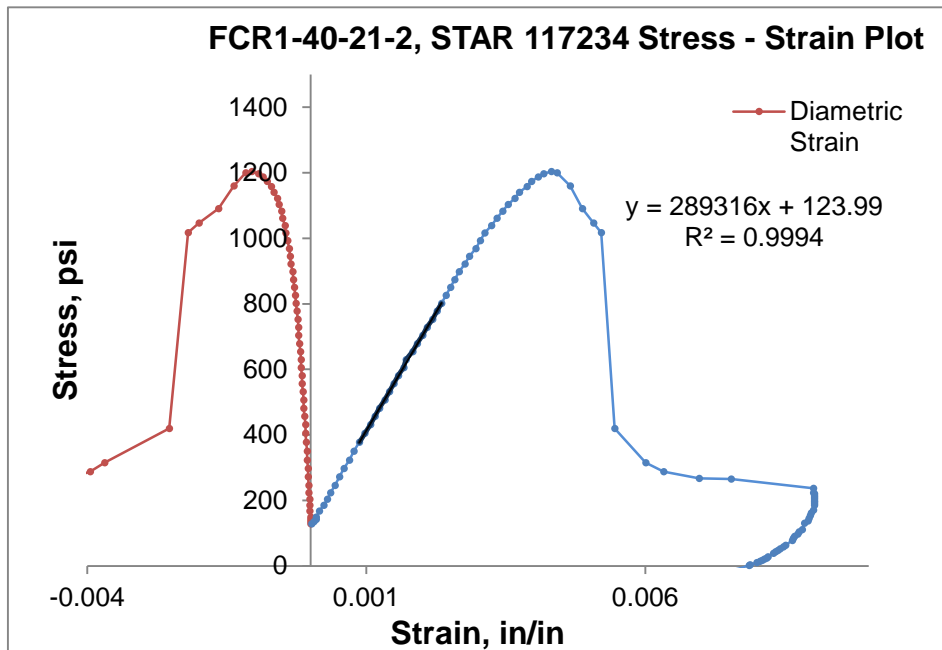


Figure 55: FCR1 - 40% Foam quality Stress - Strain Plot

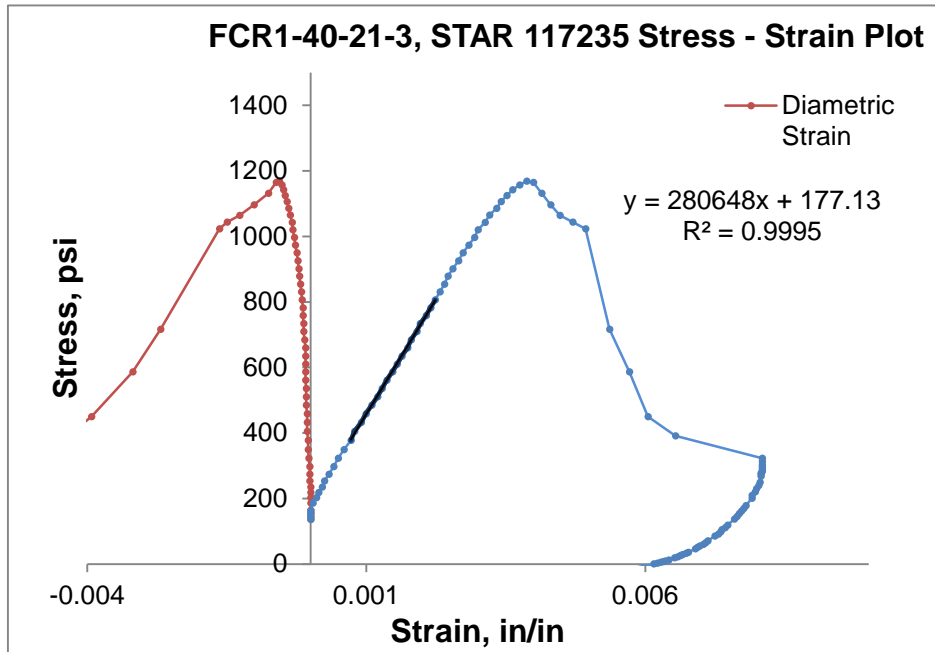


Figure 56: FCR1 - 40% Foam quality Stress - Strain Plot

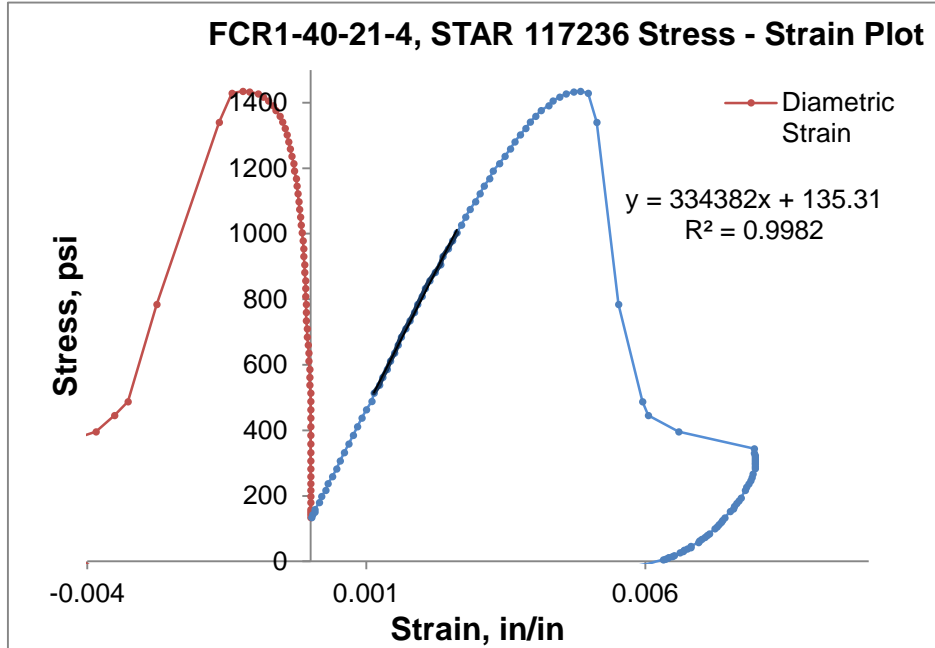
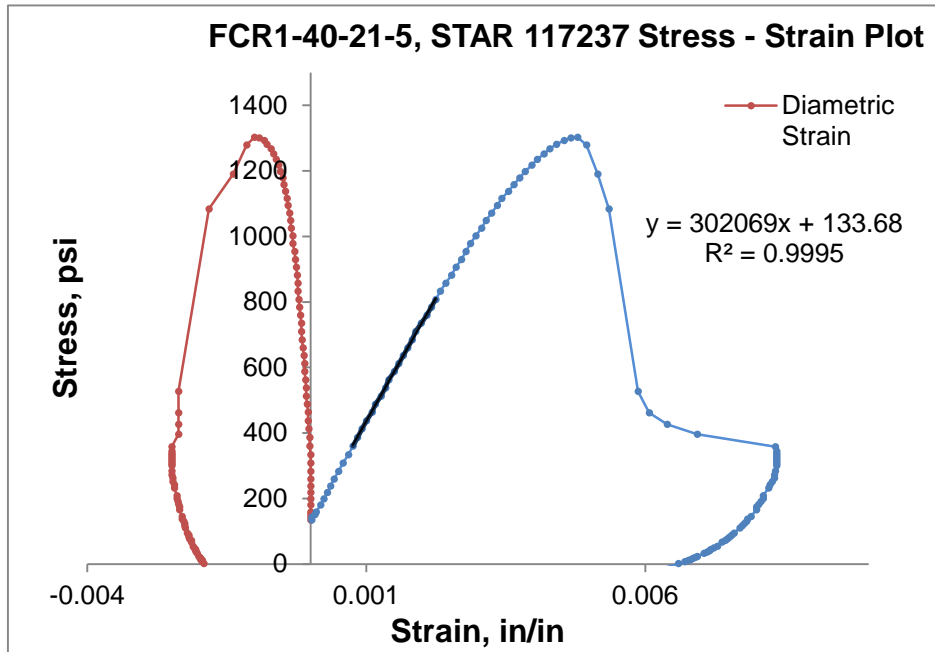


Figure 57: FCR1 - 40% Foam quality Stress - Strain Plot



FCR2 10%

Figure 58: FCR2 - 10% Foam quality Stress - Strain Plot

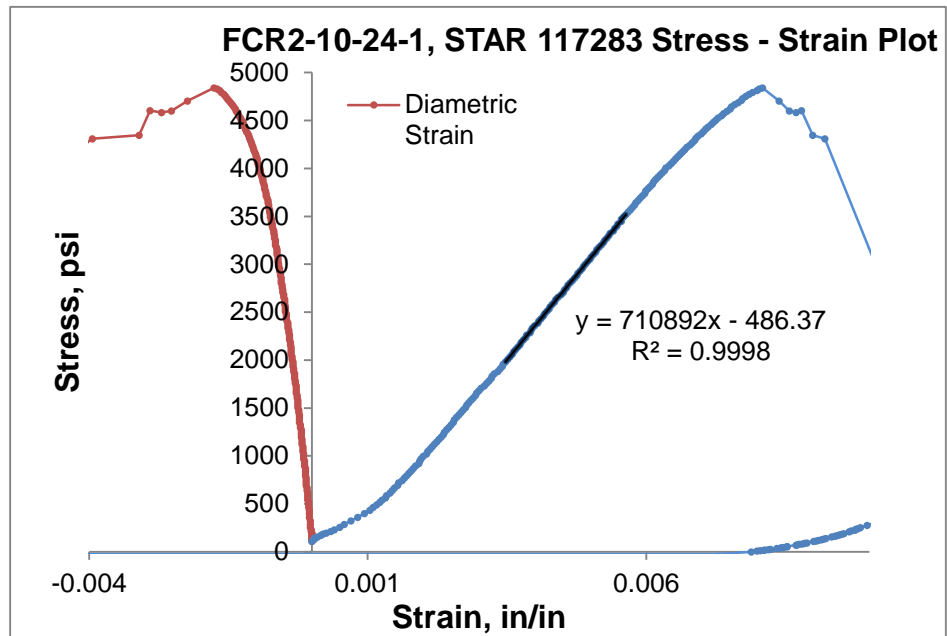


Figure 59: FCR2 - 10% Foam quality Stress - Strain Plot

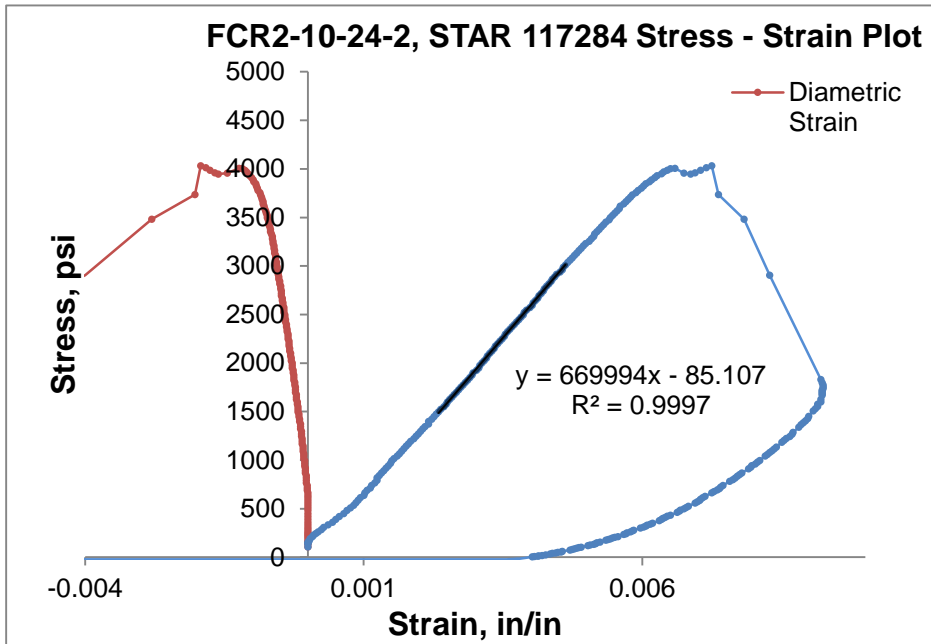


Figure 60: FCR2 - 10% Foam quality Stress - Strain Plot

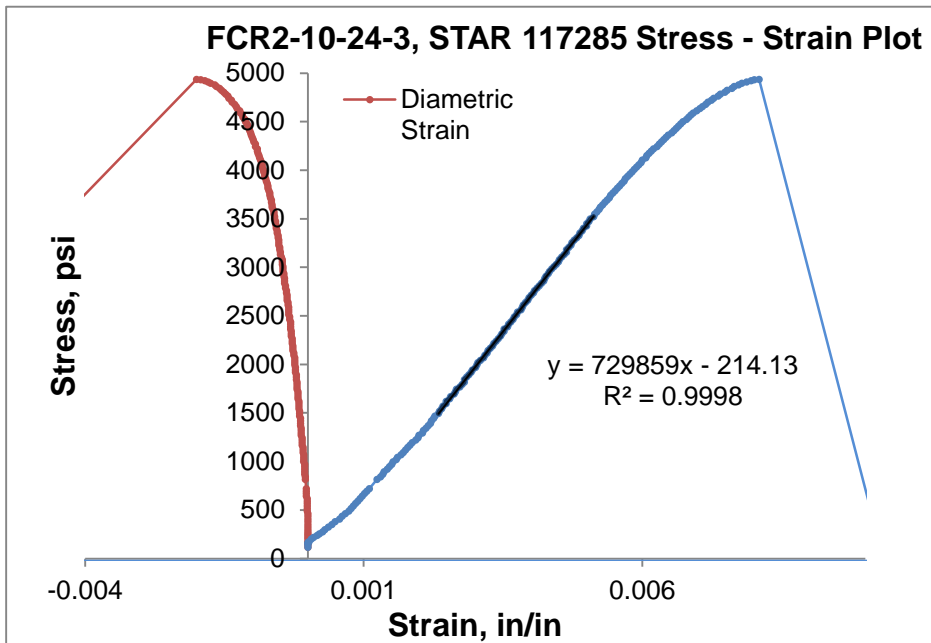


Figure 61: FCR2 - 10% Foam quality Stress - Strain Plot

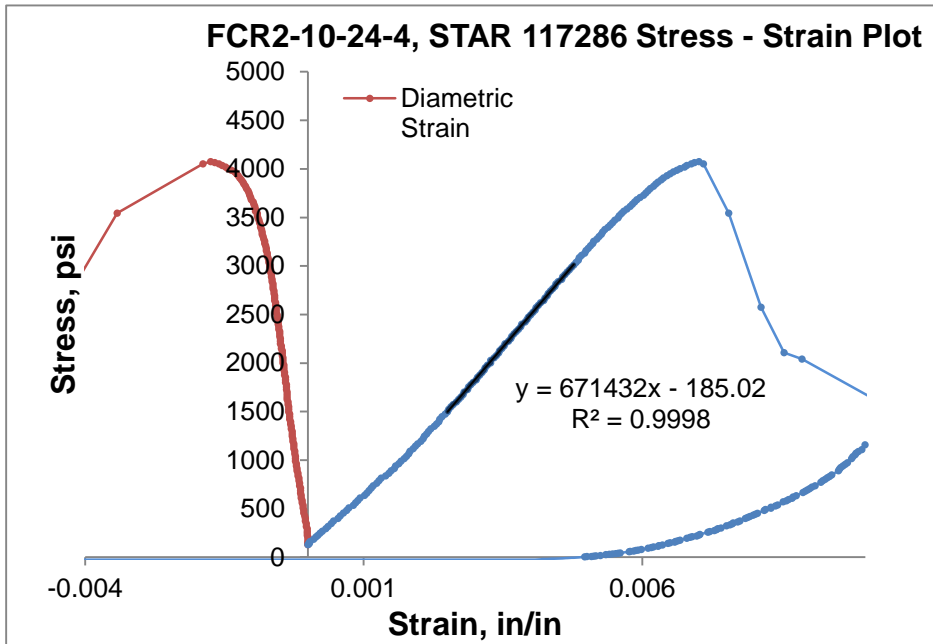
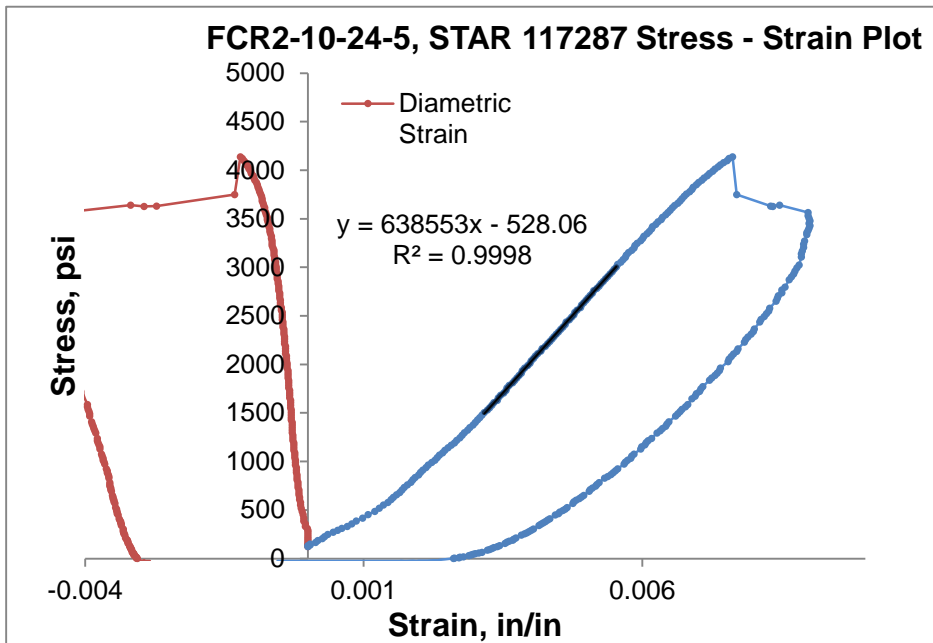


Figure 62: FCR2 - 10% Foam quality Stress - Strain Plot



FCR2 20%

Figure 63: FCR2 - 20% Foam quality Stress - Strain Plot

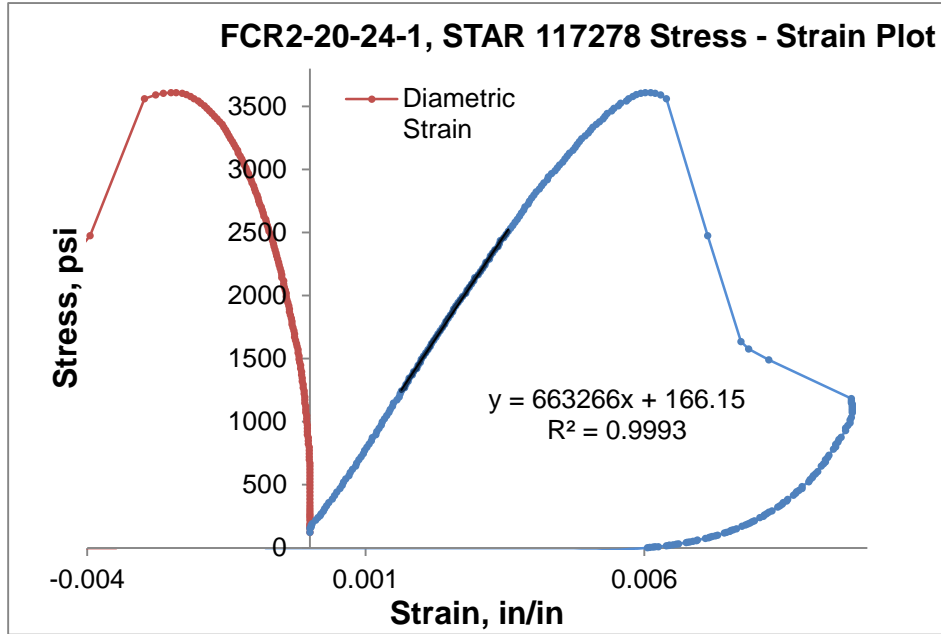


Figure 64: FCR2 - 20% Foam quality Stress - Strain Plot

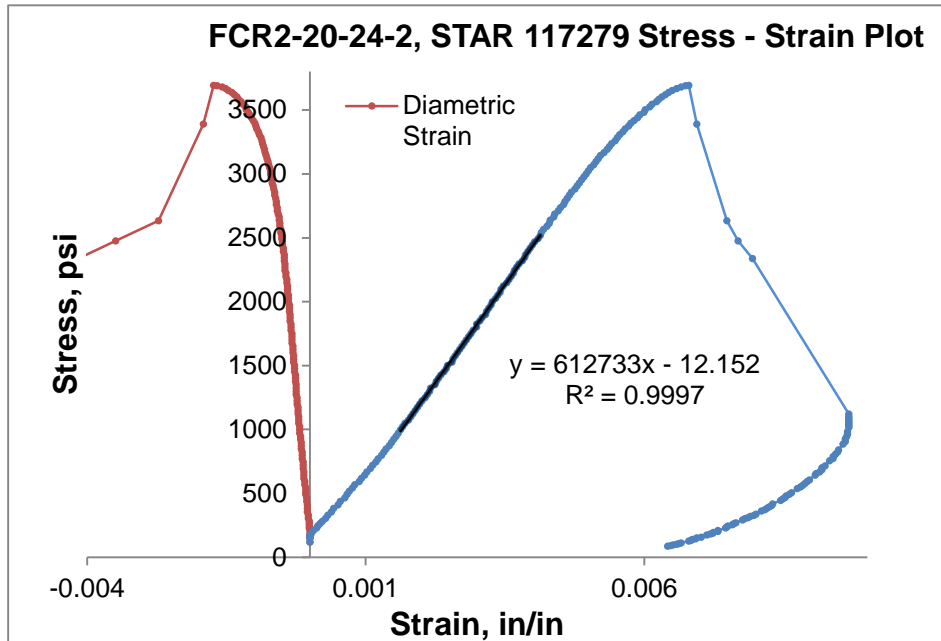


Figure 65: FCR2 - 20% Foam quality Stress - Strain Plot

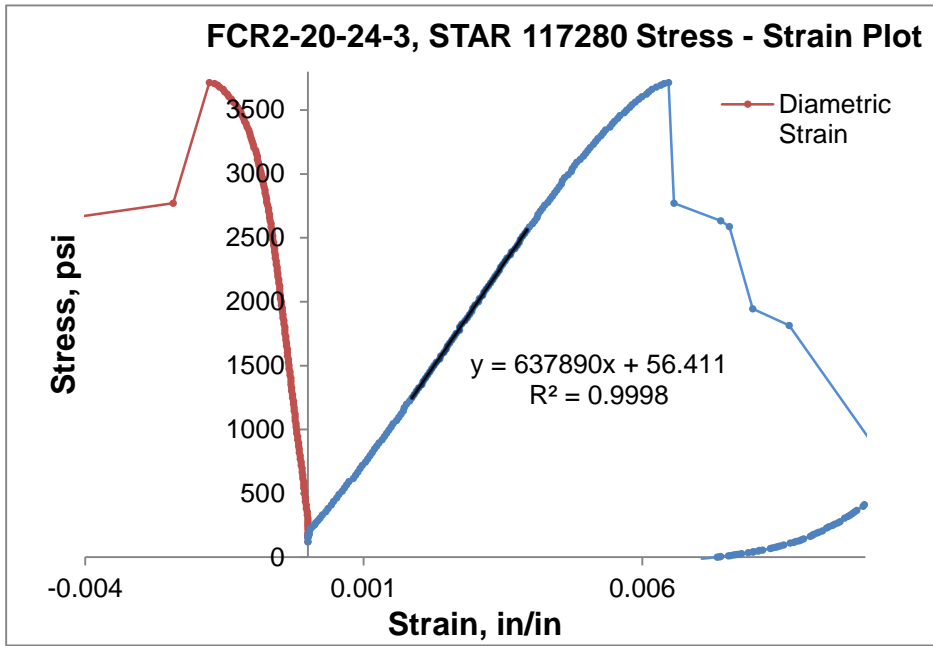


Figure 66: FCR2 - 20% Foam quality Stress - Strain Plot

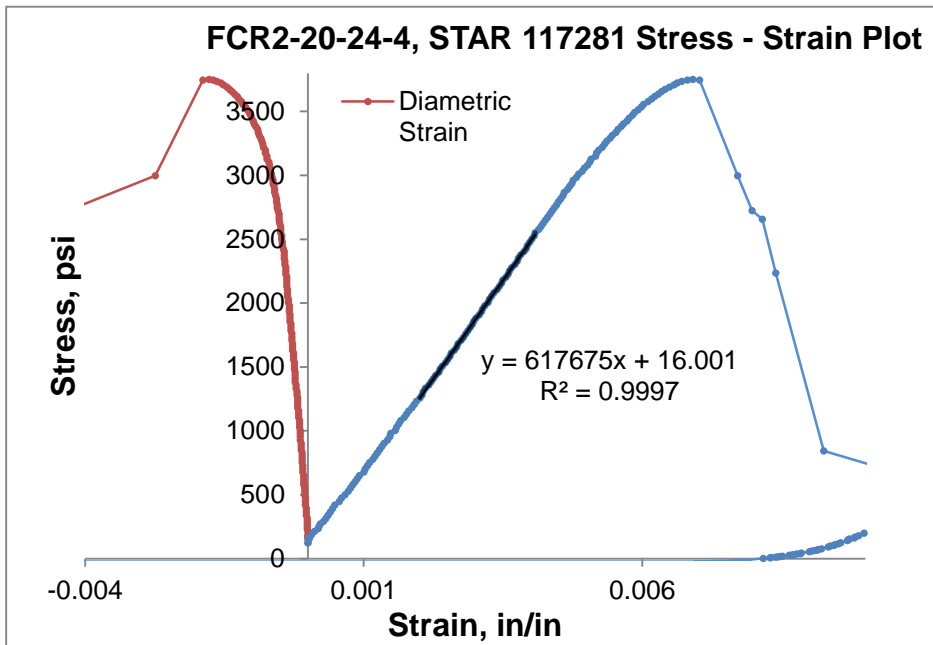
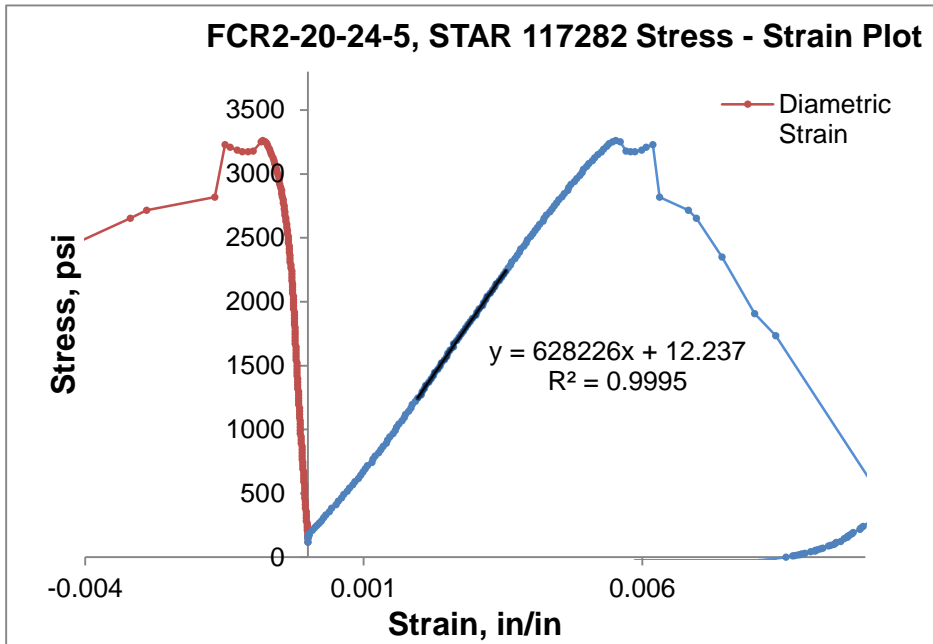


Figure 67: FCR2 - 20% Foam quality Stress - Strain Plot



FCR2 30%

Figure 68: FCR2 - 30% Foam quality Stress - Strain Plot

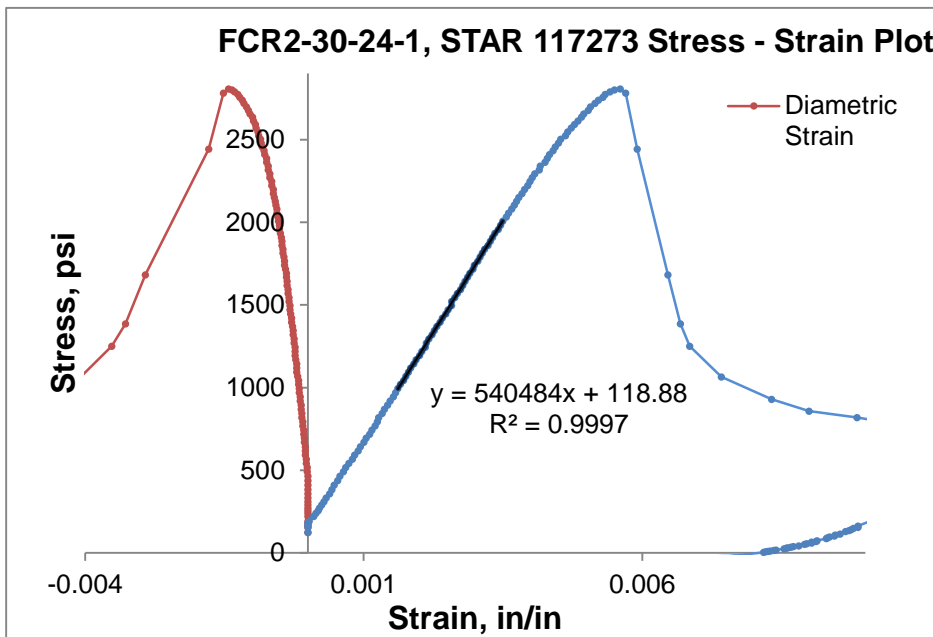


Figure 69: FCR2 - 30% Foam quality Stress - Strain Plot

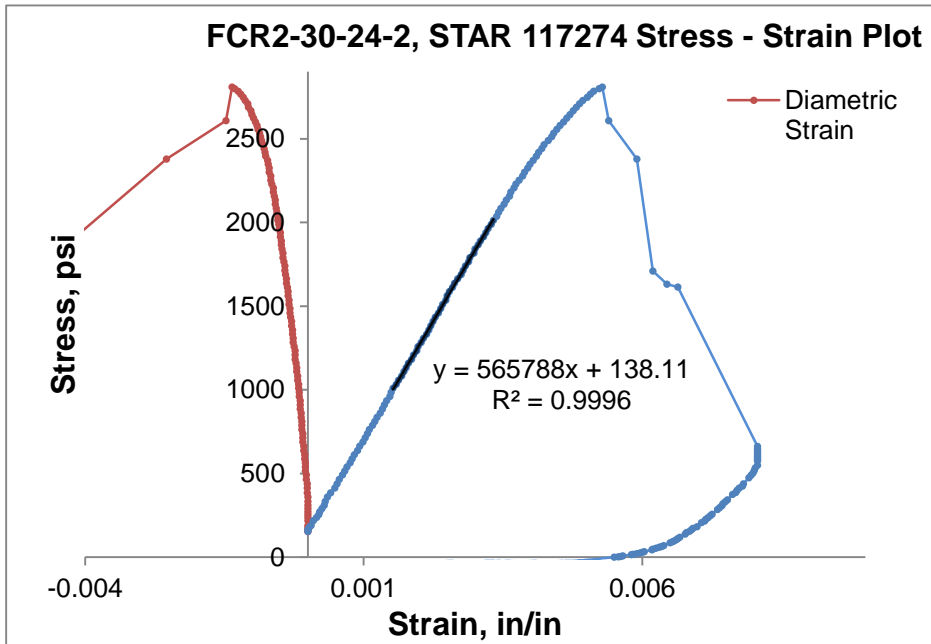


Figure 70: FCR2 - 30% Foam quality Stress - Strain Plot

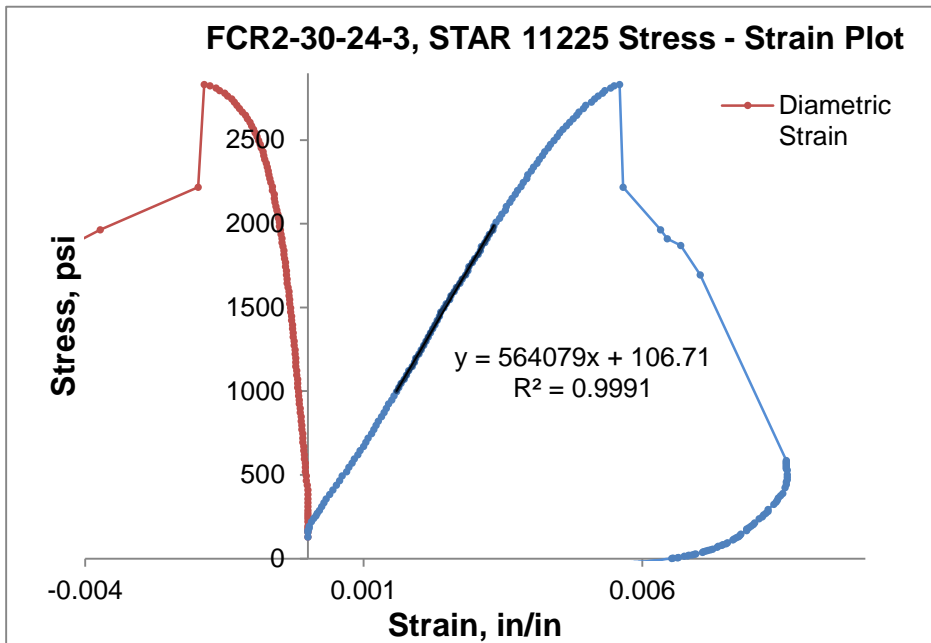


Figure 71: FCR2 - 30% Foam quality Stress - Strain Plot

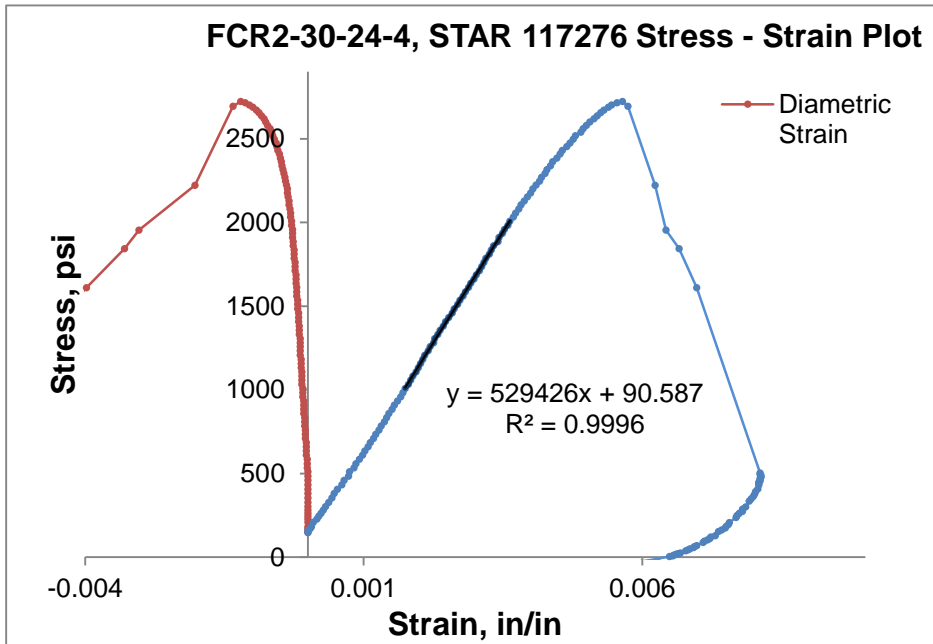
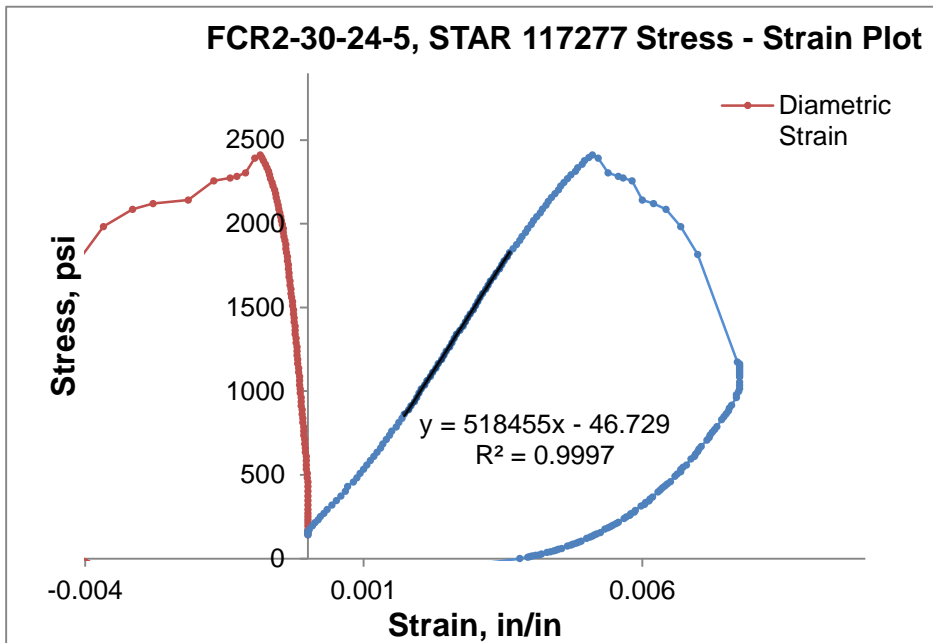


Figure 72: FCR2 - 30% Foam quality Stress - Strain Plot



FCR2 40%

Figure 73: FCR2 - 40% Foam quality Stress - Strain Plot

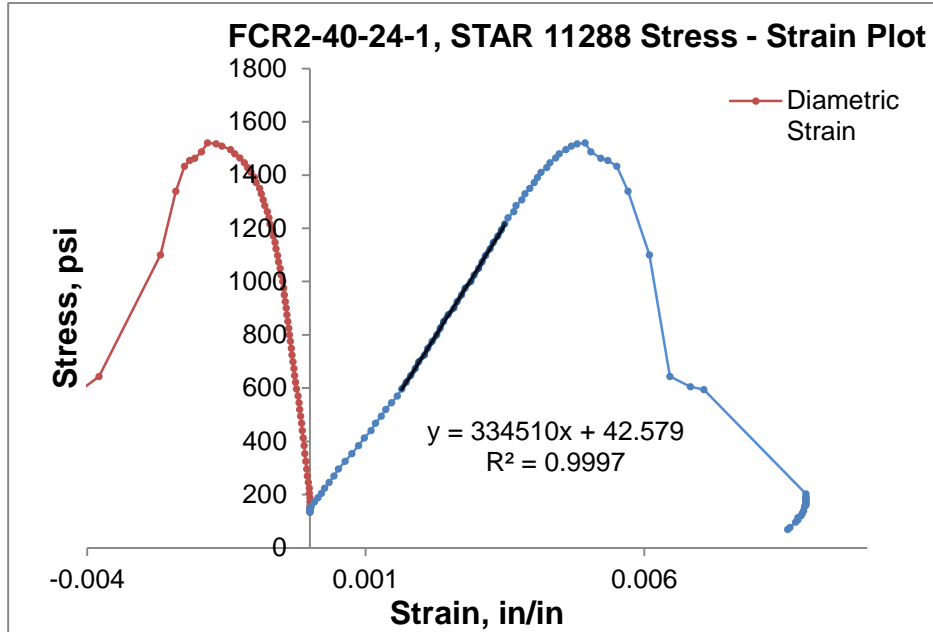


Figure 74: FCR2 - 40% Foam quality Stress - Strain Plot

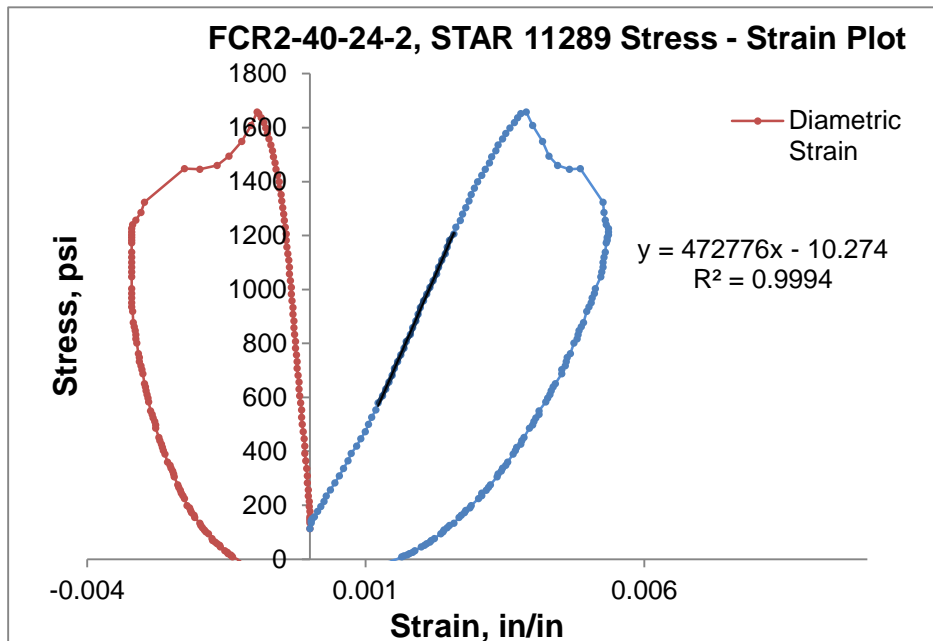


Figure 75: FCR2 - 40% Foam quality Stress - Strain Plot

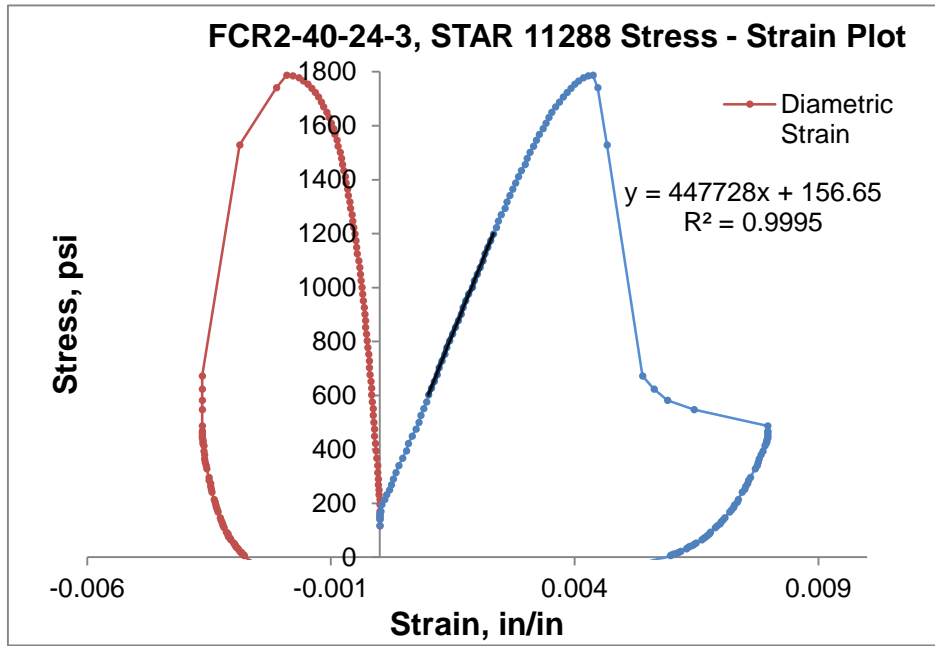


Figure 76: FCR2 - 40% Foam quality Stress - Strain Plot

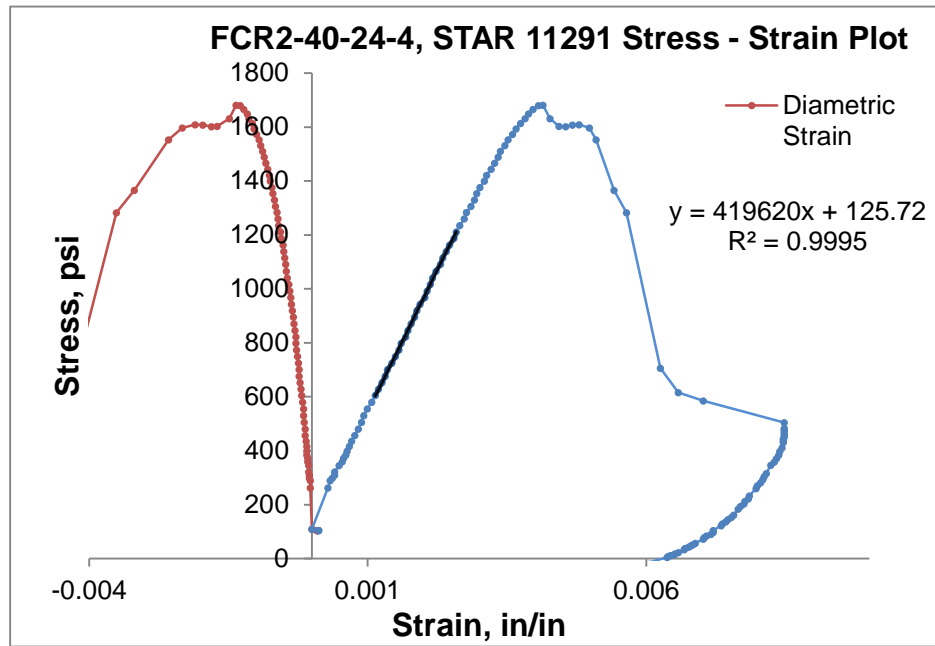
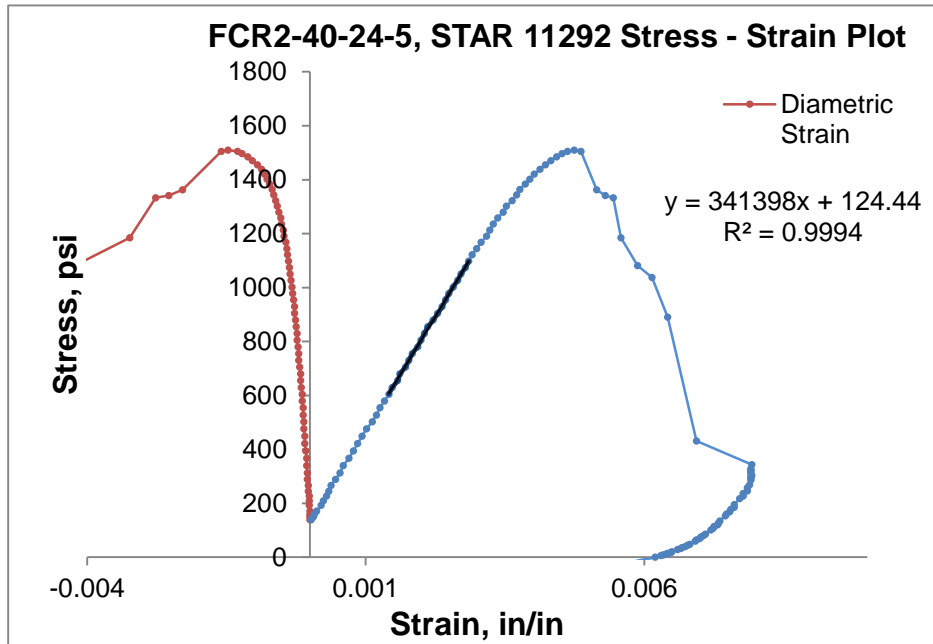


Figure 77: FCR2 - 40% Foam quality Stress - Strain Plot



BIBLIOGRAPHY

- Aldrich, C. and Mitchell, B. (1976). Strength, Permeabilities, and Porosity of oilwell foam cement. Engineering for industry.
- American Petroleum Institute. (1991). Worldwide Cementing Practices. API, Dallas, TX
- American Petroleum Institute. (1997). Recommended practice for Testing well cements: API recommended practice 10B. Washington, D.C.: API.
- American Petroleum Institute. (2004). API Recommended Practice 10B-4. Recommended Practice on Preparation and Testing of Foamed Cement Slurries at Atmospheric Pressure. Washington D.C.: American Petroleum Institute.
- Banthia, N., Biparva, A., Mindess, S. (2005). Permeability of concrete under stress. Cement and Concrete Research, 35, 1651 – 1655.
- Bartlit, F., Sankar, S., & Grimsley, S. (2011). Macondo- The Gulf Oil Disaster: The Chief Counsel's Report. National Commission on the BP Deepwater Horizon Oil Spill and Offshore Drilling.
- Benge, G.; McDermott, J.R.; Langlinais, J.C.; Griffith, J.E. (1996). Foamed Cement Job successful in deep HTHP offshore well. Oil and Gas Journal, 94, 58-63.
- Benge, G. and Poole, D. (2005). Use of foamed cement in deep water Angola. Society of Petroleum Engineers, Presented at the SPE/IADC Drilling Conference held in Amsterdam, Netherlands, 23-25 February 2005. SPE/IADC 91662.
- Bosma, M.; Ravi, K.; van Driel, W.; Schreppers, G.J. (1999). Design Approach to Sealant Selection for the Life of the Well. Society of Petroleum Engineers, Presented at the 1999 SPE Annual Technical Conference and Exhibition held in Houston, Texas, 3-6 October 1999. SPE 56536
- Bourgoyne, A. T. (1999). Sustained Casing Pressure in Offshore Producing Wells. Offshore Technology Conference.
- Bozich, M., Montman, R., and Harms, W. (1984). Application of Foamed Portland Cement to Deep Well Conditions in West Texas. Presented at the SPE Deep Drilling and Production Symposium held in Amarillo, TX, April 1-3, 1984. SPE 12612
- Coon, R. (1968). Correlation of Engineering Behaviour with the Classification of In Situ Rock. Illinois, USA: University of Illinois.
- Craig, R. R. (2011). Mechanics of Materials, 3rd Edition. Hoboken: John Wiley and Sons, Inc.

- Das, A., Nguyen, G. D., and Einav, I. (2011). Compaction bands due to grain crushing in porous rocks: A theoretical approach based on breakage mechanics. *Journal of Geophysical Research. B. Solid Earth*.
- Davies, D. R. (1981). *Foamed Cement - A Cement With Many Applications*. Society of Petroleum Engineers.
- De Beer, M. and Maina, J. (2008). Some fundamental definitions of the elastic parameters for homogeneous isotropic linear elastic materials in pavement design and analysis. *Proceedings of the 27th Southern African Transport Conference* (pp. 282-293). Pretoria: Document Transformation Technologies.
- De Rozières, J.; Ferriere, R. (1991). Foamed-Cement Characterization Under Downhole Conditions and Its Impact on Job Design. *SPE Production Engineering*, (6) 297-304
- Frisch, G.J., Graham, W.L., Griffith, J. (1999). Assessment of foamed-cement slurries using conventional cement evaluation logs and improved interpretation methods. *SPE 55649*
- Fuller, G. A. (2010). *A Gulf of Mexico Case History: Benefits of Foamed Cementing to Combat a SWF*. . Society of Petroleum Engineers.
- Galiana, C., Hitt, R., Nelson, E., Pessin, J., Poyet, M. B., Sherwood, R., and Vidick, B. (1991). Cement mixing: Better understanding and new hardware. *Oilfield Review*.
- Goodwin, K. J. (1997). *Oilwell/Gaswell Cement-Sheath Evaluation*. Society of Petroleum Engineers.
- Goodwin, K. and Crook, R. (1992). Cement Sheath Stress Failure. *SPE Drilling Engineering*, December. 291-296.
- Griffith, J. E; Lende, G.; Ravi, K.; Saasen, A.; Nødland, N. E.; Jordal, O. H. (2004). Foam cement engineering and implementation for cement sheath integrity at high temperature and high pressure. *IADC/SPE Drilling Conference*, March 2–4, 2004, Dallas, TX. *SPE 87194*.
- Harlan, T. D.; Foreman, J.; Reed, S.; Griffith, J. (2001). *Foamed Cement Selection for Horizontal Liners Proves Effective for Zonal Isolation—Case History*. Presented at the 2001 Rocky Mountain Petroleum Conference held in Keystone, Colorado, 21-23 May 2001. *SPE 71055*
- Harms, W.M. and Febus, J.S. (1985). Cementing of fragile-formation wells with foamed cement slurries. *Journal of Petroleum Technology*, 37:6, 1049-1057
- Hewlett, P.C. (1998). *Lea's Chemistry on Cement and Concrete*, Arnold, London, Great Britain.
- Hoff, G. (1972). Porosity–strength considerations for cellular concrete. *Cement and Concrete Research*, 91-100.
- Hover, K. C. (2011). The influence of water on the performance of concrete. *Construction and Building Materials*, 25 (7), 3003-3013. DOI: 10.1016/j.conbuildmat.2011.01.010

- Iverson, B.; Darbe, R.; and McMechan, D. (2008). Evaluation of Mechanical Properties of Cements. American Rock Mechanics Association. Presented at the 42nd US Rock Mechanics Symposium and 2nd U.S.-Canada Rock Mechanics Symposium, held in San Francisco, June 29- July 2, 2008. ARMA 08-293
- Judge, R.A. and Bengel, G. (1998). Advances in metering and control technology improves design and execution of foamed cement jobs. IADC/SPE 47831
- Kearsley, E. and Wainwright, P. (2002). The effect of porosity on the strength of foamed concrete. Cement and Concrete Research, 233–239.
- Kopp, K.; Reed, S.; Foreman, J.; Carty, B.; and Griffith, J. (2000). Foamed Cement vs. Conventional Cement for Zonal Isolation-Case Histories. Society of Petroleum Engineers, Presented at the 2000 SPE Annual Technical Conference and Exhibition held in Dallas, Texas, October 1-4. SPE 62895
- Kutchko, B., Crandall, D., Gill, M., McIntyre, D., Spaulding, R., Strazisar, B., et al. (2013). Computed Tomography and Statistical Analysis of Bubble Size Distributions in Atmospheric-Generated Foamed Cement. Pittsburgh: DOE-NETL internal Publication.
- Kutchko, B., Crandall, D., Moore, J., Gill, M., Haljasmaa, I., Spaulding, R., . . . Shine, J. (2014). Assessment of Foamed Cement Used in Deep Offshore Wells. Society of Petroleum Engineers. SPE 170298
- Le Roy-DeLange, S.; Baumgarte, C.; Thiercelin, M.; and Vidick, B. (2000). New Cement Systems for Durable Zonal Isolation. Presented at the IADC/SPE Drilling Conference held in New Orleans, Louisiana, 23-25 February 2000. New Orleans: Society of Petroleum Engineers. IADC/SPE 59132.
- Mashinsky, E. (2003). Differences between static and dynamic elastic moduli of rocks: Physical causes. Russian Geology and Geophysics, Vol. 44, No 9, Pages 953-959.
- McDaniel, J. W., Watters, L., Shadravan, A. (2014). Cement Sheath Durability: Increasing Cement Sheath Integrity to Reduce Gas Migration in the Marcellus Shale Play. Presented at the SPE Hydraulic Fracturing Technology Conference held in The Woodlands, Texas, 4-6 February 2014. SPE 168650
- McElfresh, P. M. (1982). Applications of Foam Cement. Society of Petroleum Engineers.
- Mindess, S. and Young, J. F. (1981). Concrete. Englewood Cliffs: Prentice-Hall.
- Moore, S., Miller, M. Faul, R. (2000). Foam cementing applications of a deepwater subsalt well – case history. IADC/SPE 59170
- Morales, R., Brady, B., and Ingraffea, A. (1993). Three-Dimensional Analysis and Visualization of the Wellbore and the Fracturing Process in Inclined Wells. Society of Petroleum Engineers, presented at the SPE Rocky Mountain Regional/Low Permeability Reservoirs Symposium, Denver, Colorado.

- Mueller, D. T. (1990). The Determination of the Static and Dynamic Properties of Nitrified Cements. Presented at the Permian Basin Oil and Gas Recovery Conference held in Midland, Texas, March 8-9, 1990. SPE 20116
- Mueller, D. T., GoBoncan, V., Dillenbeck, R.L., Heinold, T. (2004). Characterizing Casing-Cement-Formation Interactions Under Stress Conditions: Impact on Long-Term Zonal Isolation. Society of Petroleum Engineers, presented at the SPE Annual Technical Conference and Exhibition, 26-29 September, Houston, Texas. SPE-90450-MS
- Mueller, D. and Eid, R. (2006). Characterizing early-state physical properties, mechanical behavior of cement designs. *Drilling Contractor*, May/June, 50-52.
- Murayama, R., Kobayashi, M., and Jen, C. (2013). Study of Material Evaluation Probe Using a Longitudinal Wave and a Transverse Wave. *Journal of Sensor Technology*. Vol.3. No.2. pp. 25-29. doi: 10.4236/jst.2013.32005.
- Nelson, E.B. and Guillot, D. Ed. (2006). *Well Cementing*. Schlumberger Educational Services. Sugar Land, TX.
- Neville, A.M. (2004). *Properties of Concrete (4th Edition)*, John Wiley and Sons: New York.
- Pavement Interactive. (2007, August 15). Elastic modulus Modulus. Retrieved from Pavement Interactive: <http://www.pavementinteractive.org/article/elastic-modulus/>
- Pine, M. H. (2003). Selection of Foamed Cement for HPHT Gas Well Proves Effective for Zonal Isolation-Case History. Society of Petroleum Engineers.
- Rae, P. and Lullo, G.D. (2004). Lightweight cement formulations for deep water cementing: Fact and fiction. SPE 91002
- Ravi, K.; Gray, D.; and Pattillo, P. (2006). Procedures to Optimize Cement Systems for Specific Well Conditions. Presented at the AADE Drilling Fluids Technical Conference in Houston, Texas, April 11-12, 2006. AADE-06-DF-HO-35.
- Ravi, K.; McMechan, D.; Reddy, B.R.; Crook, R. (2007). A comparative study of Mechanical properties of density reduced cement compositions. SPE: *Drilling and Completion*, 119-126.
- Reddy, B. R.; Santra, A.; McMechan, D.; Gray, D.; Brenneis, C.; and Dunn, R. (2007). Cement Mechanical Property Measurements Under Wellbore Conditions. Society of Petroleum Engineers. doi:10.2118/95921-PA
- Sideris, K.K., Savva, A.E., and Papayianni, J. (2006). Sulfate resistance and carbonation of plain and blended cements. *Cement and Concrete Research*, 28, 47-56.
- Singamshetty, K. C. (2004). An Investigation to Determine the Effect of Synthetic Mud Compressibility in Deepwater Cementing Operations. . Society of Petroleum Engineers.

- Siriwardane, H., Haljasmaa, I., McLendon, R., Irdi, G., Soong, Y., and Bromhal, G. (2009). Influence of Carbon Dioxide on coal permeability determined by pressure transient methods. *International Journal of Coal Geology*-Vol. 77, issues 1-2, 109-118.
- SPE International. (2015, June 25). Foamed cement. Retrieved from PetroWiki: http://petrowiki.org/Foamed_cement
- Starzec, P. (1999). Dynamic elastic properties of crystalline rocks from south-west Sweden. *International Journal of Rock Mechanics and Mining Sciences*, 265-272.
- Taylor, H.F.W. (1997). *Cement Chemistry*, Academic Press, New York.
- Thayer, R.D., Ford, D.G., Holekamp, S., Pferdehirt, D.J. (1993). Real-time quality control of foamed cement jobs: A case study. SPE 26575
- Thiercelin, M. J., Dargaud, B., Baret, J. F., and Rodriguez, W. J. (1998). Cement Design Based on Cement Mechanical Response. Society of Petroleum Engineers. doi:10.2118/52890-PA
- van Heerden, W. (1987). General Relations Between Static and Dynamic Moduli of Rocks. *International Journal of Rock Mechanics and Mining Sciences and Geomechanics Abstracts*, Vol. 24, No. 6, 381-385.
- White, J., Moore, S., Miller, M., Faul, R. (2000). Foaming cement as a deterrent to compaction damage in deepwater production., IADC/SPE 59136
- Zimmer, M. (2003). *Rock Physics Basics*. Doctoral Thesis. Stanford University.